Doctoral Thesis

Studies on Synthesis, Structure, and Properties of Optically Active Poly(benzene-1,4-diyl) Derivatives

（光学活性ポリ(ベンゼン-1,4-ジイル)誘導体の合成、構造および物性に関する研究）

Qingyu WANG (王 慶宇)

Hokkaido University

Contents

Chapter 1. General Introduction

1.1 Helical polymers

Helix is the molecular conformation of a spiral nature, generated by regularly repeating rotations around the backbone bonds of a macromolecule. It is the most representative among so many conformations possible for a macromolecule. There are several macromolecular conformations that have been unambiguously identified for real chain, including helical conformation,[1] flat, zig-zag conformation as found in β-sheets of peptides,[2] and π-stacked conformation[3] which possesses both zig-zag and helical characteristics. Among these conformations, helix is well known to be essential for natural macromolecules such as proteins,[4] polysaccharides,[5] and DNAs[6] whose biological activities in living systems are believed to have deep connections to the conformation. Helix is a chiral form and may be right- or left-handed, and right- left-handed helices are enantiomers to each other. If either enantiomer is enriched, the polymer sample is preferred-handed helical and may show chiroptical properties. If a helical polymer is composed purely of right- or left-handed helical macromolecules, the polymer is called single-handed helix though proving single-handed helicity has been attained only in limited case.[7]

Helix has been found not only in natural polymers but also in synthetic polymers. There were two breakthroughs in synthetic polymer studies. The first one was attained through the pioneering work on isotactic polypropylene by Natta[8] in 1955 who for the first time found the formation of racemic helix in the solid state. This work stimulated remarkable progresses in the field of helical synthetic polymers with noticeable mile-stone reports that include the finding of preferred helical polyolefins having chiral side-chain groups whose helicity is maintained in solution.[9] The second breakthrough was about poly(triphenylmethyl methacrylate) (poly(TrMA)) bearing a bulky, achiral side-chain group invented by Okamoto and coworkers in 1979.[1d] This polymers prepared in an optically active form by the asymmetric anionic polymerization (helix-sense-selective polymerization or asymmetric helix-chirogenic

polymerization) using complexes of organolithiums and chiral diamine ligands including (-)-sparteine. Through very careful examinations, Okamoto concluded that poly(TrMA) has a single-handed helical conformation, not just a preferred-handed one. Following these two landmark findings, many examples of synthetic helical polymers were developed; the examples are not limited to vinyl polymers[10] but encompass various chemical structures including polyaldehydes,[11] polyisocyanides,[12] polyisocyanates,[13] polyacetylenes,[14] poly(aryleneethynylene)s,[15] polyarylenes[16] and others.[17]

Helical conformation can be formed by one or more among the following four mechanisms: (1) steric repulsion between side-chain groups, (2) attraction between side-chain or main-chain moieties, (3) inherent rigidity of the main chain, and (4) non-covalent interactions with external molecules which temporarily modify the chain structure. For example, helices of peptides, polysaccharides, and DNAs are supported by intramolecular or intermolecular hydrogen bonding through the second mechanism and helices of poly(meth)acrylates are maintained by steric repulsion between bulky side-chain groups through the first mechanism. Further, single-handedness or preferred-handedness can be induced to a polymer chain by one or more among the following three mechanisms: (1) by polymerization through kinetic control where a chiral ligand is often used as a source of chirality, or (2) on the basis of configurational chirality present in the monomeric unit or in the main chain through thermodynamic stability, or (3) through interactions of a polymer chain with external chiral molecule. Single-handed helical structure of poly(meth)acrylates can be controlled by kinetics or by thermodynamics (mechanism 1 and 2). Although the nature of single-handed helix formation of natural polymers is not completely clear, single-handedness is based at least in part on configuration of centers of chirality in the chain (mechanism 2).

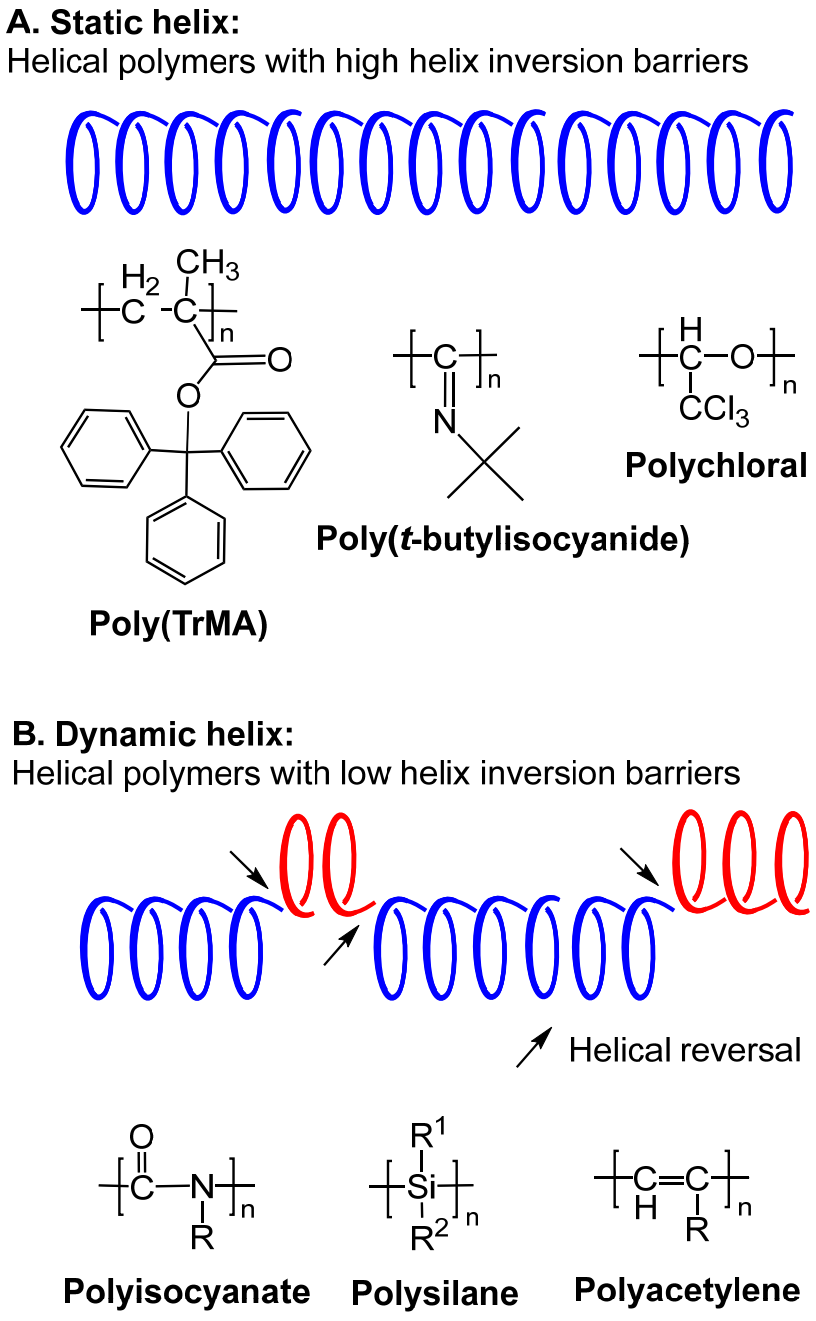

Fig. 1. Static and dynamic helical polymers.[18]

1.2 Poly(benzenediyl)s (polyphenylenes)

This thesis focuses on the synthesis and properties of poly(benzene-1,4-diyl)s. In the discipline of chiral polymers, poly(benzene-1,2-diyl)s [poly(1,2-phenylene), poly(*o*-phenylene)s were the focus of research work including poly(1,10-phenanthroline-5,6-diyl).[19] (add ref. 3) Such polymers have been proved to be helical. Helix is considered to be maintained by limited rotation around single

bonds connecting aromatic groups due partially to electronic conjugation and partially to steric repulsion about constituent atoms of the chain. Helix may also be stabilized through intramolecular π-stacking. The polymers prepared in this work were designed to be candidates of polymer ligands, inspired by the conformation poly(benzene-1,2-diyl) derivatives in which the aromatic groups are densely accumulated. Phenanthrolines accumulated in a helical manner may provide a controlled reaction field (space) for catalytic reactions including asymmetric ones.

Examples of synthesis and structural analysis of poly(benzene-1,2-diyl)s and its derivatives are far more limited compared with poly(benzene-1,3-diyl)s and poly(benzene-1,4-diyl)s and their derivatives. The first synthesis of poly(1,2-phenylene) was attempted by Wittig[20] through coupling of *ortho*-dilithiobenzene in the presence of transition metal salt resulting in products that seem to be cyclic compounds (Fig. 2A). Later, Ullmann reaction,[21] Kumada coupling[22] and electrochemical polymerization[23] aiming at poly(1,2-phenylene) were also reported. Conventional step-by-step methods such as Suzuki coupling[24] (Fig. 2B) and copper-mediated oxidative coupling[25] (Fig. 2C) were also used. Polymerizations of aryne and oxabicyclic alkene with copper and palladium catalysis, respectively (Fig. 2D), were developed.[26] In addition, our group synthesized poly(1,10-phenanthroline-5,6-diyl) by asymmetric Yamamoto coupling (Figure 2E). As one of the most noticeable achievements, uniform poly(*o*-phenylene) derivatives up to 48-mer were synthesized through copper-mediated oxidative reaction of lithiated precursors starting from a 2,2'-biphenyl derivative and *n*-BuLi, and a tight helical conformation was clarified through X-ray crystal analysis.[25] In this case, single-handed helix was obtained through resolution by triage of conglomerate crystals[26a] as well as chiral HPLC.[25a]

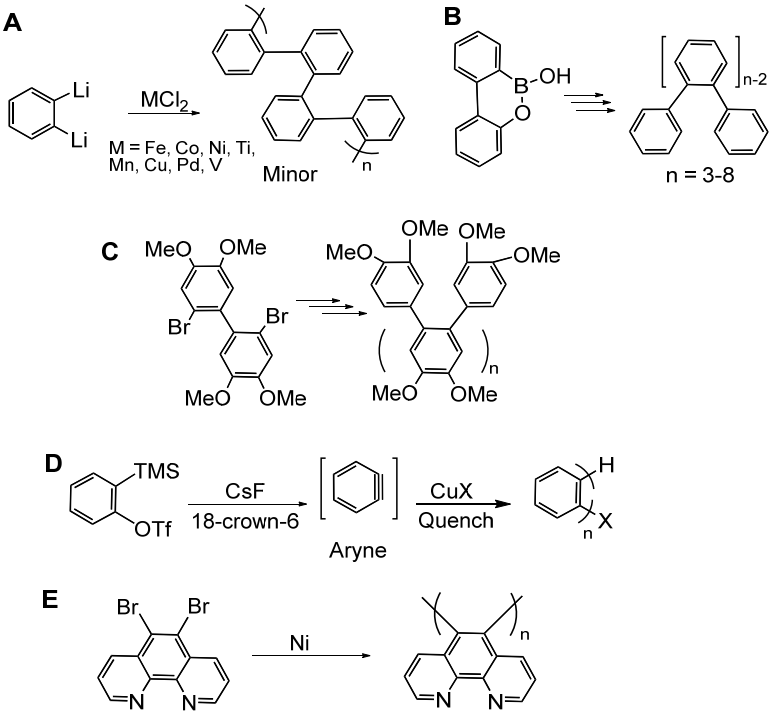

Fig. 2. Examples of poly(benzene-1,2-diyl) synthesis: coupling of *ortho*-dilithiobenzene with transition metal salt (A); Suzuki coupling (B); copper-mediated oxidative coupling (C); polymerizations of aryne and oxabicyclic alkene with copper and palladium catalysis (D); and Yamamoto coupling (E).

A related and well-surveyed class of polymer is poly(benzene-1,3-diyl)s [poly(1,3-phenylene)s, poly(*m*-phenylene)s]. 5_1-Helical conformation of poly(1,3-phenylene) in solid state by single crystal X-ray diffraction analysis and computational study,[27] while it is readily unraveled to adopt a random coil conformation in solution. Yashima[28] successfully synthesized a poly(*m*-phenylene) derivative with an optical active oligo(ethylene oxide) chain as substituent at the 5-position via the nickel catalyzed homo-coupling polymerization. The polymer took a single helical conformation in protic media, double-helical conformation in water through aromatic interactions, and random coil conformation in chloroform. Similarly, oligo(pryidine-*alt*-pyrimidine)s[29] were found to take a helical conformation, and characterized by distinct chemical shifts (upfield shift), NOE effects, and excimer emission due to the overlap of aromatic groups, as well as X-ray single crystal analysis in solid state.

Another category of polymers related to poly(benzene-1,2-diyl) is helicenes whose internal rotation is completely locked although they are not polymers. They are polycyclic aromatic compounds with nonplanar screw-shaped skeletons made up of *ortho*-fused benzene or other aromatic rings.[30]

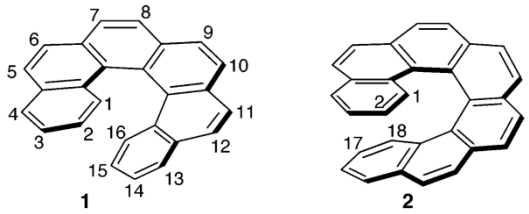

Fig. 4. Examples of helicenes. **1**: Hexahelicene ([6]helicene); **2**: Heptahelicene ([7]helicene).[31]

1.3 Application of Helical Polymers

Helical macromolecules can be used as source compounds for chiral, functional polymeric materials. Functions included (1) resolution of racemic compounds, (2) chiral catalysis, and (3) circularly polarized light (CPL) emission. Among these three, resolution of racemates has the longest history and some polymer have been successfully commercialized.[32] Chiral catalysis is a rather newer function of helical polymers, and recently remarkable advances have been made using poly(quinoxaline)s.[33] CPL emission is currently drawing attention because CPL-based organic light emitting diodes (OLED's) has been pointed out save energy in emission compared with conventional OLED's emission non-polarized light.[34]

1.4 Thesis Contents

This thesis work presents the preparation, structure and chiral properties and functions of poly(benzene-1,4-diyl)s including poly(naphthalene-1,4-diyl). In a sharp contrast to the rich accumulation of studies on poly(benzene-1,2-diyl)s, examples of research work on poly(benzene-1,4-diyl)s from a view of chirality has been limited in spite of the fact that studies on electronic properties have been reported in a number of papers that looked at the polymers as conducting polymers. In this work, it was

clarified that a wide variety of poly(benzene-1,4-diyl)s bearing chiral side-chain with random and alternating copolymer sequences can take helical conformation in the solid state while helicity is not remarkable in solution. Further, in the case of poly(naphthalene-1,4-diyl), asymmetric polymerization led to a preferred-handed helical polymer in solution, and also a CPL-irradiation method was applied to create chiral conformation in the solid state. This thesis is comprised for four chapters.

Chapter 1 described the general background of this work including the history of helical polymer developments.

Chapter 2 describes the preparation, structure, and functions of poly(benzene-1,4-diyl)s bearing chiral side chain groups. The polymers were copolymers composed of units with chiral side chain and achiral units having different bulkiness. The copolymers have either random or alternating sequence with the same monomer unit combinations. Although the polymers did not show any remarkable chiroptical properties in solution, they exhibited intense circular dichroism (CD) spectra based on preferred-handed helical conformation. The conformation was not stable in solution but is stabilized through inter-macromolecular interactions in the solid state. In addition, some of the polymers studied in this work showed resolution abilities for several racemic compounds, indicating that they can be good candidates for chiral stationary phase materials for HPLC. Further, some of the polymers indicated efficient CPL emission properties, indicating that the preferred-handed helical conformation is stable not only in the ground state but also in excited states.

Chapter 3 explores into the synthesis of poly(naphthalene-1,4-diyl) by asymmetric Suzuki-Miyaura cross coupling polymerization and Kumada coupling polymerization using chiral ligands having P atoms where helix-sense excess was estimated using optically active 1,1’-binaphthyl, a model 2-mer, whose e.e. is know by chiral HPL resolution, as a reference compound. In addition, CPL irradiation to an optically inactive, racemic poly(naphthalene-1,4-diyl) in the solid state afforded optically active polymer. Both optically active poly(naphthalene-1,4-diyl)s prepared by asymmetric polymerization or by CPL irradiation exhibited efficient CPL luminescence.

Chapter 4 describes general conclusion.

References

1. (a) Cahn, R. S.; Ingold, C.; Prelog, V. *Angew. Chem. Int. Ed.* **1966,** *5* (4), 385-415; (b) Vogl, O.; Jaycox, G. D. *Polymer* **1987,** *28* (13), 2179-2182; (c) Pino, P.; Lorenzi, G. P. *J. Am. Chem. Soc.* **1960,** *82* (17), 4745-4747; (d) Okamoto, Y.; Suzuki, K.; Ohta, K.; Hatada, K.; Yuki, H. *J. Am. Chem. Soc.* **1979,** *101* (16), 4763-4765; (e) Millich, F.; Baker, G. K. *Macromolecules* **1969,** *2* (2), 122-128; (f) Ciardelli, F.; Lanzillo, S.; Pieroni, O. *Macromolecules* **1974,** *7* (2), 174-179; (g) Corley, L. S.; Vogl, O. *Polym. Bull.* **1980,** *3* (4), 211-217.

2. (a) Schmidt, V. *Angew. Makromol. Chem.* **1970,** *14*, 185-202; (b) Chen, F.; Lepore, G.; Goodman, M. *Macromolecules* **1974,** *7* (6), 779-783; (c) Yuki, H.; Okamoto, Y.; Taketani, Y.; Tsubota, T.; Marubayashi, Y. *J. Polym. Sci., Part A: Polym. Chem.* **1978,** *16* (9), 2237-2251; (d) Yuki, H.; Okamoto, Y.; Doi, Y. *J. Polym. Sci., Part A: Polym. Chem.* **1979,** *17* (7), 1911-1921; (e) Fernandez-Santin, J. M.; Aymami, J.; Rodriguez-Galan, A.; Munoz-Guerra, S.; Subirana, J. A. *Nature* **1984,** *311* (5981), 53-54.

3. (a) Nakano, T.; Takewaki, K.; Yade, T.; Okamoto, Y. *J. Am. Chem. Soc.* **2001,** *123* (37), 9182-9183; (b) Nakano, T.; Yade, T. *J. Am. Chem. Soc.* **2003,** *125* (50), 15474-15484; (c) Nakano, T.; Nakagawa, O.; Tsuji, M.; Tanikawa, M.; Yade, T.; Okamoto, Y. *Chem. Commun.* **2004,** (2), 144-145; (d) Nakano, T.; Yade, T.; Fukuda, Y.; Yamaguchi, T.; Okumura, S. *Macromolecules* **2005,** *38* (20), 8140-8148; (e) Nakano, T.; Tanikawa, M.; Nakagawa, O.; Yade, T.; Sakamoto, T. *J. Polym. Sci., Part A: Polym. Chem.* **2009,** *47* (1), 239-246; (f) Nakano, T. *Polym. J.* **2010,** *42* (2), 103-123.

4. (a) Pauling, L.; Corey, R. B. *J. Am. Chem. Soc.* **1950,** *72* (11), 5349-5349; (b) Pauling, L.; Corey, R. B.; Branson, H. R. *Proc. Natl. Acad. Sci.* **1951,** *37* (4), 205-211.

5. (a) Hanes, C. S. *New Phytologist* **1937,** *36* (2), 101-141; (b) Hanes, C. S. *New Phytologist* **1937,** *36* (3), 189-239; (c) Freudenberg, K.; Schaaf, E.; Dumpert, G.; Ploetz, T. *Naturwissenschaften* **1939,** *27* (51), 850-853.

6. Watson, J. D.; Crick, F. H. C. *Nature* **1953,** *171* (4356), 737-738.

7. Nakano, T.; Pietropaolo, A.; Kamata, M. *Chemistry Teacher International* **2020,** *3* (1), 67-76.

8. (a) Natta, G.; Pino, P.; Corradini, P.; Danusso, F.; Mantica, E.; Mazzanti, G.; Moraglio, G. *J. Am. Chem. Soc.* **1955,** *77* (6), 1708-1710; (b) Natta, G.; Danusso, F.; Sianesi, D. *Makromo. Chem.* **1958,** *28* (1), 253-261; (c) Natta, G. *Angew. Chem.* **1964,** *76* (13), 553-566; (d) Ziegler, K. *Angew. Chem.* **1964,** *76* (13), 545-553.

9. (a) Ciardelli, F.; Benedetti, E.; Montagnoli, G.; Lucarini, L.; Pino, P. *Chemical Communications (London)* **1965,** (13), 285-286; (b) Pino, P.; Ciardelli, F.; Lorenzi, G. P. *J. Am. Chem. Soc.* **1963,** *85* (23), 3888-3890; (c) Pino, P.; Ciardelli, F.; Lorenzi, G.; Montagnoli, G. *Die Makromolekulare Chemie: Macromolecular Chemistry and Physics* **1963,** *61* (1), 207-224; (d) Pino, P.; Lorenzi, G. P. *J. Am. Chem. Soc.* **1960,** *82* (17), 4745-4747.

10. (a) Okamoto, Y.; Yashima, E. *Prog. Polym. Sci.* **1990,** *15* (2), 263-298; (b) Ren, C.; Chen, C.; Xi, F.; Nakano, T.; Okamoto, Y. *J. Polym. Sci., Part A: Polym. Chem.* **1993,** *31* (11), 2721-2728; (c) Tamaki, N.; Akihiro, M.; Yoshio, O. *Polym. J.* **1996,** *28* (6), 556-558; (d) Tamaki, N.; Kyoichi, T.; Yoshio, O. *Polym. J.* **1997,** *29* (6), 540-544; (e) Tamaki, N.; Yoichi, S.; Yoshio, O. *Polym. J.* **1998,** *30* (8), 635-640.

11. (a) Goodman, M.; Abe, A. *J. Polym. Sci.* **1962,** *59* (168), S37-S39; (b) Abe, A.; Goodman, M. *J. Polym. Sci., Part A: General Papers* **1963,** *1* (6), 2193-2205; (c) Vogl, O.; Miller, H. C.; Sharkey, W. H. *Macromolecules* **1972,** *5* (5), 658-659; (d) Jaycox, G. D.; Vogl, O. *Makromo. Chem. , Rapid Commun.* **1990,** *11* (2), 61-66.

12. (a) Nolte, R. J. M.; Van Beijnen, A. J. M.; Drenth, W. *J. Am. Chem. Soc.* **1974,** *96* (18), 5932-5933; (b) Van Beijnen, A. J. M.; Nolte, R. J. M.; Drenth, W.; Hezemans, A. M. F. *Tetrahedron* **1976,** *32* (16), 2017-2019.

13. (a) Green, M. M.; Gross, R. A.; Crosby, C.; Schilling, F. C. *Macromolecules* **1987,** *20* (5), 992-999; (b) Green, M. M.; Andreola, C.; Munoz, B.; Reidy, M. P.; Zero, K. *J. Am. Chem. Soc.* **1988,** *110* (12), 4063-4065; (c) Green, M. M.; Reidy, M. P.; Johnson, R. D.; Darling, G.; O'Leary, D. J.; Willson, G. *J. Am. Chem. Soc.* **1989,** *111* (16), 6452-6454.

14. (a) Simionescu, C.; Dumitrescu, S.; Percec, V. *Polym. J.* **1976,** *8* (2), 139-149; (b) Simionescu, C. I.; Percec, V.; Dumitrescu, S. *J. Polym. Sci., Part A: Polym. Chem.* **1977,** *15* (10), 2497-2509; (c) Simionescu, C. I.; Dumitrescu, S.; Grigoras, M. *Eur. Polym. J.* **1978,** *14* (12), 1051-1057; (d) Simionescu, C. I.; Percec, V. *Prog. Polym. Sci.* **1982,** *8* (1–2), 133-214; (e) Moore, J. S.; Gorman, C. B.; Grubbs, R. H. *J. Am. Chem. Soc.* **1991,** *113* (5), 1704-1712; (f) Yashima, E.; Maeda, Y.; Okamoto, Y. *J. Am. Chem. Soc.* **1998,** *120* (34), 8895-8896.

15. (a) Prince, R. B.; Saven, J. G.; Wolynes, P. G.; Moore, J. S. *J. Am. Chem. Soc.* **1999,** *121* (13), 3114-3121; (b) Gin, M. S.; Yokozawa, T.; Prince, R. B.; Moore, J. S. *J. Am. Chem. Soc.* **1999,** *121* (11), 2643-2644; (c) Prince, R. B.; Barnes, S. A.; Moore, J. S. *J. Am. Chem. Soc.* **2000,** *122* (12), 2758-2762; (d) Prince, R. B.; Brunsveld, L.; Meijer, E. W.; Moore, J. S. *Angew. Chem. Int. Ed.* **2000,** *39* (1), 228-230; (e) Hill, D. J.; Mio, M. J.; Prince, R. B.; Hughes, T. S.; Moore, J. S. *Chem. Rev.* **2001,** *101* (12), 3893-4012; (f) Gin, M. S.; Moore, J. S. *Org. Lett.* **2000,** *2* (2), 135-138.

16. (a) Bedworth, P. V.; Tour, J. M. *Macromolecules* **1994,** *27* (2), 622-624; (b) Langeveld-Voss, B. M. W.; Janssen, R. A. J.; Christiaans, M. P. T.; Meskers, S. C. J.; Dekkers, H. P. J. M.; Meijer, E. W. *J. Am. Chem. Soc.* **1996,** *118* (20), 4908-4909; (c) Langeveld-Voss, B. M. W.; Christiaans, M. P. T.; Janssen, R. A. J.; Meijer, E. W. *Macromolecules* **1998,** *31* (19), 6702-6704; (d) Bassani, D. M.; Lehn, J.-M.; Baum, G.; Fenske, D. *Angew. Chem. Int. Ed.* **1997,** *36* (17), 1845-1847; (e) Yu, H.-B.; Hu, Q.-S.; Pu, L. *J. Am. Chem. Soc.* **2000,** *122* (27), 6500-6501.

17. (a) Berni, E.; Kauffmann, B.; Bao, C.; Lefeuvre, J.; Bassani, D. M.; Huc, I. *Chem. Eur. J.* **2007,** *13* (30), 8463-8469; (b) Berni, E.; Garric, J.; Lamit, C.; Kauffmann, B.; Leger, J.-M.;

Huc, I. *Chem. Commun.* **2008,** (17), 1968-1970; (c) Dai, Y.; Katz, T. J.; Nichols, D. A. *Angew. Chem. Int. Ed.* **1996,** *35* (18), 2109-2111; (d) Fujiki, M. *J. Am. Chem. Soc.* **1994,** *116* (26), 11976-11981; (e) Nakashima, H.; Fujiki, M.; Koe, J. R. *Macromolecules* **1999,** *32* (22), 7707-7709; (f) Fujiki, M. *J. Am. Chem. Soc.* **2000,** *122* (14), 3336-3343; (g) Fujiki, M. *Macromol. Rapid. Comm.* **2001,** *22* (8), 539-563; (h) Fujiki, M.; Koe, J. R.; Motonaga, M.; Nakashima, H.; Terao, K.; Teramoto, A. *J. Am. Chem. Soc.* **2001,** *123* (26), 6253-6261.

18. Yashima, E.; Maeda, K.; Iida, H.; Furusho, Y.; Nagai, K. *Chem. Rev.* **2009,** *109* (11), 6102-6211.

19. Yang, W.; Nakano, T. *Chem. Commun.* **2015,** *51* (97), 17269-17272.

20. (a) Wittig, G.; Lehmann, G. *Chem. Ber.* **1957,** *90* (6), 875-892; (b) Winkler, H. J. S.; Wittig, G. *J. Org. Chem.* **1963,** *28* (7), 1733-1740.

21. (a) Ibuki, E.; Ozasa, S.; Kazue, M. *Bull. Chem. Soc. Jpn.* **1975,** *48*, 7; (b) Ozasa, S.; Fujioka, Y.; Fujiwara, M.; Ibuki, E. *Chem. Pharm. Bull.* **1980,** *28* (11), 3210-3222.

22. Ibuki, E.; Ozasa, S.; Fujioka, Y.; Okada, M. *Chem. Pharm. Bull.* **1982,** *30* (7), 2369-2379.

23. (a) Xu, J.; Liu, H.; Pu, S.; Li, F.; Luo, M. *Macromolecules* **2006,** *39* (17), 5611-5616; (b) Dong, B.; Zheng, L.; Xu, J.; Liu, H.; Pu, S. *Polymer* **2007,** *48* (19), 5548-5555.

24. (a) Blake, A. J.; Cooke, P. A.; Doyle, K. J.; Gair, S.; Simpkins, N. S. *Tetrahedron Lett.* **1998,** *39* (49), 9093-9096; (b) He, J.; Crase, J. L.; Wadumethrige, S. H.; Thakur, K.; Dai, L.; Zou, S.; Rathore, R.; Hartley, C. S. *J. Am. Chem. Soc.* **2010,** *132* (39), 13848-13857; (c) Mathew, S. M.; Engle, J. T.; Ziegler, C. J.; Hartley, C. S. *J. Am. Chem. Soc.* **2013,** *135* (17), 6714-6722; (d) Mathew, S. M.; Hartley, C. S. *Macromolecules* **2011,** *44* (21), 8425-8432.

25. (a) Ando, S.; Ohta, E.; Kosaka, A.; Hashizume, D.; Koshino, H.; Fukushima, T.; Aida, T. *J. Am. Chem. Soc.* **2012,** *134* (27), 11084-11087; (b) Ohta, E.; Sato, H.; Ando, S.; Kosaka, A.; Fukushima, T.; Hashizume, D.; Yamasaki, M.; Hasegawa, K.; Muraoka, A.; Ushiyama, H.; Yamashita, K.; Aida, T. *Nat. Chem.* **2011,** *3* (1), 68-73; (c) Kajitani, T.; Suna, Y.; Kosaka, A.; Osawa, T.; Fujikawa, S.; Takata, M.; Fukushima, T.; Aida, T. *J. Am. Chem. Soc.* **2013,** *135* (39), 14564-14567.

26. (a) Ito, S.; Takahashi, K.; Nozaki, K. *J. Am. Chem. Soc.* **2014,** *136* (21), 7547-7550; (b) Mizukoshi, Y.; Mikami, K.; Uchiyama, M. *J. Am. Chem. Soc.* **2015,** *137* (1), 74-77.

27. (a) Williams, D. J.; Colquhoun, H. M.; O'Mahoney, C. A. *J. Chem. Soc., Chem. Commun.* **1994,** (14), 1643-1644; (b) Berresheim, A. J.; Müller, M.; Müllen, K. *Chem. Rev.* **1999,** *99* (7), 1747-1786; (c) Kobayashi, N.; Sasaki, S.; Abe, M.; Watanabe, S.; Fukumoto, H.; Yamamoto, T. *Macromolecules* **2004,** *37* (21), 7986-7991; (d) Hong, S. Y.; Kim, D. Y.; Kim, C. Y.; Hoffmann, R. *Macromolecules* **2001,** *34* (18), 6474-6481.

28. (a) Ben, T.; Furusho, Y.; Goto, H.; Miwa, K.; Yashima, E. *Org. Biomol. Chem.* **2009,** *7* (12), 2509-2512; (b) Ben, T.; Goto, H.; Miwa, K.; Goto, H.; Morino, K.; Furusho, Y.; Yashima, E. *Macromolecules* **2008,** *41* (12), 4506-4509; (c) Katagiri, H.; Miyagawa, T.; Furusho, Y.; Yashima, E. *Angew. Chem. Int. Ed.* **2006,** *45* (11), 1741-1744.

29. (a) Ohkita, M.; Lehn, J.-M.; Baum, G.; Fenske, D. *Chem. Eur. J.* **1999,** *5* (12), 3471-3481; (b) Hanan, G. S.; Lehn, J.-M.; Kyritsakas, N.; Fischer, J. *J. Chem. Soc., Chem. Commun.* **1995,** (7), 765-766.
30. Shen, Y.; Chen, C.-F. *Chem. Rev.* **2011,** *112* (3), 1463-1535.
31. Paruch, K.; Vyklický, L.; Wang, D. Z.; Katz, T. J.; Incarvito, C.; Zakharov, L.; Rheingold, A. L. *J. Org. Chem.* **2003,** *68* (22), 8539-8544.
32. (a) Shen, J.; Okamoto, Y. *Chem. Rev.* **2015,** *116* (3), 1094-1138; (b) Nakano, T. *Journal of Chromatography A* **2001,** *906* (1–2), 205-225; (c) Okamoto, Y.; Ikai, T. *Chemical Society Reviews* **2008,** *37* (12), 2593-2608; (d) Okamoto, Y.; Kawashima, M.; Hatada, K. *Journal of the American Chemical Society* **1984,** *106* (18), 5357-5359; (e) Okamoto, Y.; Yashima, E. *Angew Chem Int Edit* **1998,** *37* (8), 1020-1043; (f) Yashima, E. *Journal of chromatography A* **2001,** *906* (1), 105-125.
33. (a) Ke, Y.-Z.; Nagata, Y.; Yamada, T.; Suginome, M. *Angew. Chem., Int. Ed.* **2015,** *54* (32), 9333-9337; (b) Yamamoto, T.; Suginome, M. *Angew. Chem., Int. Ed.* **2009,** *48* (3), 539-542.
34. Wan, L.; Wade, J.; Shi, X.; Xu, S.; Fuchter, M. J.; Campbell, A. J. *ACS applied materials & interfaces* **2020,** *12* (35), 39471-39478.

Chapter 2. Synthesis and Functions of Helical Polyphenylenes

2.1 Introduction

Optically active macromolecules having single-handed or preferred-handed helical conformation are an important class polymeric material as they exhibit various useful functions based on polymer chirality including chiral recognition, asymmetric catalysis, and circularly polarized light (CPL) emission.[1-6] Typical examples of helical polymers are characterized by a rigid main chain having twisted bonds connecting constitutional atoms and include vinyl polymers such as poly(meth)acrylates, conjugated polymers such as polyacetylenes and polythiophenes, and polymers obtained through condensation and polyaddition such as polyamides and polyurethanes. Among these examples, conjugated polymers having π-electronic monomeric units are of particular interest from the view of electronic properties including photo absorbance and emission, and one of the simplest conjugated polymers is poly(benzene-1,4-diyl) [poly(*p*-phenylene)]. Although this polymer itself have very low solubility,[7-9] derivatives having alky substituents at the 2- and 5-positions of the main-chain benzene rings were found soluble in solvents.[10,11] In addition, soluble, optically active derivatives were synthesized and were proposed to assume preferred-handed helical conformation on the basis of their chiroptical properties, and the examples of chiral homopolymers and copolymers composed of benzene-1,4-diyl units involve those prepared using chiral monomers having cholesteryl group, 2-methylbutyl group, 1-phenylethyl group, and 1-methyl octyl group, and monomers with planar chirality, and each of them shows characteristic chirality features.[12-18]

However, there have not been systematic studies on poly(benzene-1,4-diyl)s units from a view of effects of side-chain bulkiness on chirality. This is in a sharp contrast to the fact that side-chain bulkiness is a key aspect in the formation of helix[3-6, 19, 20] and also of other specific conformation including π-stacked structure[21-23] for vinyl

polymers. In addition, properties so far studied for optically active poly(benzene-1,4-diyl)s have been limited to circularly polarized (CPL) emission. Chiral recognition ability has never been examined using this class of polymers although racemic resolution is often facilitated by a helical polymer chain.[24-30]

With such a background, we herein report a systematic study on the synthesis and chiroptical properties of the poly(benzene-1,4-diyl) derivatives with random and alternating copolymer sequences composed of bulky, achiral monomeric units and less bulky, chiral monomeric units. The copolymers exhibited distinctive chiroptical properties depending on the chemical structure, and also their chiroptical properties were remarkably amplified in suspension and in film. Further, some of the polymers exhibited efficient CPL emission in film and also showed chiral recognition toward racemic *trans*-stilbene oxide, Tröger's base, and flavanone (Chart 2-1).

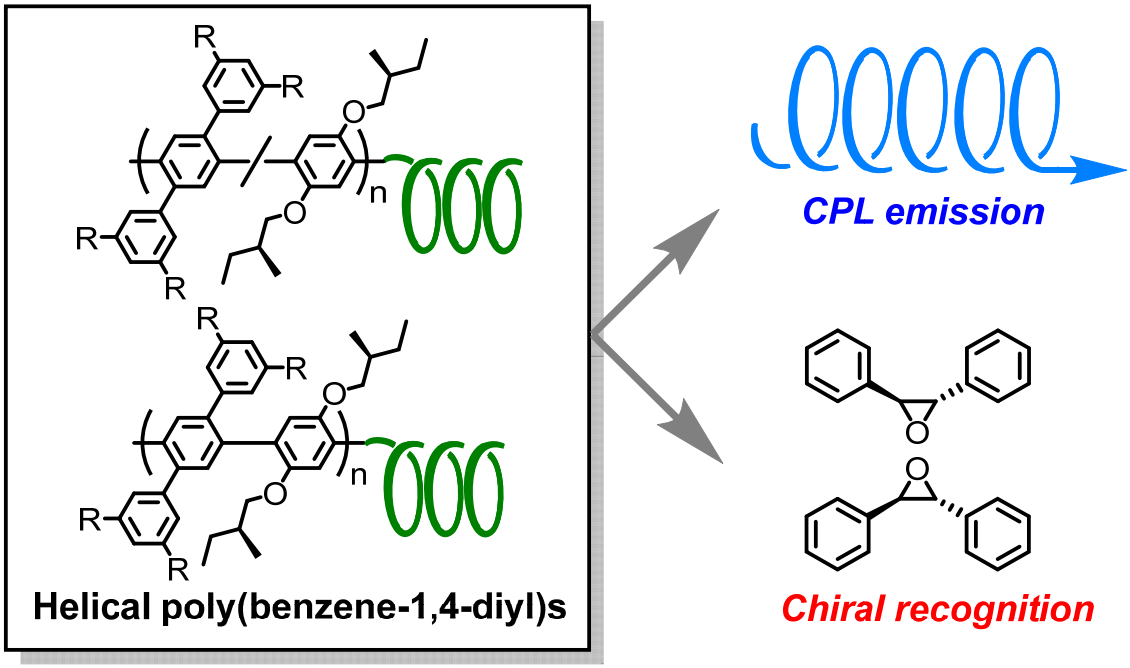

Chart 2-1. Helical poly(benzene-1,4-diyl)s exhibited CPL emission and showed chiral recognition.

2.2 Monomer Synthesis

In this work, Random copolymers comprised of chiral and achiral benzene-1,4-diyl units were prepared by Ni-mediated copolymerization of optically active

1,4-dibromo-2,5-bis((*S*)-2-methylbutoxy)benzene with bulky, achiral monomers, i.e., 1,4-dibromo-2,5-diphenylbenzene, 1,4-dibromo-2,5-bis(3,5-dimethylphenyl)benzene, 1,4-dibromo -2,5-bis(3,5-bis(trifluoromethyl)phenyl) benzene, and 1,4-dibromo-2,5-bis(3,5-diphenylphenyl)-benzene, and the corresponding alternating copolymers were synthesized by Pd-catalyzed Suzuki-Miyaura cross coupling of optically active 1,4-bis(dihydroxyboranyl)-2,5-bis((*S*)-2-methyl-butoxy)benzene with the bulky, achiral monomers (Chart 2-2).

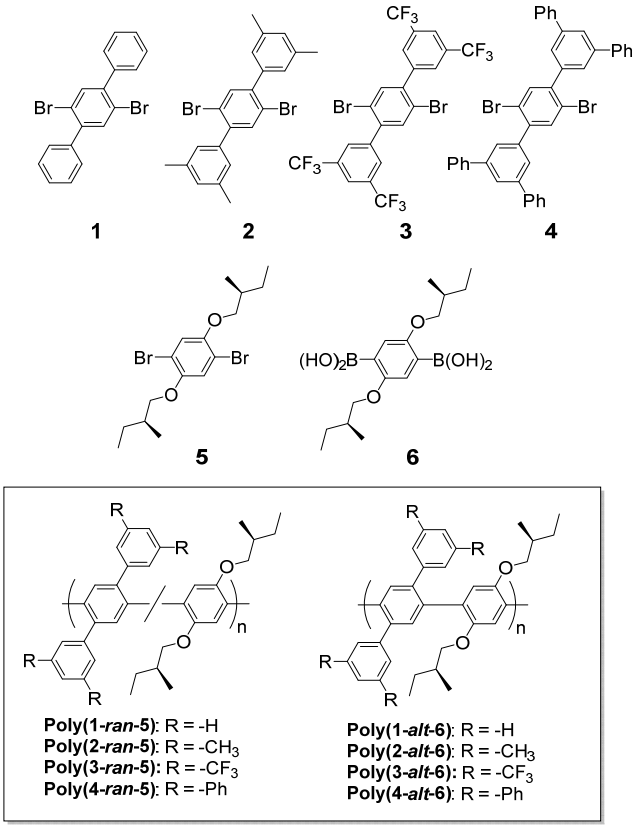

Chart 2-2. Structures of monomers and copolymers.

The monomers (**1-4**) were made through Pd-catalyzed Suzuki-Miyaura cross coupling of 1,4-dibromo-2,5-diiodobenzene with the phenylboronic acid derivatives. As a chiral monomer for polymers, 1,4-dibromo-2,5-bis((*S*)-2-methylbutoxy)benzene (**5**) and 1,4-dihyroxyboranyl-2,5-bis((*S*)-2-methylbutoxy)benzene (**6**) were synthesized according to the method indicated in Scheme 2-1[5]. The yields of target products **1-6** were 34%, 36%, 53%, 45%, 91% and 27%.

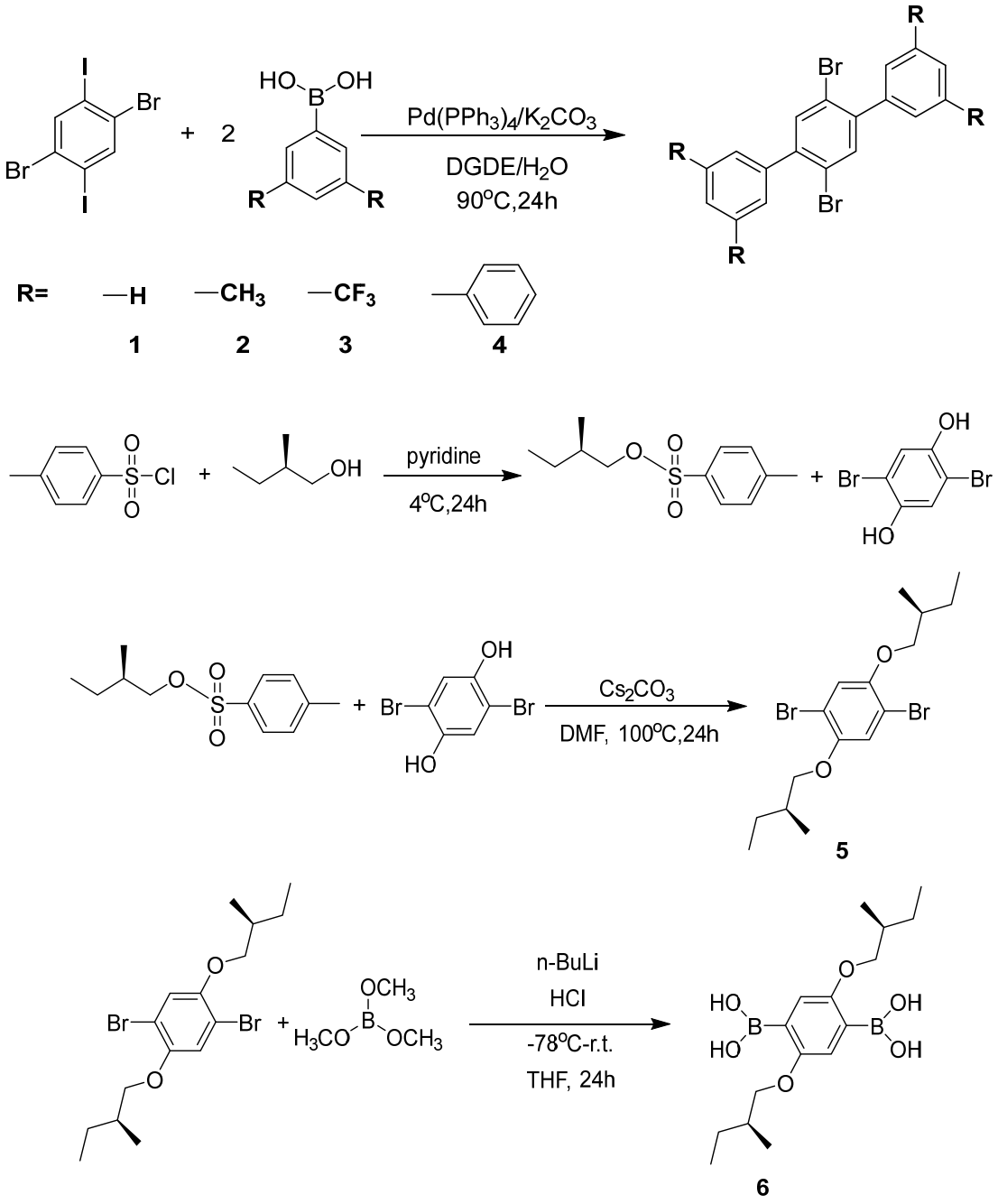

Scheme 2-1. Monomer synthesis.

2.3 Random Copolymers Synthesis

The random copolymers were prepared by Yamamoto coupling polymerization using Ni species of achiral monomer, *i.e.*, 1,4-dibromo-2,5-diphenylbenzene (**1**), 1,4-dibromo-2,5-bis(3,5-dimethylphenyl)benzene (**2**),[31] 1,4-dibromo-2,5-bis(3,5-bis(trifluoromethyl)phenyl)benzene (**3**), and 1,4-dibromo-2,5-bis(3,5-diphenylphenyl)benzene (**4**) with chiral

1,4-dibromo-2,5-bis((*S*)-2-methylbutoxy)benzene (**5**)[15] in toluene at [**1**-**4**]/[**5**] = 1/1 in feed (Scheme 2-2). The random copolymers were purified by reprecipitation in MeOH and were found to compose of THF-insoluble and -soluble parts. The THF-soluble parts were further purified by preparative SEC and by washing with a $CHCl_3$-MeOH (1/9 (v/v)) mixture. The conditions and results of polymerization are shown in Table 2-1.

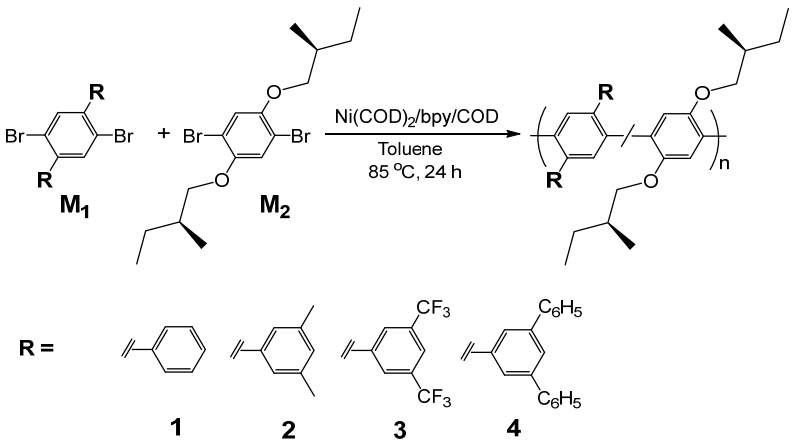

Scheme 2-2. Synthesis of poly(benzene-1,4-diyl) derivatives composed of achiral and chiral monomeric units by Yamamoto coupling in toluene.

In all the random copolymerizations of **1**-**3** with **5**, the monomers were consumed at high conversions, indicating monomers **1**-**3** were reactive enough in spite of their bulky structures. In the random copolymerization of **4** with **5**, the conversion of **4** was only 43%, suggesting that the highest bulkiness of **4** reduced its polymerization activity due to steric hindrance. Also, in the random copolymerization of **1**-**4** with **5**, the ratios of **5**-based monomeric units were higher than those of **1**-**4**-based monomeric units. This observation may be explained also by the bulkiness of **1**-**4.**

As an example, the synthetic procedure for poly(**1**-*ran*-**5**) is described. A solution of 1,5-cyclooctadiene (0.3 mmol, 31.8 mg), 2,2'-bipyridine (0.3 mmol, 45.9 mg) and $Ni(COD)_2$ (0.3 mmol, 80.5 mg) in distilled toluene (1.5 mL) was placed in a dried 10-mL flask equipped with a three-way stopcock under N_2. The mixture was heated to 85 °C for 30 min, leading to a deep purple solution. 1,4-Dibromo-2,5-diphenybenzene (0.05 mmol, 19.0 mg) and 1,4-dibromo-2,5-bis((*S*)-2-methylbutoxy)benzene (0.05 mmol, 20.0 mg) dissolved in distilled toluene (1 mL) was introduced into the

Ni-species-containing, deep purple solution with stirring. The polymerization reaction was carried out at 85 ºC for 24 h. Crude products were washed twice with methanol (50 mL) and then twice with aq. EDTA (pH= 5 and 9, 50 mL) in this order and were collected with a centrifuge. The washed material was washed twice with THF (50mL) and collected with a centrifuge, resulting in THF-insoluble part (yield 7.3 mg, 15 %) and THF-soluble part (yield 7.0 mg, 14 %, M_n 4550, M_w/M_n 4.32 (SEC using polystyrene standard)). THF-soluble polymer was further purified by preparative SEC and by washing with $CHCl_3$-MeOH (9/1 (v/v)): ^{1}H NMR (400 MHz, $CDCl_3$, r.t.) δ/ppm: 7.63-6.55, 3.76-3.21, 1.86-0.81. FT-IR (KBr) υ/cm^{-1}: 2959, 2920, 2870, 1462, 1380, 1277, 1260, 1201, 898, 862, 800, 766, 699. The conditions and results of polymerization are summarized in Table 2-1.

Table 2-1. Random copolymerization of achiral **1-4** (M_1) with chiral **5** (M_2) by Yamamoto coupling in toluene at 85ºC for 24 h[a]

Run	M_1	Conv.[b] (%)		MeOH-insoluble product				
				THF-insol.	THF-sol.[c]			
		M_1	M_2	Yield (%)	Yield (%)	M_n[c,d]	M_w/M_n[c,d]	$[M_1]/[M_2]$[e]
1	**1**	>99	>99	15	14	10940	3.60	41/59
2	**2**	>99	>99	31	65	8970	2.67	27/73
3[f]	**3**	>99	>99	17	49	27640	1.86	29/71
4	**4**	43	>99	4	43	5890	2.27	36/64

[a]M_1 0.05 mmol, M_2 0.05 mmol, $Ni(COD)_2$ 0.30 mmol, bpy 0.30 mmol, COD 0.30 mmol, toluene 3 mL. [b]Determined by ^{1}H NMR analysis of reaction mixture. [c]Determined by SEC using polystyrene standard. [d]Purified by preparative SEC and washed with $CHCl_3$-MeOH (1/9, v/v)) to remove a small amount of impurities. [e]Determined by ^{1}H NMR spectra of the polymers. [f]A lower-molar-mass fraction was obtained from the THF-soluble part by preparative SEC (M_n 9400, M_w/M_n 1.37) in order to study molar mass effects on chiroptical properties.

2.4 Chemical Structure of Random Copolymers

Chemical structure of random copolymers was identified by IR and NMR spectra. In FT-IR spectra (Figure 2-1, 2-2, 2-3, 2-4), the polymers indicated much broader signals compared with those monomers. NMR spectroscopy measurement of the polymers were carried out in $CDCl_3$. (Figure 2-5, 2-6, 2-7, 2-8).

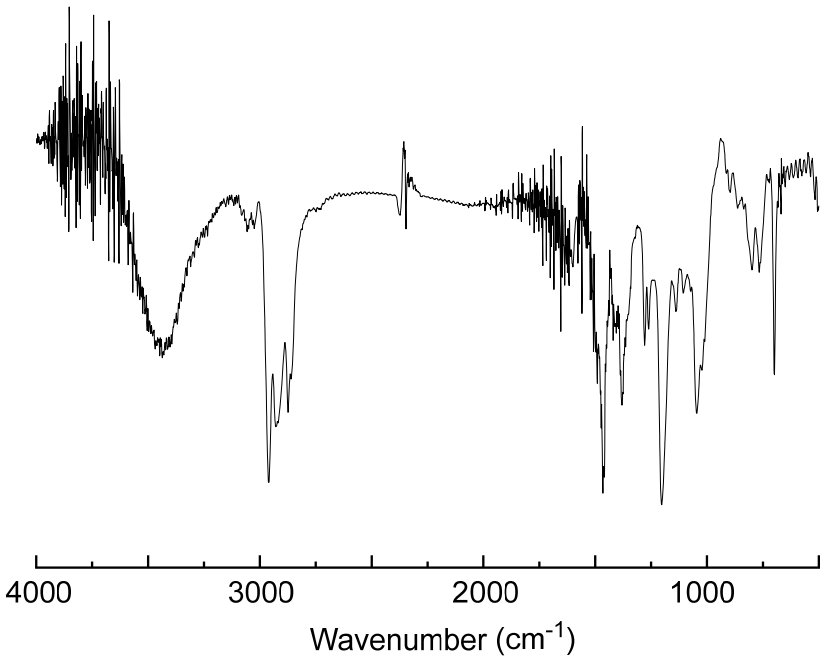

Figure 2-1. IR spectrum of poly(1-ran-5).

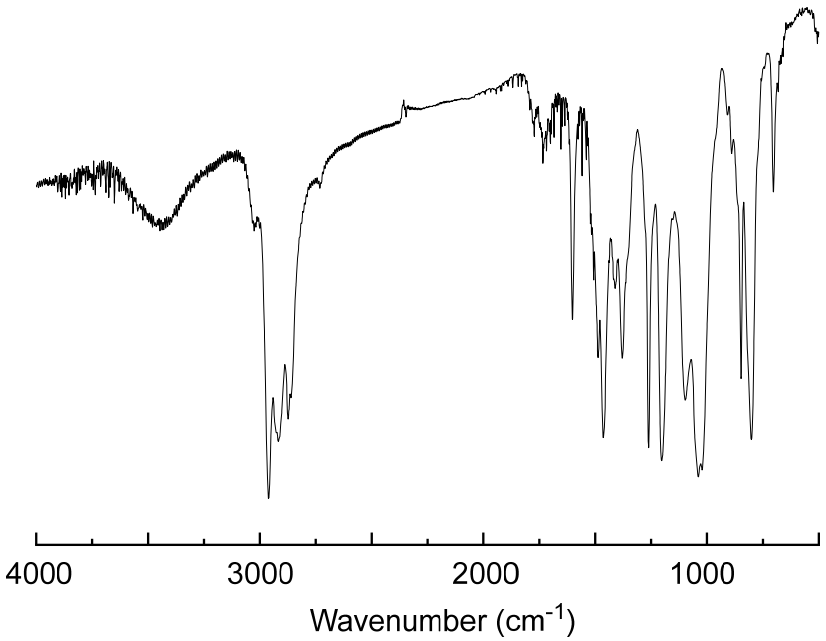

Figure 2-2. IR spectrum of poly(2-ran-5).

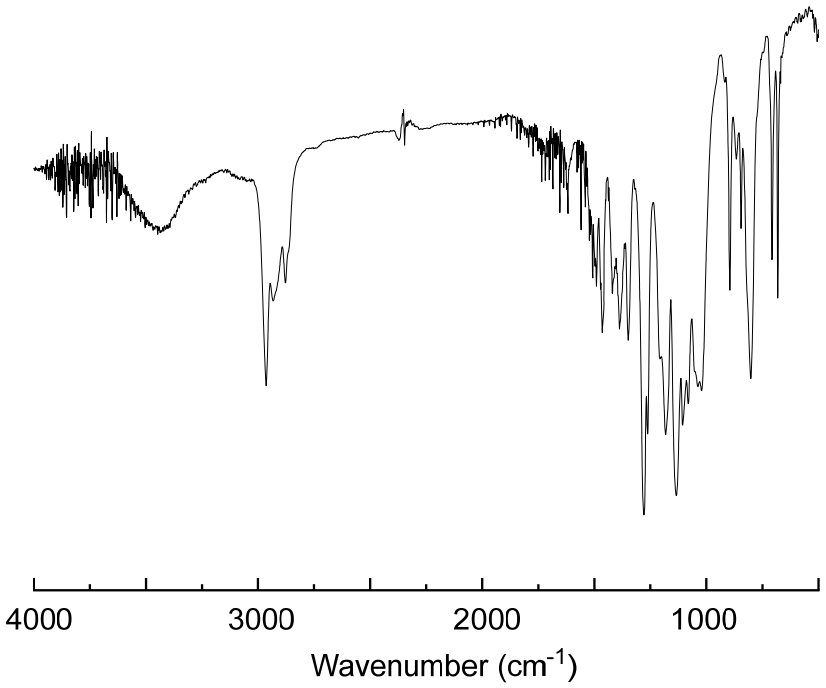

Figure 2-3. IR spectrum of poly(3-ran-5).

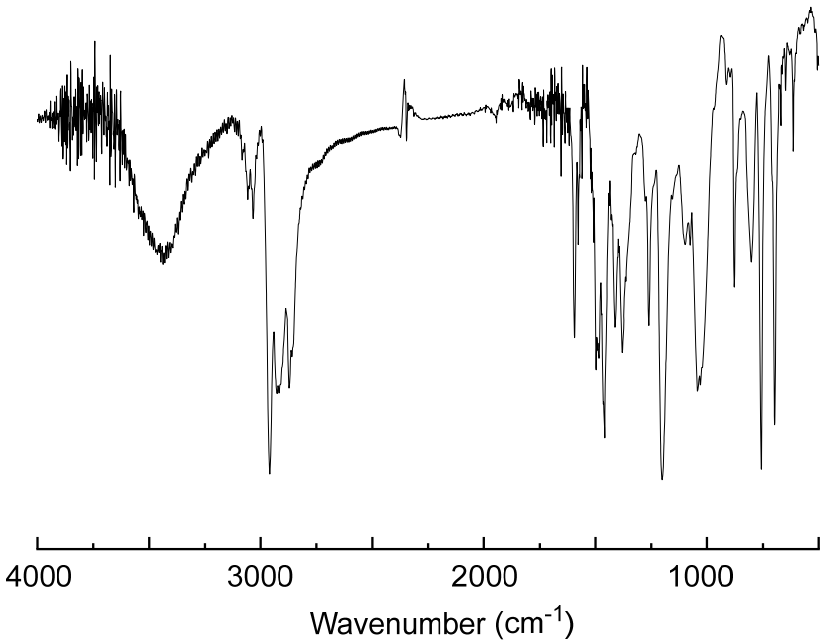

Figure 2-4. IR spectrum of poly(4-ran-5).

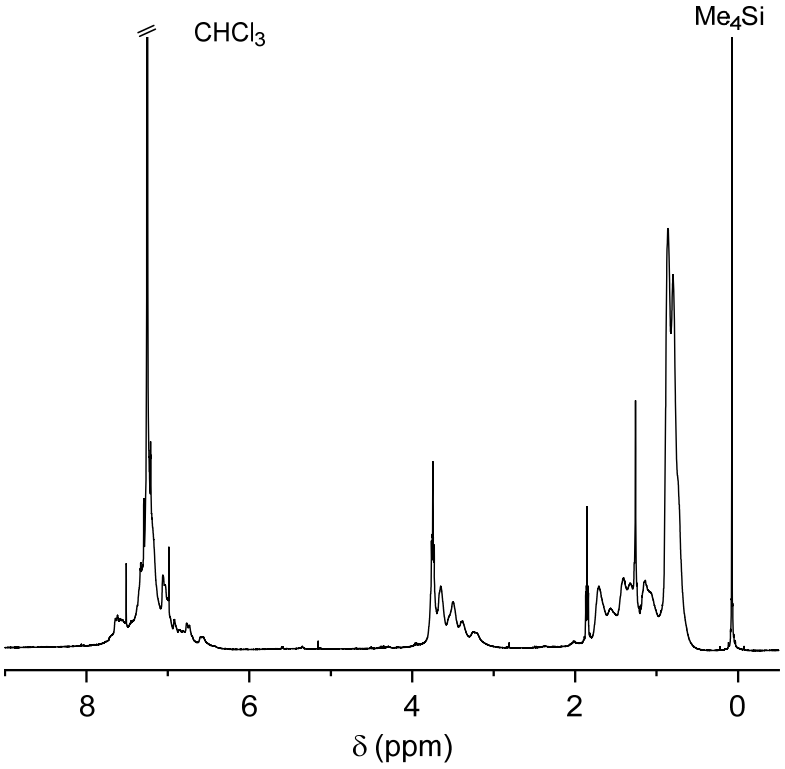

Figure 2-5. ^{1}H NMR spectrum of poly(**1**-*ran*-**5**). [400 MHz, $CDCl_3$, r.t.].

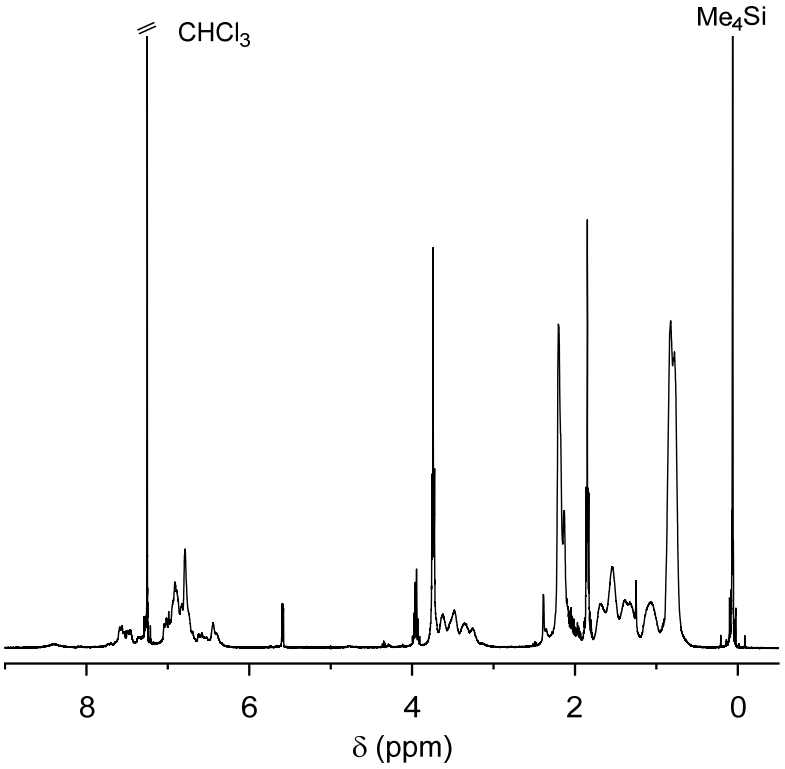

Figure 2-6. ^{1}H NMR spectrum of poly(2-ran-5). [400 MHz, $CDCl_3$, r.t.].

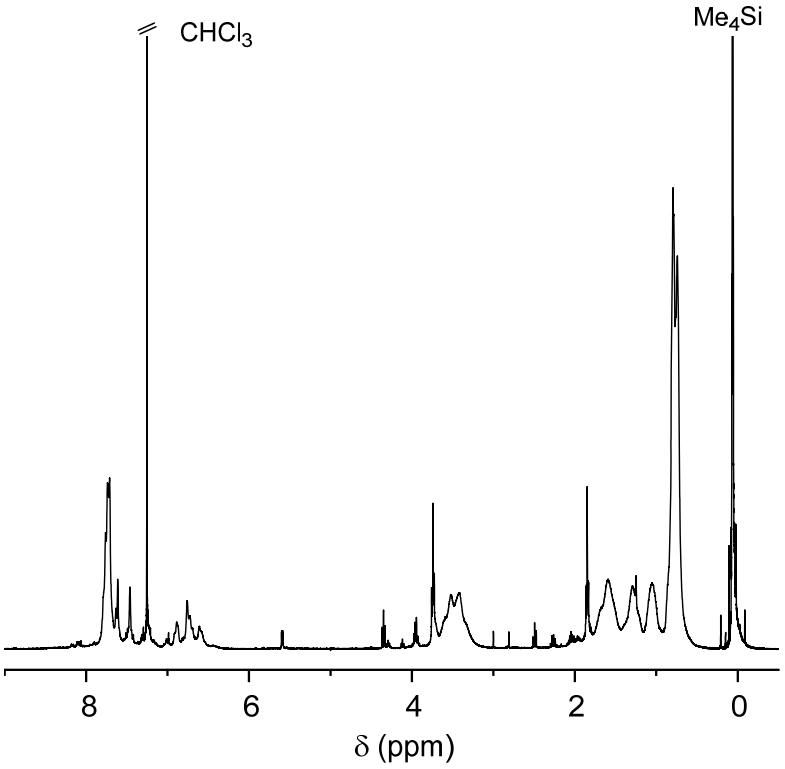

Figure 2-7. ^{1}H NMR spectrum of poly(**3**-*ran*-**5**). [400 MHz, $CDCl_3$, r.t.].

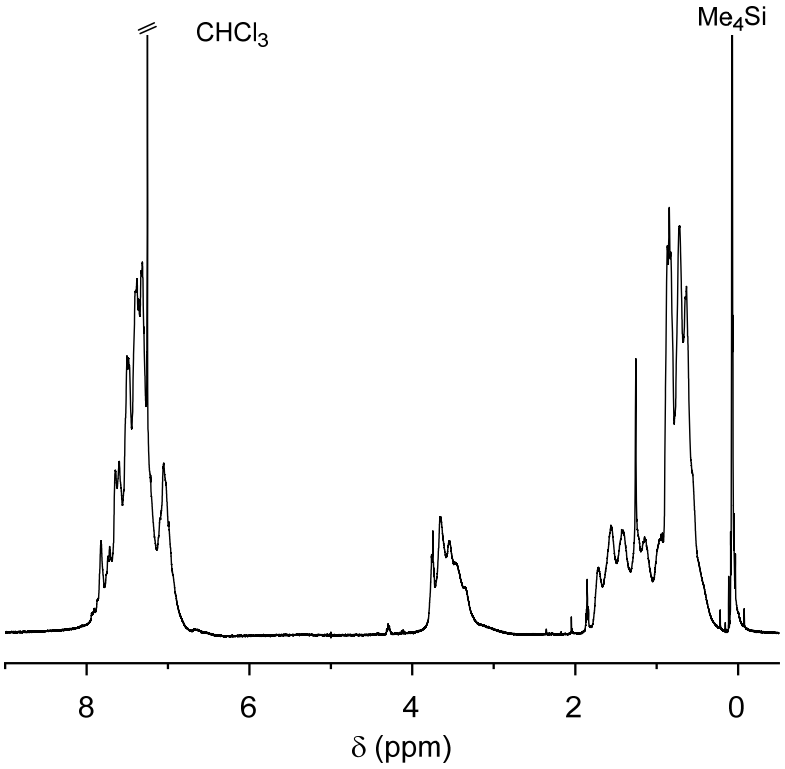

Figure 2-8. ^{1}H NMR spectrum of poly(**4**-*ran*-**5**). [400 MHz, $CDCl_3$, r.t.].

2.5 Alternating Copolymers Synthesis

The alternating copolymers were prepared by Suzuki reaction (Suzuki-Miyaura coupling) polymerization using Pd species of achiral monomer, *i.e.*, 1,4-dibromo-2,5-diphenylbenzene (**1**), 1,4-dibromo-2,5-bis(3,5-dimethylphenyl)benzene (**2**),[31] 1,4-dibromo-2,5-bis(3,5-bis(trifluoromethyl)phenyl)benzene (**3**), and 1,4-dibromo-2,5-bis(3,5-diphenylphenyl)benzene (**4**) with chiral 1,4-bis(dihydroxyboranyl)-2,5-bis((*S*)-2-methylbutoxy)benzene (**6**)[15] in 1,2-dimethoxyethane (DME) at [**1**-**4**]/[**6**] = 1/1 in feed (Scheme 2-3).

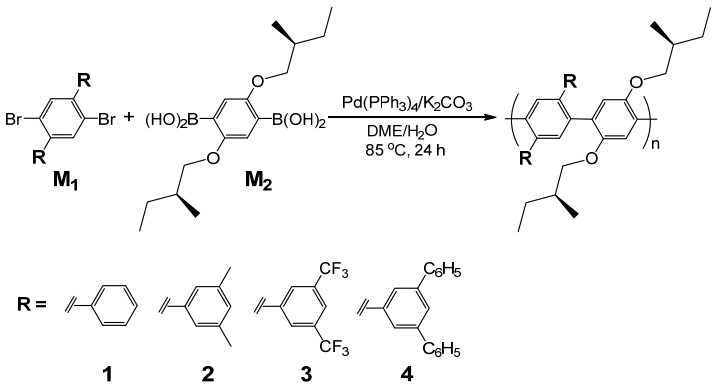

Scheme 2-3. Synthesis of poly(benzene-1,4-diyl) derivatives composed of achiral and chiral monomeric units by Suzuki-Miyaura cross coupling.

The alternating copolymers had lower molar masses compared with the random copolymers and were all soluble in THF. The THF-soluble parts were further purified by preparative SEC and by washing with a $CHCl_3$-MeOH (1/9 (v/v)) mixture. In the alternating copolymerizations where the bulky achiral monomers have to be incorporated into the chain at every two steps of reaction, bulkiness effects reducing polymerization activity seem to be more significant than in the random copolymerizations.

Also, it should be pointed out that molar masses of the random and alternating copolymers made using **3** tended to be higher than those of the others. The presence of $-CF_3$ groups in **3** may have reaction-facilitating effects apart from simple bulkiness.

Alternating copolymers were synthesized according to the Suzuki-Miyaura cross coupling using $Pd(PPh_3)_4$ as catalyst. As an example, the synthetic procedure for

poly(**1**-*alt*-**6**) is described. To a solution of 1,4-dibromo-2,5-diphenyldibromobenzene (0.15 mol, 57.4 mg) and 1,4-dihyroxyboranyl-2,5-bis((*S*)-2-methylbutoxy)benzene (0.15 mmol, 50.0 mg) in a degassed DME (0.8 mL) was added a degassed aqueous solution of K_2CO_3 (2 M, 0.3 mL). $Pd(PPh_3)_4$ (10 mol%, 17.0 mg) was then introduced to the system, and the reaction mixture was stirred under N_2 at 85 °C for 24 h. The reaction mixture was quenched by the addition of aq. HCl solution (2 N, 0.6 mL). Crude products were washed twice with H_2O (50 mL) and twice with methanol (50 mL×2 times) in this order and collected with a centrifuge. The obtained polymer was further purified by preparative SEC and by washing with $CHCl_3$-MeOH (9/1 (v/v)) (yield 20.8 mg, 29 %, M_n 3210, M_w/M_n 1.60 (SEC using polystyrene standard): ^{1}H NMR (400 MHz, $CDCl_3$, r.t.) δ/ppm: 7.75-6.42, 3.75-3.16, 1.86-0.72. FT-IR (KBr) υ/cm^{-1}: 3054, 3024, 2960, 2930, 2877, 1599, 1499, 1466, 1414, 1384, 1203, 1073, 1039, 903, 869, 795, 766, 699. The conditions and results of polymerization are shown in Table 2-2.

Table 2-2. Alternating copolymerization of achiral **1**-**4** (M_1) with chiral **6** (M_2) by Suzuki-Miyaura coupling in DME at 85°C for 24 h[a]

Run	M_1	Conv.[b] (%)		MeOH-insoluble product				
				THF-insol.	THF-sol.[c]			
		M_1	M_2	Yield (%)	Yield (%)	M_n [c,d]	M_w/M_n [c,d]	$[M_1]/[M_2]$[e]
1	**1**	>99	>99	0	29	3210	1.60	41/59
2	**2**	>99	>99	0	52	3470	1.64	27/73
3	**3**	>99	>99	0	57	7030	1.70	29/71
4	**4**	>99	>99	0	51	3820	1.92	36/64

[a]M_1 0.15 mmol, M_2 0.15 mmol, $Pd(PPh_3)_4$ 0.01 mmol, K_2CO_3 0.96 mmol, DME 0.8 mL, H_2O 0.3 mL. [b]Determined by ^{1}H NMR analysis of reaction mixture. [c]Determined by SEC using polystyrene standard. [d]Further washed with $CHCl_3$-MeOH (1/9, v/v) to remove a small amount of impurities. [e]Determined by ^{1}H NMR spectra of the polymers.

2.6 Chemical Structure of Alternating Copolymers

Chemical structure of random copolymers was identified by IR and NMR spectra. In FT-IR spectra (Figure 2-9, 2-10, 2-11, 2-12), the polymers indicated much broader signals compared with those monomers. NMR spectroscopy measurement of the polymers were carried out in $CDCl_3$. (Figure 2-13, 2-14, 2-15, 2-16).

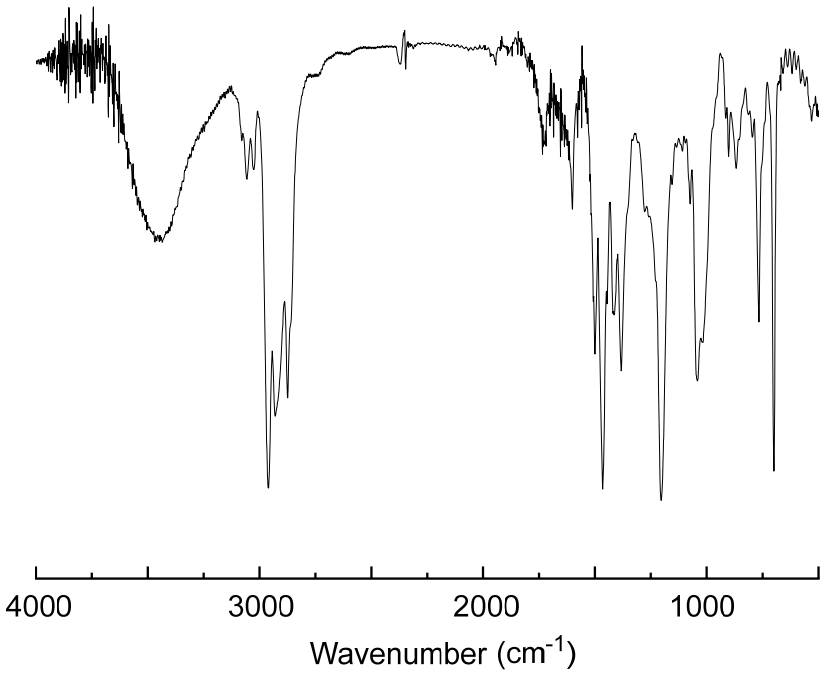

Figure 2-9. IR spectrum of poly(1-alt-6).

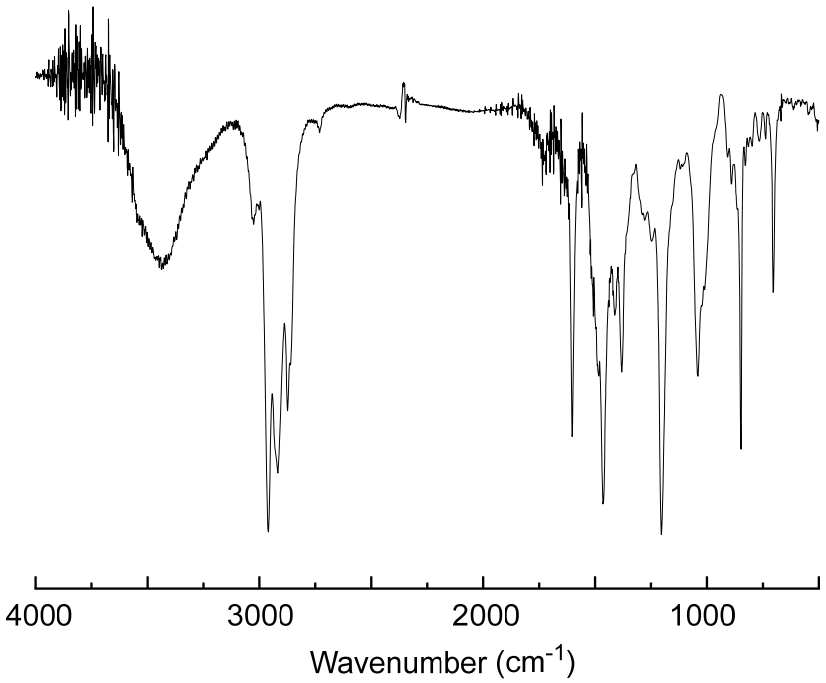

Figure 2-10. IR spectrum of poly(2-alt-6).

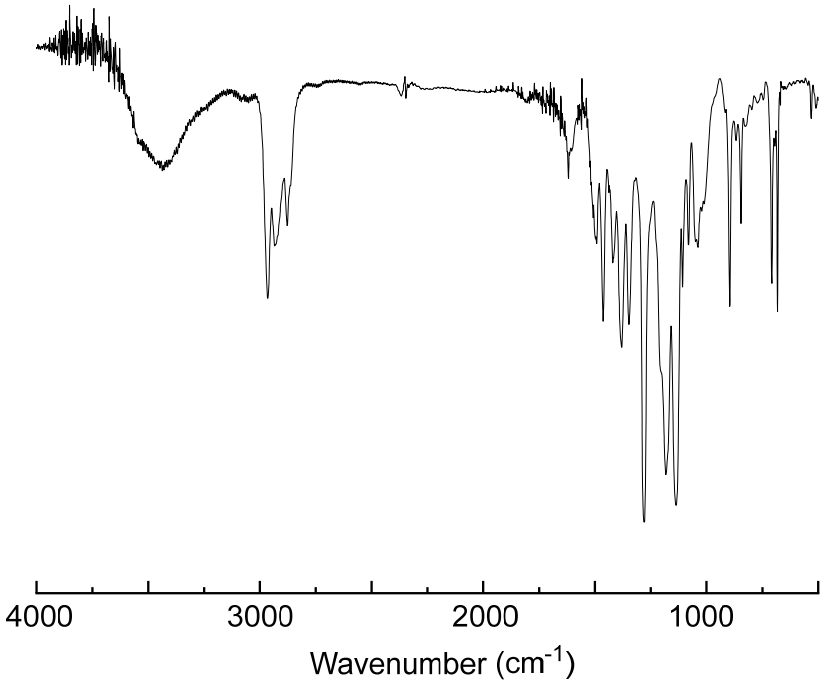

Figure 2-11. IR spectrum of poly(3-alt-6).

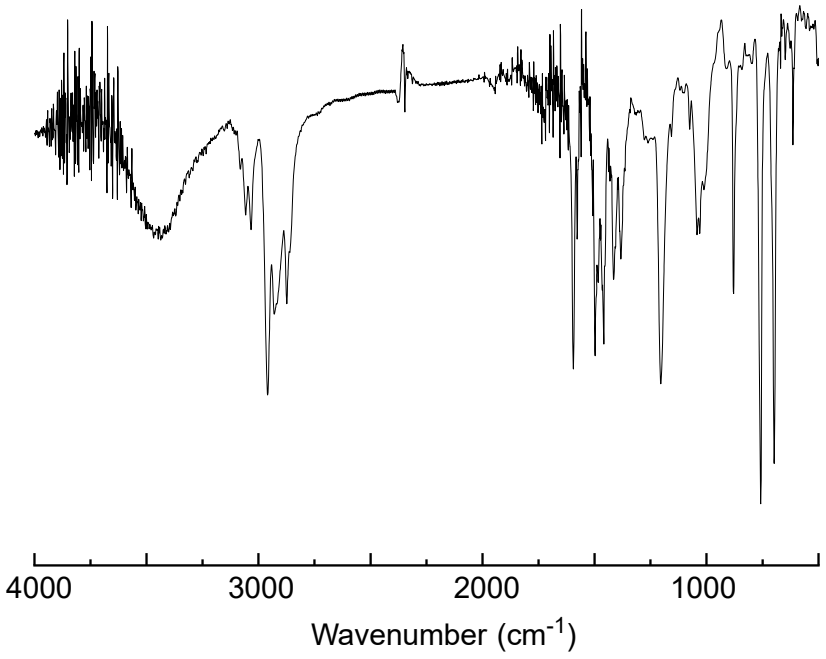

Figure 2-12. IR spectrum of poly(4-alt-6).

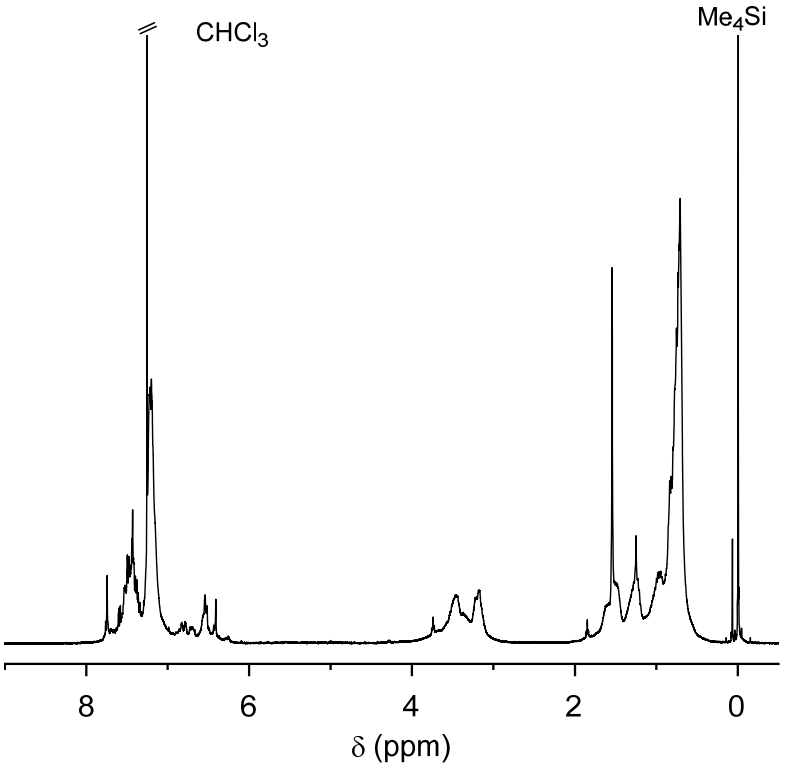

Figure 2-13. ^{1}H NMR spectrum of poly(**1**-*alt*-**6**). [400 MHz, $CDCl_3$, r.t.].

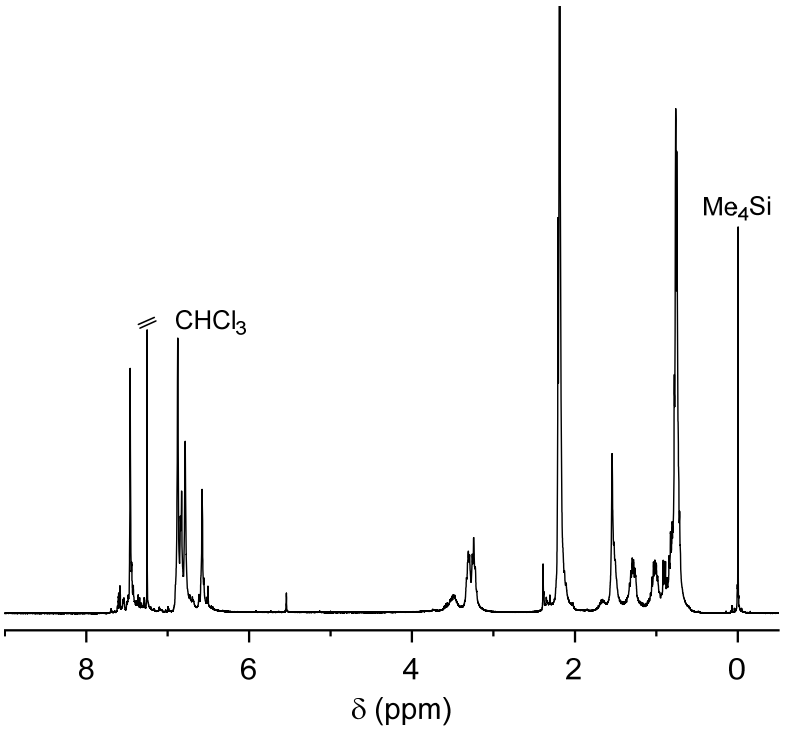

Figure 2-14. ^{1}H NMR spectrum of poly(**2**-*alt*-**6**). [400 MHz, $CDCl_3$, r.t.].

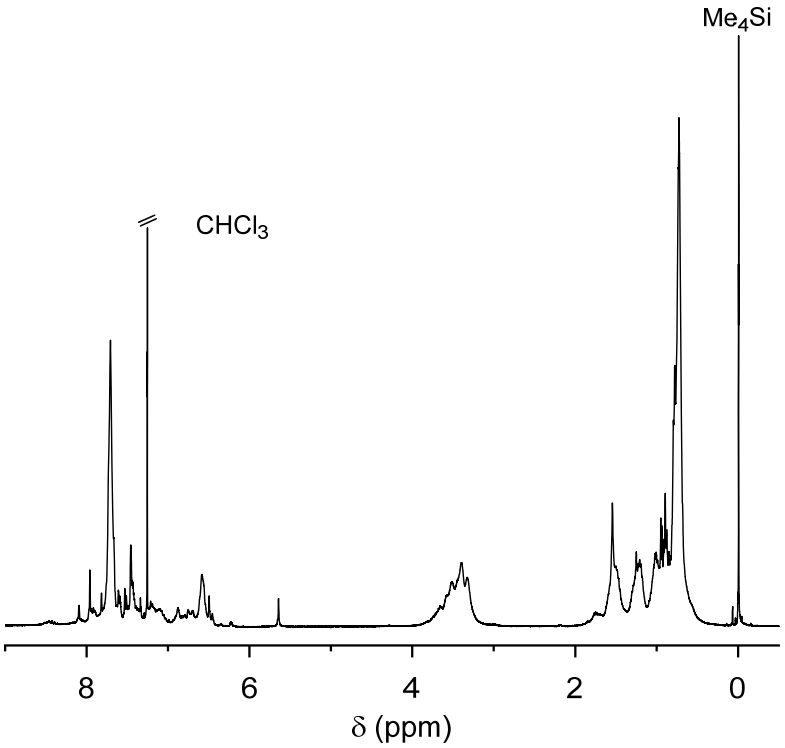

Figure 2-15. ^{1}H NMR spectrum of poly(**3**-*alt*-**6**). [400 MHz, $CDCl_3$, r.t.].

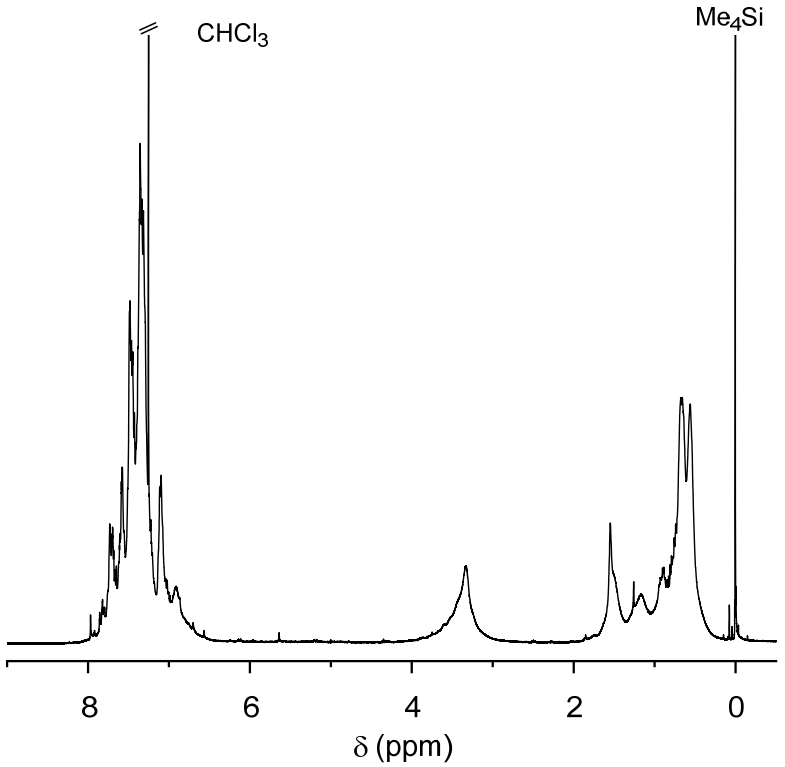

Figure 2-16. ^{1}H NMR spectrum of poly(**4**-*alt*-**6**). [400 MHz, $CDCl_3$, r.t.].

2.7 Conformation of the Polymers

Prior to the analyses of chiroptical properties and chiral recognition ability of the copolymers, thermal analysis and X-ray diffraction (XRD) experiments were conducted. The copolymers showed the onset temperature of major thermal decomposition in the range of 300-350 °C. Figure 2-17 shows differential scanning calorimetry (DSC) profiles of copolymers obtained in the second heating scans. None of the eight copolymers showed transitions that may be connected with liquid crystallinity while poly(benzene-1,4-diyl) is reported to have a stiff conformation.[32,33] All the copolymers showed glass transition, and Tg's were in the range of 2-24 °C, indicating that the properties observed at around room temperature reflect soft and amorphous solid-state structure of the polymers.

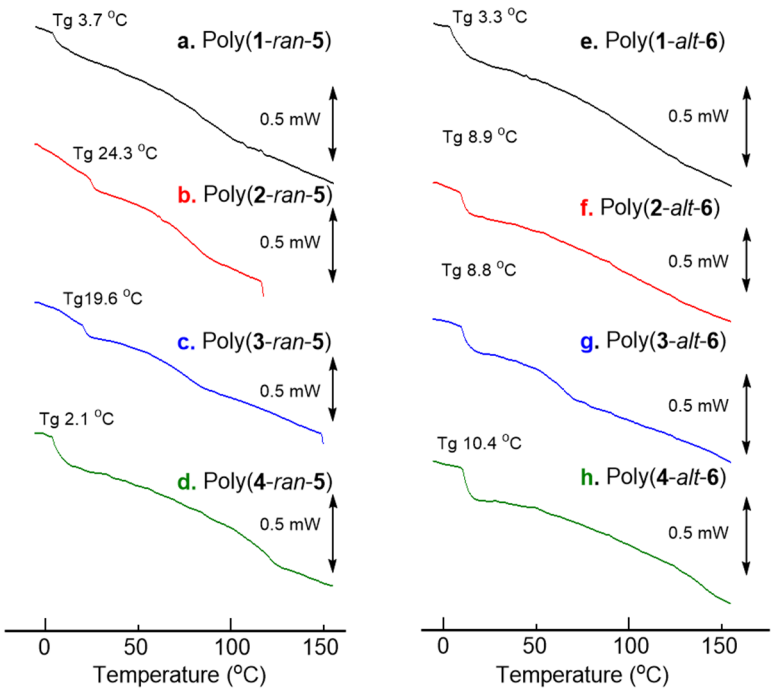

Figure 2-17. DSC profiles of the random (**a**-**d**) and alternating (**e**-**h**) copolymers obtained in second heating scans at 10 °C min^{-1} in the temperature range of -25 °C to 200 °C.

XRD profiles of the copolymers except for poly(**2**-*alt*-**6**) showed broad patterns with broad signals at around 2θ = 20 deg and 10-12 deg, suggesting that the samples are rather amorphous, which is in line with the conclusions from the thermal analyses

(Figure 2-18). Poly(**2**-*alt*-**6**) indicated several sharper signals than those of the other copolymers, implying that this copolymer may have crystalline domains in which chains may be aligned. However, as mentioned above, this polymer did not show any clear melting points in the DSC analysis, indicating that the proposed ordered domains may be only partial from the view of thermal transitions.

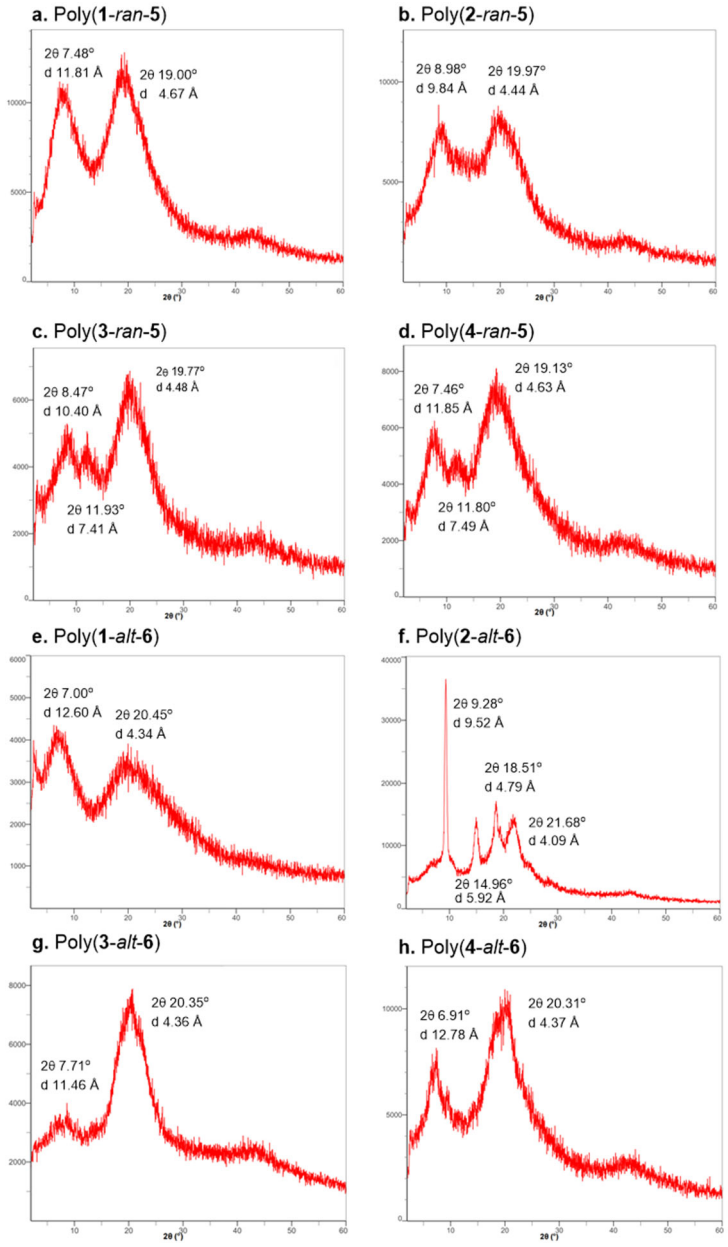

Figure 2-18. XRD profiles of the random (a-d) and alternating (e-h) copolymers.

The chirality of the obtained polymers was assessed by circular dichroism (CD) spectra (Figure 2-19 A-D, Figure 2-20 A-D). In THF solution, both the random and

alternating copolymers showed overall rather low intensities of CD responses where there was no clear tendency of increase or decrease in intensity according to bulkiness of the achiral monomeric units (Figure 3 A-1, A-2, B-1, B-2, C-1, C-2, D-1, D-2, Figure 4 A-1, A-2, B-1, B-2, C-1, C-2, D-1, D-2). Bulkiness of the four types of achiral side-chain groups, i.e., phenyl, 2,5-dimethylphenyl, 2,5-bis(trifluoromethyl)phenyl, and 2,5-diphenylphenyl, may not be high enough to make the polymers assume a stable helical conformation in solution. On the other hand, the polymers except for poly(**1**-*ran*-**5**) and poly(**1**-*alt*-**6**) showed CD spectra with slightly to largely enhanced intensities in suspension in $CHCl_3$-MeOH (1/9 (v/v)) with respect to in solution (Figure 3 B-3, B-4, C-3, C-4, D-3, D-4, Figure 4 B-3, B-4, C-3, C-4, D-3, D-4). In addition, spectral patterns changed in these cases from monotonous ones to split ones. There results suggest that chain aggregation in the solid state increased the bias of right- or left-handed enantiomeric structure of chiral conformation such as helix and also altered the conformations to ones showing higher optical anisotropy probably due to greater twist angles around the single bonds connecting the benzene rings (chirality amplification). The little effects observed for poly(**1**-*ran*-**5**) and poly(**1**-*alt*-**6**) imply that bulkiness effects of the substituents, $-CH_3$, $-CF_3$, and $-C_6H_5$, on the side-chain benzene rings of monomeric units derived from **2**-**4** play an important role in creating the chiral conformations showing remarkable CD spectra in the solid state. This conclusion was further supported by the CD spectra of film samples prepared by casting a THF-solution onto a quartz glass and thermally annealed at 100ºC for 2h in order to facilitate aggregates formation. Also in film, the copolymers except for poly(**1**-*ran*-**5**) and poly(**1**-*alt*-**6**) showed remarkably increased CD intensities and clear splitting patterns (Figure 2-19 B-5, B-6, C-5, C-6, D-5, D-6, Figure 2-20 B-5, B-6, C-5, C-6, D-5, D-6).

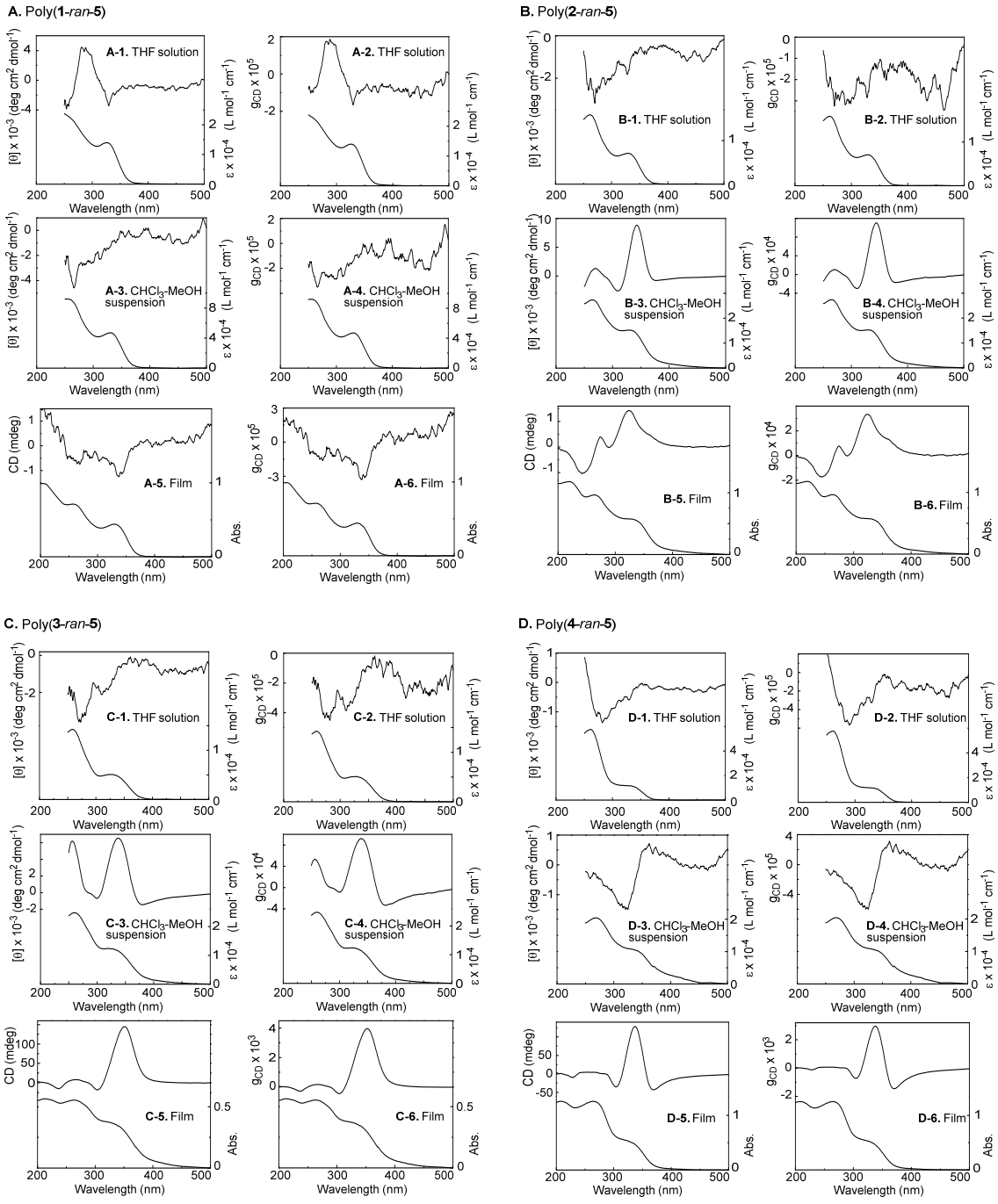

Figure 2-19. CD-UV and g_{CD}-UV spectra of the random copolymers in THF solution, in $CHCl_3$-MeOH (1/9 (v/v)) suspension, and in film after annealing at 100 ºC for 2h. [Concentrations in THF solution and in $CHCl_3$-MeOH (1/9 (v/v)) suspension (per residue) = 4.2 x 10^{-5} M (Poly(**1**-*ran*-**5**)), 6.0 x 10^{-5} M (Poly(**2**-*ran*-**5**)), 6.5 x 10^{-5} M (Poly(**3**-*ran*-**5**)), and 1.8 x 10^{-5} M (Poly(**4**-*ran*-**5**)); cell path = 10 mm].

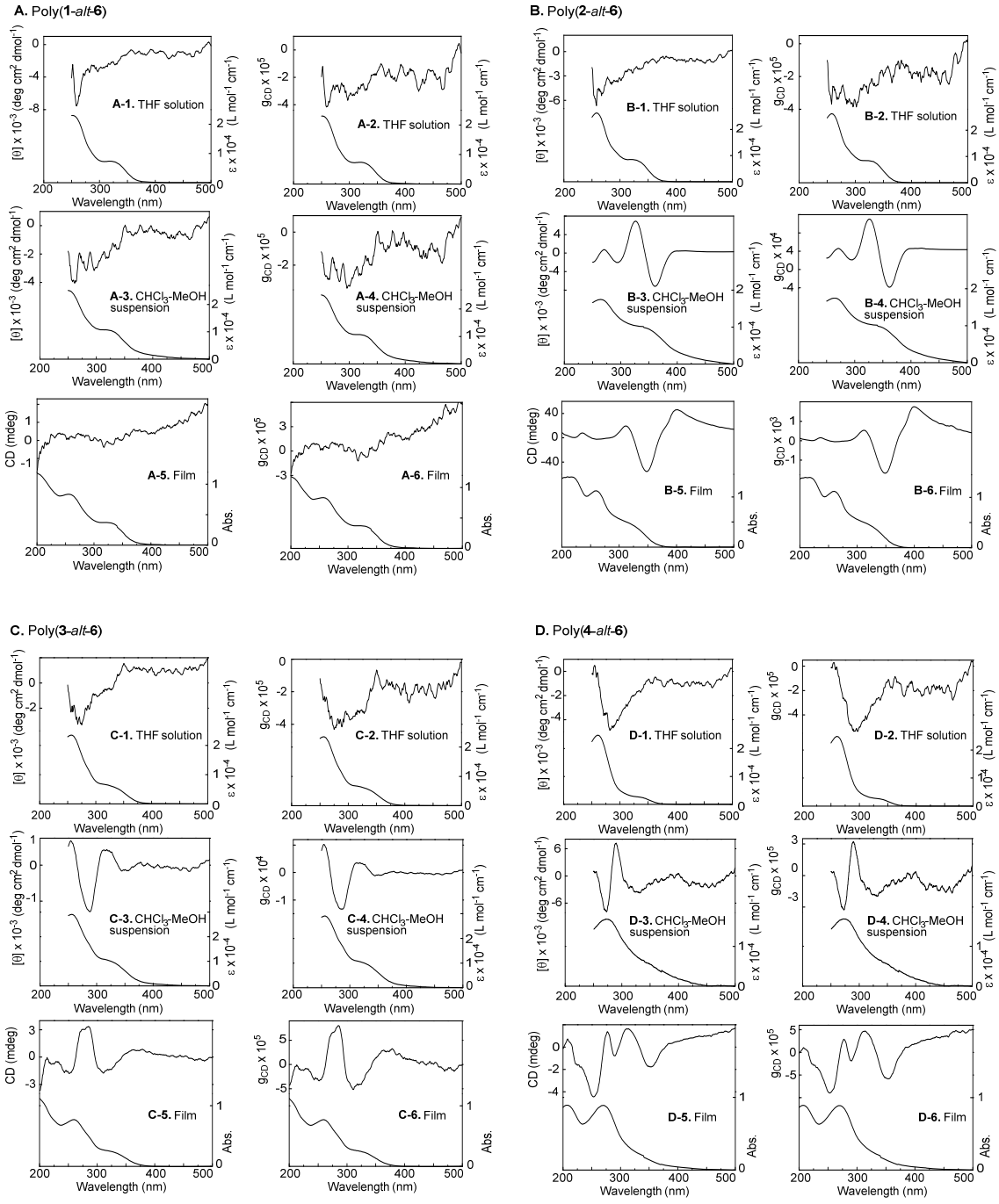

Figure 2-20. CD-UV and g_{CD}-UV spectra of the alternating copolymers in THF solution, in $CHCl_3$-MeOH (1/9 (v/v)) suspension, and in film after annealing at 100 ºC for 2h. [Concentrations in THF solution and in $CHCl_3$-MeOH (1/9 (v/v)) suspension (per residue) = 4.1 x 10^{-5} M (Poly(**1**-*alt*-**6**)), 4.2 x 10^{-5} M (Poly(**2**-*alt*-**6**)), 4.4 x 10^{-5} M (Poly(**3**-*alt*-**6**)), and 4.2 x 10^{-5} M (Poly(**4**-*alt*-**6**)); cell path = 10 mm].

From these results, it may be concluded that side-chain bulkiness effects of the achiral monomeric units indeed play a role in creating a chiral conformation such as helix with high anisotropy *in the solid state through inter-chain interactions but not in solution*. Side-chain phenyl group without substituents for both the random and alternating sequences appeared not bulky enough to induce a chiral conformation with large bias on one hand even in the solid state. Also, it is notable that the spectral patterns in the $CHCl_3$-MeOH suspension samples and the film samples are not necessarily the same, implying that polymer conformations in the solid state may reflect the sample preparation procedure.

The effects of side-chain structure of the achiral monomeric units and effects of random and alternating sequences may be overviewed as follows from a view of the anisotropy factor, $g_{CD} = 2(\varepsilon_L - \varepsilon_R)/(\varepsilon_L + \varepsilon_R)$ where ε_L and ε_R are molar absorptivities toward L- and R-CPL, respectively. The maximum g_{CD} (absolute values) of the random copolymers was in the order of 3,5-dimethylphenyl (max. g_{CD} $+1.2 \times 10^{-3}$ at 340 nm) $\simeq$ 3,5-bis(trifluoromethyl)phenyl (max. g_{CD} $+0.9 \times 10^{-3}$ at 350 nm) > 3,5-diphenylphenyl (max. g_{CD} -6×10^{-5} at 320 nm) > phenyl (max. g_{CD} -3×10^{-5} at 300 nm) in $CHCl_3$-MeOH (1/9 (v/v)) suspension and in the order of 3,5-bis(trifluoro)methylphenyl (max. g_{CD} $+4 \times 10^{-3}$ at 350 nm) $\simeq$ 3,5-diphenylpheny (max. g_{CD} $+3 \times 10^{-3}$ at 335 nm) > 3,5-dimethylphenyl (max. g_{CD} $+3 \times 10^{-4}$ at 320 nm) > phenyl (max. g_{CD} -3×10^{-5} at 300 nm) in film. On the other hand, the maximum g_{CD} (absolute values) of the alternating copolymers was in the order of 3,5-dimethylphenyl (max. g_{CD} -6×10^{-4} at 360 nm) > 3,5-bis(trifluoromethyl)phenyl (max. g_{CD} -1×10^{-4} at 290 nm) > 3,5-diphenylpheny (max. g_{CD} -3×10^{-5} at 320 nm) $\simeq$ phenyl (max g_{CD} 3×10^{-5} at 300 nm) in $CHCl_3$-MeOH (1/9 (v/v)) suspension and in the order of 3,5-dimethylphenyl (max. g_{CD} -1.8×10^{-3} at 350 nm) > 3,5-diphenylpheny (max. g_{CD} -9×10^{-5} at 260 nm) $\simeq$ 3,5-bis(trifluoro)methylphenyl (max. g_{CD} $+8 \times 10^{-5}$ at 290 nm) > phenyl (max. $g_{CD} < 1 \times 10^{-5}$) in film. Overall, the 3,5-disubstituted phenyl groups led to greater g_{CD} values of the polymers than unsubstituted phenyl group for both the random and the alternating copolymers regardless of the state of the samples, film or suspension. The order among the three 3,5-disubstituted phenyl

groups seems not to obey the order of seeming bulkiness as single species which is 3,5-diphenylphenyl > 3,5-dimethylphenyl ≃ 3,5-bis(trifluoro)methylphenyl.

In this regard, it is interesting that poly(**2**-*ran*-**5**) having 3,5-dimethylphenyl showed the greatest g_{CD} value in suspension and that poly(**2**-*alt*-**6**) having 3,5-dimethylphenyl as side-chain group showed the greatest g_{CD} values both in suspension and in film among the alternating copolymers. In the solid state where inter-chain interactions would significantly affect polymer conformation, the size and shape of 3,5-dimethylphenyl may be suited to induce a helix showing high optical anisotropy.

Between the random and alternating copolymers with the same side-chain group, the random copolymers tended to show higher g_{CD} values even considering the random copolymers have higher amounts of the chiral units. This may mean that diad or triad sequence composed of neighboring bulky, achiral units which does not exist in the alternating copolymers may be important in creating greater anisotropy of the chain.

In addition, in order to obtain information on molar-mass effects on chiroptical properties, CD spectra were compared between the poly(**3**-*ran*-**5**) sample from run 3 in Table 2-1 (M_n 27640) and a sample from the same polymer with lower molar mass (M_n 9400, footnote f to Table 2-1) obtained from the former sample by preparative SEC fractionation. The two samples showed rather similar CD spectral shapes and intensities in solution, in suspension and in film, suggesting that molar-mass effects may not seriously affect chiral conformation of the polymer in the ground state (Figure 2-21).

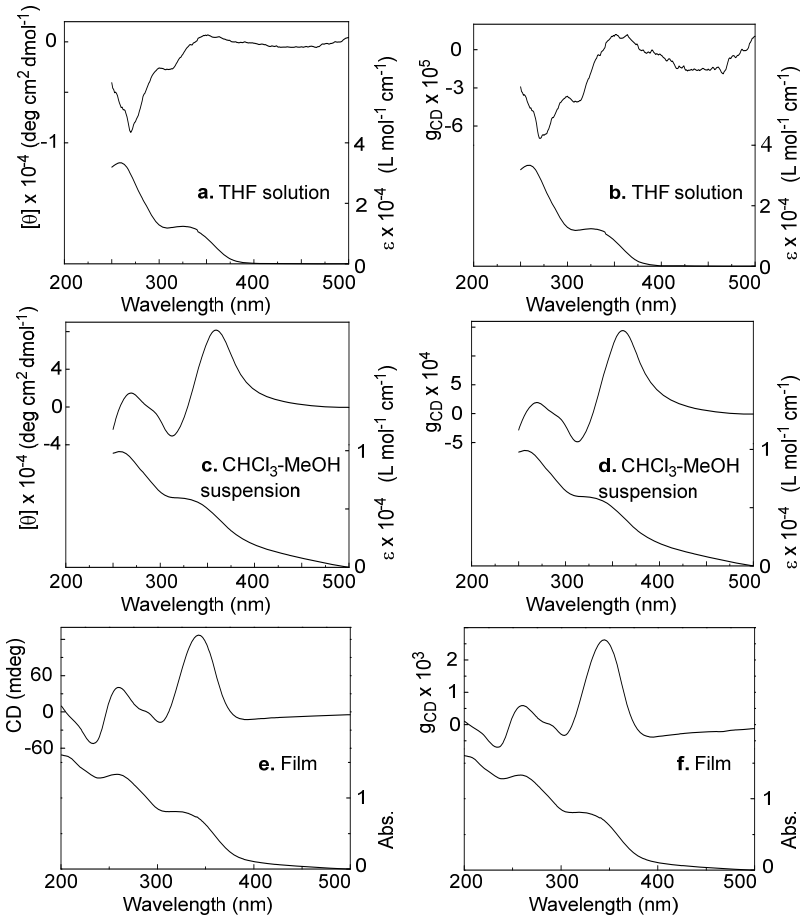

Figure 2-21. CD-UV and g_{CD}-UV spectra of poly(**3**-*ran*-**5**) (M_n 9400) in THF solution, in $CHCl_3$-MeOH (1/9 (v/v)) suspension, and in film after annealing at 100 °C for 2h. [Concentration in THF solution and in $CHCl_3$-MeOH (1/9 (v/v)) suspension (per residue) = 6.5 x 10^{-5} M; cell path = 10 mm].

A question about the chirality of the polymers may be whether the observed CD spectra are contributed by the main-chain helix of the poly(benzene-1,4-diyl) backbone or by the side-chain twist, axial chirality around single bonds connecting the side-chain groups and the main chain. While clear distinguishment between the two types of chirality is not simple, regarding this aspect, the intensity of the CD spectrum of poly(**2**-*alt*-**6**) was found to decrease at 60°C with respect to at ambient temperature (around 23°C) to a larger extent at a shorter-wavelength (Figure 2-22). This result may mean that a CD signal at a shorter-wavelength is contributed more by side-chain axial chirality than by main-chain helix because side-chain conformation would be more readily affected at a higher temperature. The polymers showing clear

CD bands at roughly around 320 nm or longer wavelengths may be proposed to have a preferred-handed helical conformation of the main chain as far as those studied here are concerned though accurate distinction between side-chain chirality and main-chain chirality in CD spectra would generally need very careful analyses.

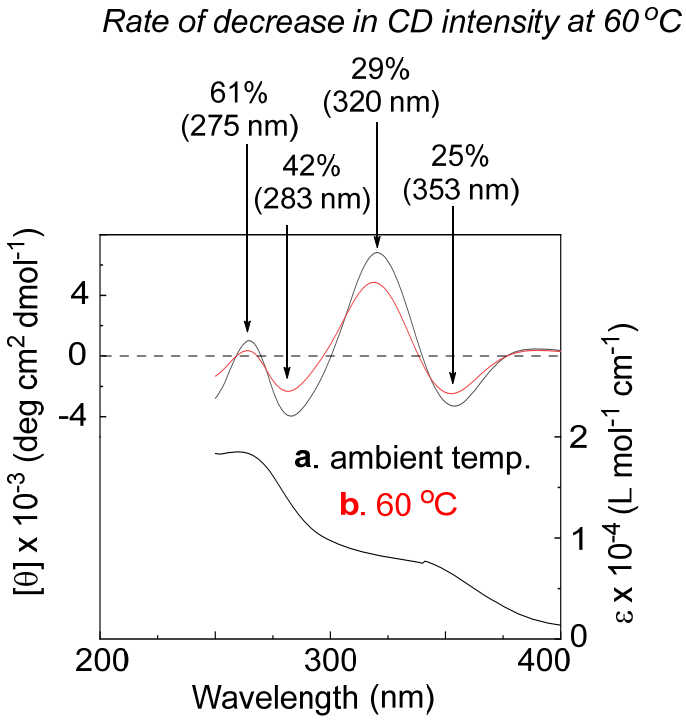

Figure 2-22. CD-UV spectra of poly(**2**-*alt*-**6**) in $CHCl_3$-MeOH (1/9 (v/v)) suspension measured at ambient temperature (around 23 °C) (a) and 60 °C (b) with rates of decrease in CD intensity at 60 °C. [Concentration (per residue) = 4.2 x 10^{-5} M; cell path = 10 mm].

As discussed so far, side-chain bulkiness remarkably affected chiroptical properties of the polymers. This point was further assessed by computational studies on single chain 12-mer models of the four alternating copolymers (Figure 2-23). Four types of models were considered for each alternating copolymer, *i.e.,* right- and left-handed helical models (Figure 2-23 I,II) and two enantiomeric zigzag twist models (Figure 2-23 III,IV). Because the polymers in this work have substituents at 2- and 5-five positions on benzene-1,4-diyl units, the zigzag twist models are asymmetric as well as the helical models. The models were optimized by molecular mechanics with COMPASS force field,[34] and total steric energies were compared (Figure 2-23 A-D).

The results indicate that left-handed helical models have smaller steric energies than the other models for poly(**2**-*alt*-**6**), poly(**3**-*alt*-**6**), and poly(**4**-*alt*-**6**) while the four models of poly(**1**-*alt*-**6**) showed rather similar energies.

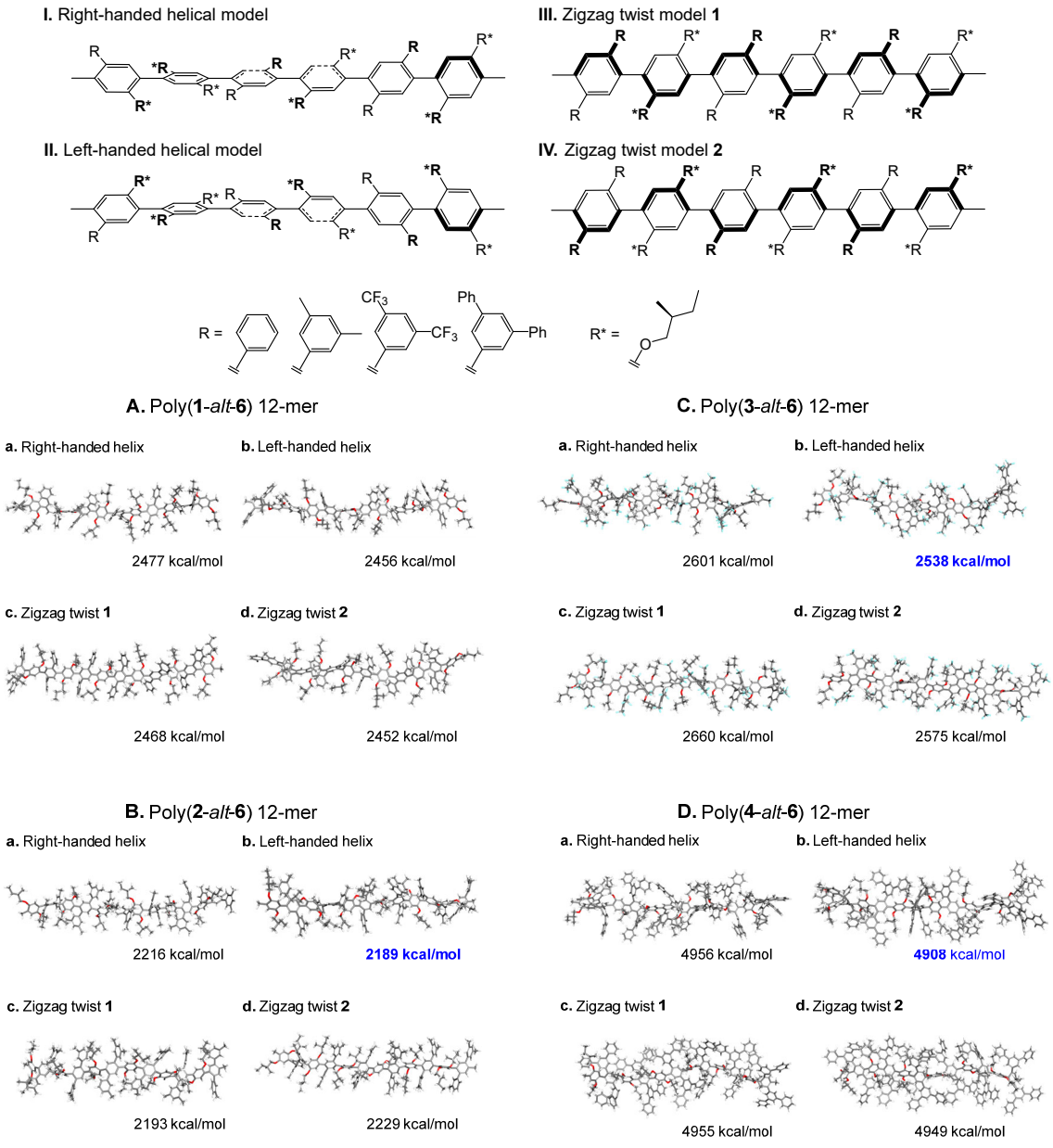

Figure 2-23. Right-handed helix (I) and left-handed helix (II) models and zigzag twist models 1 and 2 having enantiomeric conformations (III and IV) of alternating copolymer chains, and optimized conformations of 12-mer models of the alternating copolymers with total steric energies calculated by COMPASS force field (A-D).

Although the differences in steric energy among the four models are not conclusively large even for the former, three polymers with bulkier side chains, left-handed helix may be regarded as a preferred conformation for them where the other conformations may co-exist. Side-chain bulkiness is thus found significant through single-chain computation. In addition, the left-handed models of poly(**1**-*alt*-**6**) and poly(**2**-*alt*-**6**) maintained their helicity through molecular dynamics (MD) simulations, implying that their handedness is stable once it is formed through polymerization (Figure 2-24).

a. Left-handed helical 12-mer of poly(**1**-*alt*-**6**)

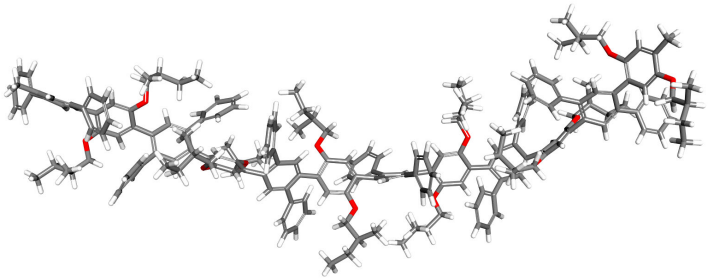

b. Left-handed helical 12-mer of poly(**2**-*alt*-**6**)

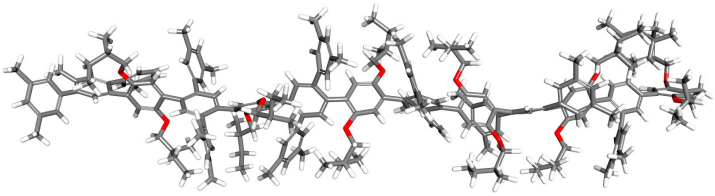

Figure 2-24. Left-handed helical 12-mer models of poly(**1**-*alt*-**6**) (a) and poly(**2**-*alt*-**6**) (b) obtained through MD simulations using COMPASS force field (NVT, 1 nsec, 300 K) .

However, it should be noted that the four conformers of 6-mer models of the four alternating copolymers had steric energies which are much closer to each other compared with the 12-mer models (Figure 2-25). This suggests that side chain bulkiness may take greater effect when side-chain groups are more congested in a longer chain with less conformational freedom. The chirality amplification observed in the solid state may support this conclusion. In the solid state where chains are densely packed and confined in small space, side-chain bulkiness effects may be maximized through inter-chain interactions. This aspect was assessed by MD simulations of 12-mer models of poly(**1**-*alt*-**6**) and poly(**2**-*alt*-**6**) in which ensembles of rather randomly located five chains were used for calculations (Figure 2-26). It can

be seen that methyl groups attached at the 3- and 5-positions of the side-chain phenyl groups are located in close proximity to other chains in the model of poly(**2**-*alt*-**6**) which would result in significant inter-chain steric repulsion (Figure 2-26 B) while the corresponding positions seem to have greater rooms in the model of poly(**1**-*alt*-**6**) (Figure 2-26 A). These results agree with the fact that poly(**2**-*alt*-**6**) remarkably amplified its chirality in the solid state while poly(**1**-*alt*-**6**) did not.

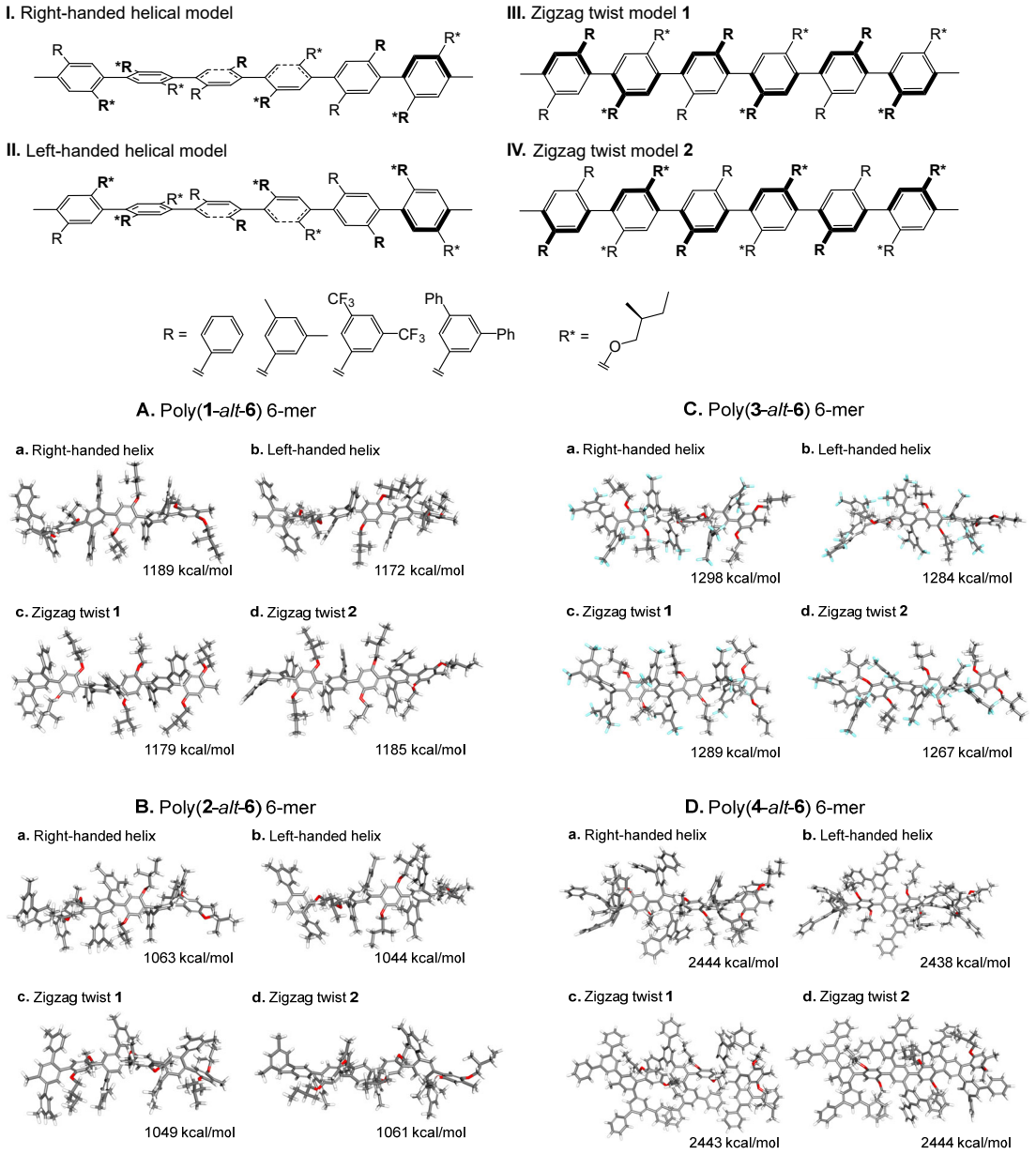

Figure 2-25. Right-handed helix (I) and left-handed helix (II) models and zigzag twist models 1 and 2 having enantiomeric conformations (III and IV) of alternating 6-mer chains, and optimized conformations of 6-mer models of the alternating copolymers with total steric energies calculated by COMPASS force field (A-D).

A. Five left-handed helical 12-mers of poly(**1**-*alt*-**6**)

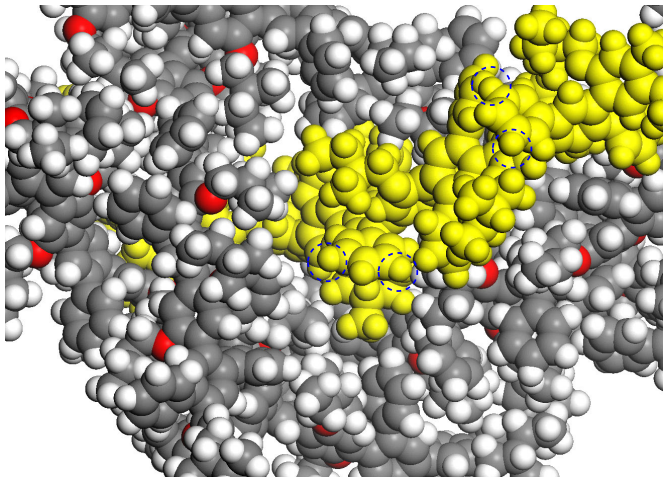

B. Five left-handed helical 12-mers of poly(**2**-*alt*-**6**)

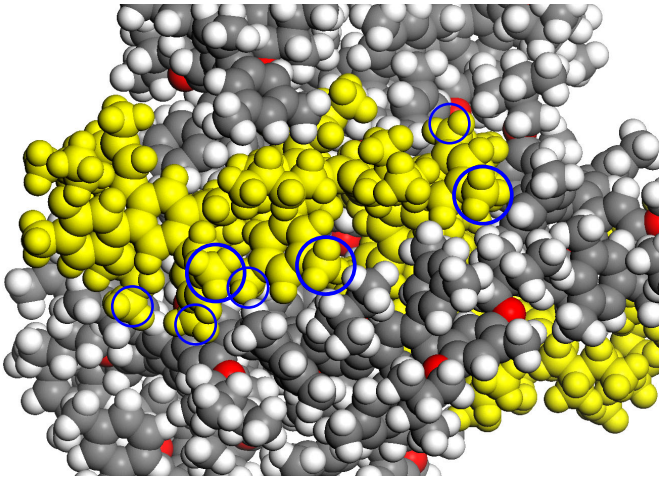

Figure 2-26. Five-chain ensemble structures of left-handed 12-mer models of poly(**1**-*alt*-**6**) (A) and poly(**2**-*alt*-**6**) (B) observed in molecular dynamics simulations (COMPASS force field, NVT, 300 K, 1 nsec). One chain is highlighted in both models for clarity. Hydrogens at the 3- and 5-positions of the side-chain phenyl group are marked by dotted blue circles in A, and methyl groups at the 3- and 5-positions of the side-chain phenyl group are marked by solid blue circles.

2.8 CPL emission of the Polymers

As a function of the copolymers, CPL emission was studied using the film samples (Figures 2-27 and 2-28). Anisotropy was quantified by luminescence anisotropy factor, $g_{lum} = 2(I_L - I_R)/(I_L + I_R)$ where I_L and I_R are the emission intensities of *L*- and

R-CPL, respectively.[35] All polymers showed emission bands centered at around 400-420 nm.

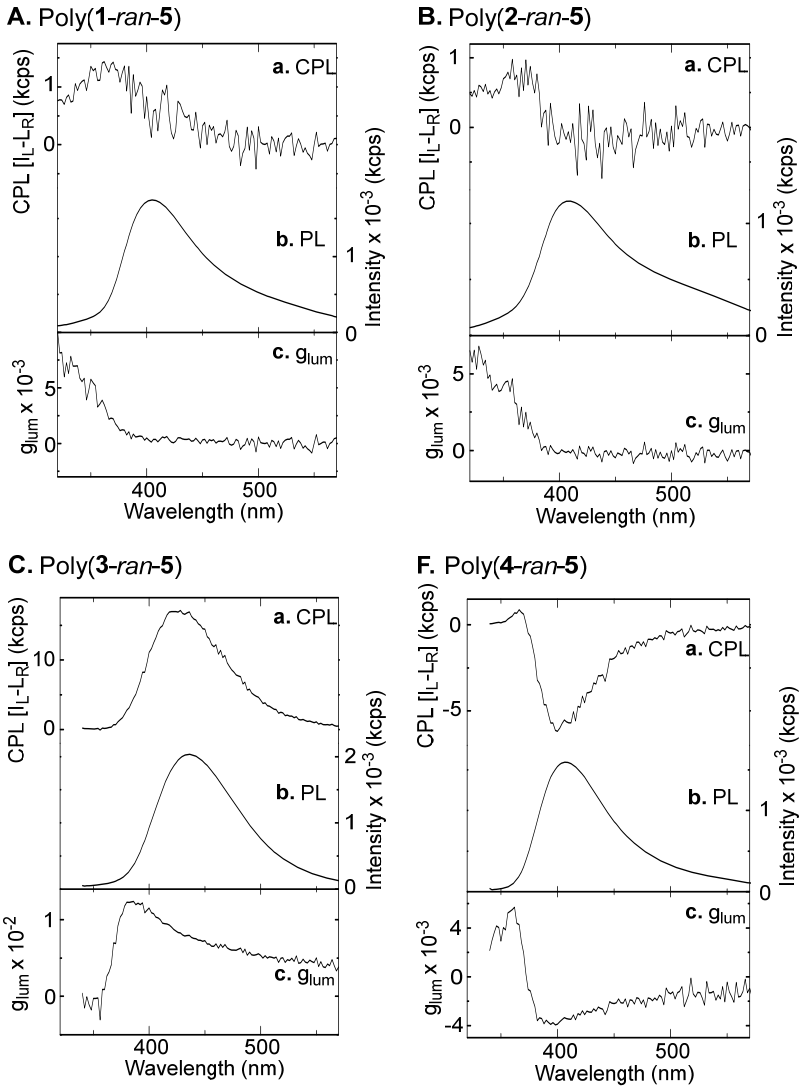

Figure 2-27. CPL emission spectra (a), total emission (PL) spectra (b), and g_{lum} spectra of the random copolymers in film after annealing at 100 ºC for 2h. [λ_{ex} = 260 nm].

Among the random copolymers, poly(**1**-*ran*-**5**) and poly(**2**-*ran*-**5**) showed only weak CPL responses in the shorter-wave-length parts of the emission bands, suggesting that chiral conformation of these polymers may be controlled for shorter sequences in excited states. On the other hand, poly(**3**-*ran*-**5**) and poly(**4**-*ran*-**5**) showed CPL spectra with shapes similar to those of PL spectra, indicating that helical conformation is controlled also for longer sequences. Poly(**3**-*ran*-**5**) and poly(**4**-*ran*-**5**) exhibited very clear positive and negative CPL spectra with g_{lum} 0.012 at 390 nm and g_{lum} -0.004 at 390 nm, respectively. The especially high g_{lum} value of poly(**3**-*ran*-**5**)

may have a connection with electron-withdrawing -CF_3 group leading to a greater dipole moment which could affect excited-state chirality. In the case of poly(**4**-*ran*-**5**), axial chirality around the bonds connecting the four benzene rings to the side-chain benzene rings directly attached to the main chain and axial chirality around the other single bonds might lead to opposite signs in CPL.

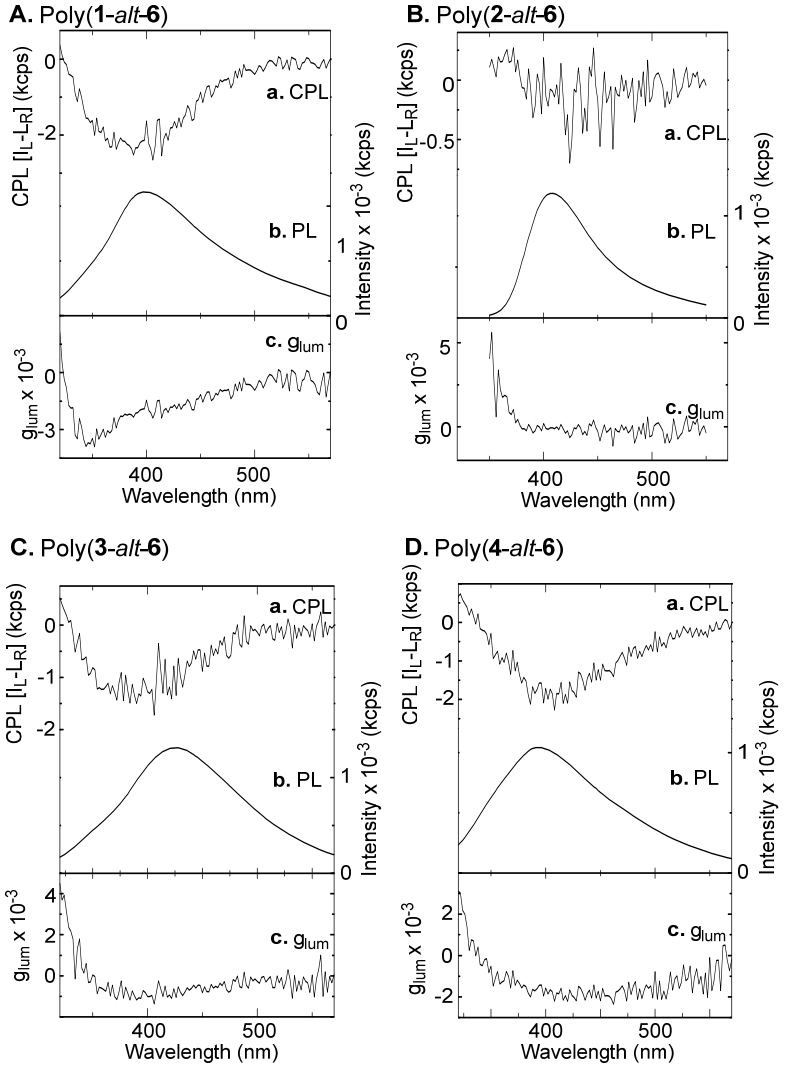

Figure 2-28. CPL emission spectra (a), total emission (PL) spectra (b), and g_{lum} spectra of the alternating copolymers in film after annealing at 100 °C for 2h. [λ_{ex} = 260 nm].

All alternating copolymers showed negative CPL with lower g_{lum} values compared with the random copolymers. The alternating sequence was thus found not as efficient as the random sequence in inducing or maintaining preferred-handed helix in excited states. Also, an intriguing fact was that poly(**1**-*alt*-**6**) with the least bulky side chain group (unsubstituted phenyl) showed a slightly higher g_{lum} than the other three

alternating copolymers. Interchain aggregation in the solid state might have role in stabilizing helix leading to higher g_{lum} where smaller, less-hindered side-chain group may result in efficient inter-chain interactions in excited states.

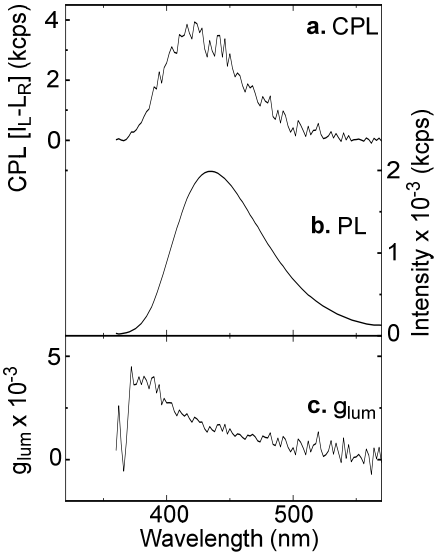

Figure 2-29. CPL emission spectra (a), total emission (PL) spectra (b), and g_{lum} spectra of poly(**3**-ran-**5**) of M_n 9400 in film after annealing at 100 °C for 2h. [λ_{ex} = 260 nm].

Molar-mass effects on CPL emission properties were studied using the poly(**3**-*ran*-**5**) sample of lower molar masses (M_n 9400) mentioned earlier (Figure 2-29). Unlike the CD spectral properties, CPL efficiency was significantly affected by molar mass. The polymer of M_n 9400 showed g_{lum} 0.004 which is about one third of that of the polymer of M_n 27640 (g_{lum} 0.012). This result may mean that a longer chain more efficiently stabilizes chiral conformation in excited states.

2.9 Chiral Recognition Ability of the Polymers in the Solid State

As another, important function of helical polymers, chiral recognition (resolution) ability toward racemic compounds was examined by a batch adsorption experiment in which a polymer film was soaked in a solution of racemic *trans*-stilbene oxide in MeOH or in hexane-2-propanol (95/5 (v/v)) or that of racemic Tröger's base in MeOH or that of flavanone in MeOH, and the amount and enantiomeric excess of unabsorbed analytes in the solution part was quantified by chiral HPLC (Tables 2-3, 2-4, 2-5, and 2-6) on the basis of which separation factors were calculated. The

detailed experimental procedure is found in the literature.[36] *trans*-Stilbene oxide, Tröger's base, and flavanone are often used as racemate in evaluation of chiral recognition ability of stationary phases of HPLC columns.[24,28,29]

Table 2-3. Chiral recognition ability of copolymers toward *trans*-stilbene oxide in MeOH at 25°C[a]

Run	Copolymer	Adsorbed analyte[b] (%)	E.e. of free analyte in supernatant solution[b] (%)	Separation factor[c]
1	Poly(**1**-*ran*-**5**)	51	~0	~1
2	Poly(**2**-*ran*-**5**)	92	0.7(-)	1.07
3	Poly(**3**-*ran*-**5**)	66	1.0(-)	1.04
4	Poly(**4**-*ran*-**5**)	72	4.5(-)	1.10
5	Poly(**1**-*alt*-**6**)	66	~0	~1
6	Poly(**2**-*alt*-**6**)	90	~0	~1
7	Poly(**3**-*alt*-**6**)	63	3.5(-)	1.10
8	Poly(**4**-*alt*-**6**)	60	2.0(-)	1.06

[a]Experimetal conditions: copolymer 1 mg; racemic analyte 0.0025 mg (0.2 mL portion from a 0.0125 mg mL^{-1} solution of *trans*-stilbene oxide in methanol; temperature ca. 25 °C; time 2 h. Determined by HPLC analysis of supernatant solution using a ChiralPak IC column. Absorption yield was estimated by comparing the peak area of the sample in question with that of the stock solution of racemate. The error of ee estimated was less than 1% judging from the data for racemate. [c]Calculated according to $\alpha = (F_{major}(\%)/F_{minor}(\%)) / (A_{minor}(\%)/A_{major}(\%))$, where F_{major} and F_{minor} are the percentages of major and minor isomers of free analyte in supernatant solution, respectively, and A_{major} and A_{minor} are those of major and minor isomers of adsorbed analyte, respectively.

Table 2-4. Chiral recognition ability of copolymers toward *trans*-stilbene oxide in hexane-2-propanol (95/5 v/v)[a]

Run	Copolymer	Adsorbed analyte[b] (%)	E.e. of free analyte in supernatant solution[b] (%)	Separation factor[c]
1	Poly(**1**-*ran*-**5**)	66	1.6(+)	1.05
2	Poly(**2**-*ran*-**5**)	n.d.[d]	n.d.[d]	n.d.[d]
3	Poly(**3**-*ran*-**5**)	n.d.[d]	n.d.[d]	n.d.[d]
4	Poly(**4**-*ran*-**5**)	60	1.3(+)	1.04
5	Poly(**1**-*alt*-**6**)	47	~0	~1
6	Poly(**2**-*alt*-**6**)	93	10.5(+)	1.25
7	Poly(**3**-*alt*-**6**)	n.d.[d]	n.d.[d]	n.d.[d]
8	Poly(**4**-*alt*-**6**)	6	~0	~1

[a]Experimetal conditions: copolymer 1 mg; racemic analyte 0.0025 mg (0.2 mL portion from a 0.0125 mg mL^{-1} solution of *trans*-stilbene oxide in hexane-2-propanol (95/5, v/v); temperature ca. 25 °C; time 2 h. [b]Determined by HPLC analysis of supernatant solution using a Chiralcel OD column. Absorption yield was estimated by comparing the peak area of the sample in question with that of the stock solution of racemate. The error of ee estimated was less than 1% judging from the data for racemate. [c]Calculated according to $\alpha = (F_{major}(\%)/F_{minor}(\%)) / (A_{minor}(\%)/A_{major}(\%))$, where F_{major} and F_{minor} are the percentages of major and minor isomers of free analyte in supernatant solution, respectively, and A_{major} and A_{minor} are those of major and minor isomers of adsorbed analyte, respectively. [d]Polymer was partially dissolved in hexane-2-propanol, and data were not obtained.

Table 2-5. Chiral recognition ability of copolymers toward Tröger's base in MeOH[a]

Run	Copolymer	Adsorbed analyte[b] (%)	E.e. of free analyte in supernatant solution[b] (%)	Separation factor[c]
1	Poly(**1**-*ran*-**5**)	60	8.6 (+)	1.33
2	Poly(**2**-*ran*-**5**)	64	5.9 (+)	1.20
3	Poly(**3**-*ran*-**5**)	63	10.2 (-)	1.38
4	Poly(**4**-*ran*-**5**)	54	0.9 (-)	1.03
5	Poly(**1**-*alt*-**6**)	62	10.8 (-)	1.42
6	Poly(**2**-*alt*-**6**)	74	3.2 (+)	1.09
7	Poly(**3**-*alt*-**6**)	66	3.5 (+)	1.11
8	Poly(**4**-*alt*-**6**)	62	0.9 (+)	1.03

[a]Experimetal conditions: copolymer 1 mg; racemic analyte 0.0025 mg (0.2 mL portion from a 0.0125 mg mL^{-1} solution of tröger's base in methanol; temperature ca. 25 °C; time 0.5 h). [b]Determined by HPLC analysis of supernatant solution using a ChiralPak AS-H column. Absorption yield was estimated by comparing the peak area of the sample in question with that of the stock solution of racemate. The error of ee estimated was less than 1% judging from the data for racemate. [c]Calculated according to $\alpha = (F_{major}\ (\%)/\ F_{minor}\ (\%))\ /\ (A_{minor}\ (\%)/\ A_{major}\ (\%))$, where F_{major} and F_{minor} are the percentages of major and minor isomers of free analyte in supernatant solution, respectively, and A_{major} and A_{minor} are those of major and minor isomers of adsorbed analyte, respectively.

Table 2-6. Chiral recognition ability of copolymers toward flavanone in MeOH[a]

Run	Copolymer	Adsorbed analyte[b] (%)	E.e. of free analyte in supernatant solution[b] (%)	Separation factor[c]
1	Poly(**1**-*ran*-**5**)	64	2.8 (-)	1.09
2	Poly(**2**-*ran*-**5**)	70	2.0 (-)	1.06
3	Poly(**3**-*ran*-**5**)	80	0.6 (-)	1.01
4	Poly(**4**-*ran*-**5**)	27	0.6 (-)	1.04
5	Poly(**1**-*alt*-**6**)	77	1.7 (-)	1.05
6	Poly(**2**-*alt*-**6**)	74	3.8 (+)	1.11
7	Poly(**3**-*alt*-**6**)	73	1.3 (-)	1.04
8	Poly(**4**-*alt*-**6**)	31	0	~1

[a]Experimetal conditions: copolymer 1 mg; racemic analyte 0.0025 mg (0.2 mL portion from a 0.0125 mg mL^{-1} solution of flavanone in methanol; temperature ca. 25 °C; time 0.5 h). [b]Determined by HPLC analysis of supernatant solution using a ChiralPak IC column. Absorption yield was estimated by comparing the peak area of the sample in question with that of the stock solution of racemate. The error of ee estimated was less than 1% judging from the data for racemate. [c]Calculated according to $\alpha = (F_{major}\ (\%)/\ F_{minor}\ (\%))\ /\ (A_{minor}\ (\%)/\ A_{major}\ (\%))$, where F_{major} and F_{minor} are the percentages of major and minor isomers of free analyte in supernatant solution, respectively, and A_{major} and A_{minor} are those of major and minor isomers of adsorbed analyte, respectively.

In the resolution of *trans*-stilbene oxide in MeOH, poly(**2**-*ran*-**5**), poly(**3**-*ran*-**5**), poly(**4**-*ran*-**5**), poly(**3**-*alt*-**6**), and poly(**4**-*alt*-**6**) showed resolution abilities (Table 3), and all these polymers preferentially adsorbed (+)-isomer of *trans*-stilbene oxide, resulting in the excess of (-)-isomer unadsorbed and left in solution. The fact that poly(**1**-*ran*-**5**), poly(**1**-*alt*-**6**), and poly(**2**-*alt*-**6**) with rather less bulkier side chains did not resolve the racemate may mean that bulkier side-chain group lead to a chain

conformation and an ordered inter-chain structure more suited for resolution. It has been known that uniformly ordered inter-chain structure in the solid state of chiral polymers as chiral selector plays a crucial role in chiral recognition.[24] In addition, compatibility between the racemate polymer side-chain groups in chemical structure should be also considered. π –π interactions between the side-chain 3,5-diphenylphenyl of poly(**4**-*ran*-**5**) and poly(**4**-*alt*-**6**) and the phenyl groups of *trans*-stilbene oxide may facilitate chiral recognition in MeOH.

The experiments with *trans*-stilbene oxide were conducted also in hexane-2-propanol (95/5 (v/v)) (Table 2-4). However, resolution data for poly(**2**-*ran*-**5**), poly(**3**-*ran*-**5**), and poly(**3**-*alt*-**6**) were not obtained because these polymers were partially dissolved in this solvent system. Resolution abilities of the polymers in this solvent were quite different than those in MeOH. Poly(**4**-*alt*-**6**) which performed well in MeOH did not resolve *trans*-stilbene oxide in hexane-2-propanol (95/5 (v/v)) while poly(**1**-*ran*-**5**) and poly(**2**-*alt*-**6**) which poorly performed in MeOH resolved *trans*-stilbene oxide in hexane-2-propanol (95/5 (v/v)). The best resolution performance of poly(**2**-*alt*-**6**) among all polymers in hexane-2-propanol (95/5 (v/v)) may be based on its partial crystalline structure as proposed on the basis of the XRD profile. In addition, all the polymers showing resolution ability preferentially adsorbed (-)-isomer of *trans*-stilbene oxide leaving (+)-isomer-enriched solutions, which indicates that resolution mechanisms are different between the MeOH systems and the hexane-2-propanol (95/5 (v/v)) systems. In hexane-2-propanol (95/5 (v/v)), rather than the π-π interactions proposed in MeOH, polar interactions between the epoxide ring of *trans*-stilbene oxide and the ether moiety of 2,5-bis((*S*)-2-methylbutoxy) group in the copolymers may play a role in resolution in a solvent with low polarity.

Tröger's base was better resolved the polymers in MeOH than *trans*-stilbene oxide where the preferentially adsorbed enantiomer varied depending on the chemical structure of the polymers in spite of the fact that all polymers have (*S*)-2-methylbutoxy group as the chirality source (Table 2-5). It is interesting that poly(**1**-*ran*-**5**) and poly(**1**-*alt*-**6**) having the least bulky side-chain group (unsubstituted

phenyl) showed rather high separation factors, 1.33 and 1.42, respectively, suggesting that the solid-state conformations of these polymers fit for resolution of this particular racemic compound. In the case of flavanone resolution, (+)-enantiomer was preferentially adsorbed except for the case with poly(**2**-*alt*-**6**), and the separation factors were not as high as those in the Tröger's base resolution.

The optically poly(bezene-1,4-diyl)s thus exhibited resolution ability toward the three racemates while the ability of the copolymers appeared not to have any simple relation with their CD intensities or CPL emission efficiencies of the polymers. Enantiomer-selective interactions with external molecule in the resolution experiments may not necessarily be connected with electronic states in the ground state or excited states whereas "chirality" of polymers designed as functional materials including chiral selectors is very often quantified by measurements of optical properties.

In addition, although various helical polymers are known to exhibit chiral recognition ability toward racemic compounds, poly(bezene-1,4-diyl)s have never been examined for this function.[27-30] The findings in this work may expand the structural scope of chiral polymers with resolution abilities.

2.10 Conclusions

Random and alternating copoly(bezene-1,4-diyl)s composed of chiral 2,5-bis((*S*)-2-methylbutoxy)bezene-1,4-diyl units and bulky, achiral 2,5-disubstituted bezene-1,4-diyl units were prepared by Ni-mediated Yamamoto coupling and Pd-catalyzed Suzuki-Miyaura coupling, respectively. The copolymers showed CD spectra whose shape and intensity largely varied depending on the state of the sample, solution or suspension or film as well as the chemical structure. CD intensity was overall much greater in suspension and in film than in solution, suggesting that significant bias on either left- or right-handedness is attained through inter-chain interactions in the solid state. Enhanced chirality expression in the solid state has been reported also for other polymer systems.[37,38] The side-chain groups were thus found not bulky enough to realize helix showing high optical anisotropy in solution unlike

the cases of acrylic polymers.[3,4,19,20] As for the effects of the chemical structure on chirality, for both the random and the alternating copolymers, the polymers with side-chain 3,5-disubstituted phenyl groups led to higher g_{CD} values than those with side-chain unsubstituted phenyl groups, clearly indicating that side-chain bulkiness plays a role in creating a preferred-handed conformation in the solid state. However, among the three 3,5-disubstituted phenyl groups, 3,5-dimethylphenyl group which is not the seemingly bulkiest one tended to result in greatest g_{CD} values. Not only simple bulkiness but also shape of side-chain groups seems to be important in inducing chirality through inter-chain interactions.

In CPL emission, side-chain 3,5-bis(trifluoro)phenyl group and unsubstituted phenyl group led to the greatest g_{lum} values of film for random and alternating copolymers, respectively, indicating that the significance of bulkiness of side-chain group varies between the ground state and excites states. This may be reasonable because axial chirality around single bonds connecting aromatic groups has been reported to be significantly affected on photo excitation. A twisted aromatic-aromatic junction in the ground state can be transformed to coplanar conformation in excited states (twisted-coplanar transition, TCT).[39-52] TCT may not simply cause racemization but may change the conformation of an entire chain for the polymers studied in this work which have various aromatic-aromatic junctions.

In addition, the polymers showed chiral recognition abilities for *trans*-stilbene oxide, Tröger's base, and flavanone in most cases. The abilities varied depending on the solvent and the combination of racemate and polymer as well as the chemical structure of the polymers. The order of separation factors was not particularly in agreement with the order of g_{CD} values while the extent of polymer chirality is often evaluated by CD spectra (g_{CD} values), and polymers' chiral functions generally tend to be anticipated to be better for a polymer with a greater g_{CD} value. Ground-state chirality (g_{CD}), excited-state chirality (g_{lum}), and resolution ability (separation factor) appeared not directly related to each other through the systematic study in this work on chiral poly(benzene-1,4-diyl)s. Appropriate designs of chiral, functional polymers should be made targeting specific functions.

2.11 Experimental

2.11.1 General Instrumentation

^{1}H NMR spectra in solution were recorded on a JEOL JNM-ECX400 spectrometer (400 MHz for ^{1}H measurement) and a JEOL JNM-ECA600 spectrometer (600 MHz for ^{13}C measurement). SEC measurements were carried out using a chromatographic system consisting of a Hitachi L-7100 chromatographic pump, a Hitachi L-7420 UV detector (254 nm), and a Hitachi L-7490 RI detector equipped with TOSOH TSK gel G3000H$_{HR}$ and G6000H$_{HR}$ columns (30 x 0.72(i.d.) cm) connected in series (eluent THF, flow rate 1.0 mL/min). Preparative SEC purification was carried out using a JAI LC-9201 chromatograph with an S-3740 detector equipped with JAIGEL-1H and 2H columns connected in series (eluent $CHCl_3$, flow rate 3.5 mL/min), a JAI LC-9201 chromatograph with a UV-50 and an RI-50 RI detectors equipped with JAIGEL-1H and 2H columns connected in series (eluent $CHCl_3$, flow rate 3.8 mL/min), and a Laboace LC-5060 chromatograph with a 4ch800LA and a 700LA detectors equipped with JAIGEL-1RH, 2RH, and 3RH connected in series (eluent $CHCl_3$, flow rate 10.0 mL/min). UV-vis absorption spectra were measured with a JASCO V-570 spectrophotometers. Emission spectra were taken on a JASCO FP-8500 fluorescence spectrophotometer. IR spectra were recorded on a JASCO FT/IR-6100 spectrometer using KBr pellet samples. Circular dichroism (CD) spectra were taken with a JASCO-820 spectrometer. CPL emission spectra were measured with a JASCO-300 spectrometer and with an apparatus based on a photo elastic modulator and a photomultiplier assembled according the literature[35] with modifications. Differential scanning calorimetry (DSC) and thermal gravity analysis (TGA) were conducted on Rigaku Thermo Plus DSC8230 and TG8120 analyzer at a heating rate of 10 K/min in nitrogen atmosphere. XRD profiles were measured using a Rigaku MiniFlex600-C diffractometer.

2.11.2 Computer Simulation

Molecular mechanics structure optimization was conducted using the COMPASS force field[34] implemented in the Discover module of the Material

Studio 2.0 (Accelrys) software package with the Fletcher-Reeves[53] conjugate gradient algorithm until the RMS residue went below 0.01 kcal/mol/Å. Molecular dynamic simulation was performed under a constant NVT condition in which the numbers of atoms, volume, and thermodynamic temperature were held constant. Berendsen's thermocouple[54] was used for coupling to a thermal bath. The step time was 1 fs and the decay constant was 0.1 ps.

2.11.3 Materials

Tetrakis(triphenylphosphine)palladium(0), 1,4-dibromo-2,5-diiodobenzene, benzeneboronic acid, 3,5-dimethylbenzeneboronic acid, 3,5-bis(trifluoromethy)benzeneboronic acid, 3,5-diphenylbenzene boronic acid, diethylene glycol dimethyl ether (DGDME), bis(1,5-cyclooctadiene)nickel(0), 1,5-cyclooctadiene, 1,2-dimethoxyethane (DME), 2,5-dibromohydroquinone, (*S*)-(-)-2-methylbutanol and *p*-toluenesulfonyl chloride were used as purchased from TCI (Tokyo, Japan). *n*-Butyllithium (1.6 M in hexane), toluene, chloroform, chloroform-d_1, 2,2'-bipyridyl, trimethyl borate, methanol, 2-propanol, pyridine, dichloromethane (DCM), *N,N*-dimethylformamide (DMF) and *N*,*N*-dimethylmethanamide were used as purchased from KANTO Chemical (Tokyo, Japan). Tetrahydrofuran (THF) was used as purchased from WAKO Chemical (Osaka, Japan). DMF was distilled and dried over molecular sieves 4A, and toluene was distilled over CaH_2. *Trans*-stilbene oxide, Tröger's base, and flavanone were used as purchased from Sigma-Aldrich (Tokyo, Japan).

2.12 Synthesis and Structural Analysis of Monomers

2.12.1 1,4-Dibromo-2,5-diphenybenzene[31]

1,4-Dibromo-2,5-diiodobenzene (2.93 g, 6.0 mmol), benzeneboronic acid (1.54 g, 12.6 mmol), K_2CO_3 (3.32 g, 24.0 mmol) and tetrakis(triphenylphosphine)palladium

(0.69 g, 0.6 mmol) were mixed with a degassed mixture of DGDME (60 mL) and H_2O (15 mL) in a 200-mL flask under nitrogen, and the reaction mixture was stirred at 90ºC for 24 h. The mixture was poured into water after cooling at ambient temperature, and the raw material was extracted with DCM. The organic layer was washed by water and dried over anhydrous $MgSO_4$, and removal of the solvent resulted in the crude product which was recrystallized from DGDME to lead to a white powder as the pure monomer: yield 0.79 g (34 %). ^{1}H NMR (400 MHz, $CDCl_3$, r.t.) δ/ppm: 7.65 (2H, s), 7.47-7.42 (10H, m). ^{13}C NMR (600 MHz, $CDCl_3$, r.t.) δ/ppm: 143.0, 139.6, 135.3, 129.4, 128.3, 128.2, 121.5. FT-IR (KBr) υ/cm^{-1}: 3061, 3021, 1459, 1442, 1348, 1086, 1035, 1008, 892, 760, 708, 699, 544. HRMS (ESI): calcd. for $C_{18}H_{12}Br_2$ 385.93; found 385.93123.

The spectral data for this compound are indicated in Figure 2-30, 2-31 and 2-32.

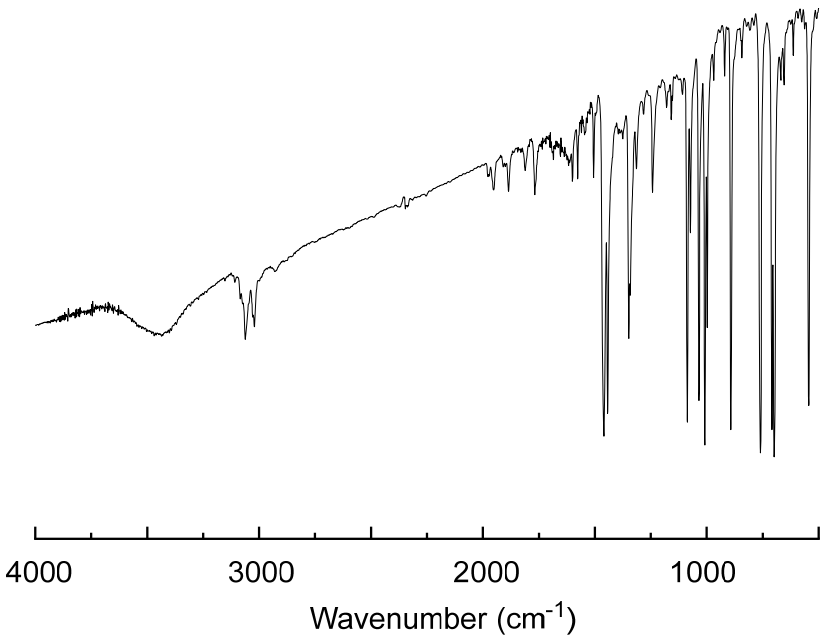

Figure 2-30. IR spectrum of 1,4-dibromo-2,5-diphenybenzene.

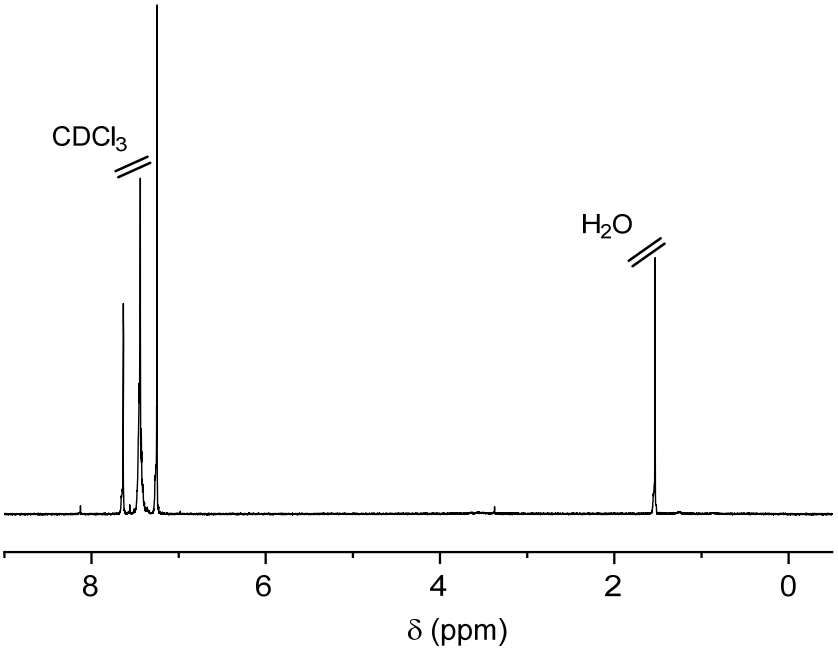

Figure2-31. ^{1}H NMR spectrum of 1,4-dibromo-2,5-diphenybenzene. [400 MHz, $CDCl_3$, r.t.].

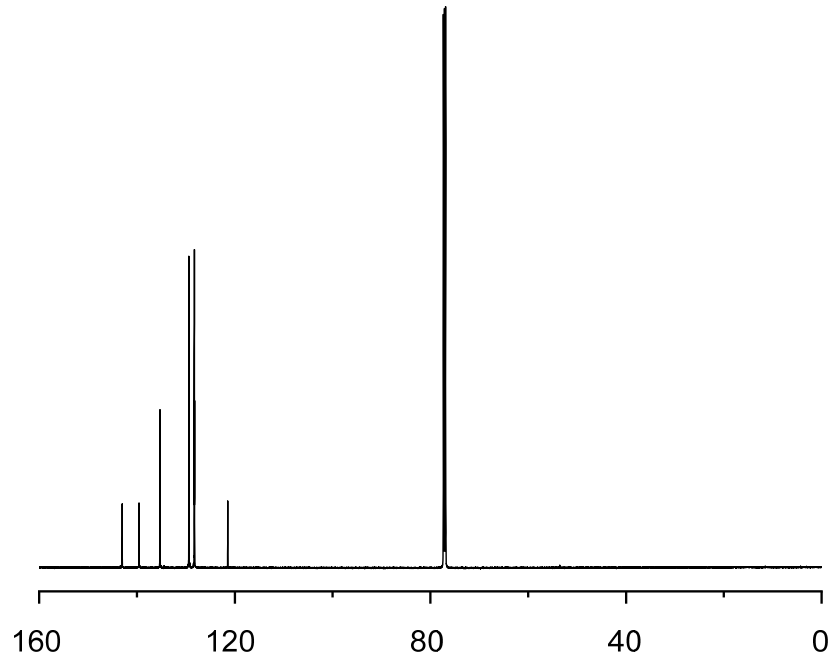

Figure 2-32. ^{13}C NMR spectrum of 1,4-dibromo-2,5-diphenybenzene. [600 MHz, $CDCl_3$, r.t.].

2.12.2 1,4-Dibromo-2,5-bis(3,5-dimethylphenyl)benzene

1,4-Dibromo-2,5-diiodobenzene (1.22 g, 2.5 mmol), 3,5-dimethylbenzeneboronic

acid (0.90 g, 6.0mmol), K_2CO_3 (1.38 g, 10.0 mmol) and tetrakis(triphenylphosphine)palladium (0.28 g, 0.25 mmol) were mixed with a degassed mixture of DGDME (20 mL) and H_2O (5 mL) in a 100-mL flask under nitrogen, and the reaction mixture was stirred at 90ºC for 24 h. The mixture was poured into water after cooling at ambient temperature, and the raw material was extracted with DCM. The organic layer was washed by water and dried over anhydrous $MgSO_4$. Removal of the solvent led to the crude product which was recrystallized from DGDME to lead to a white powder as the pure monomer: yield 0.40 g (36 %). ^{1}H NMR (400 MHz, $CDCl_3$, r.t.) δ/ppm: 7.60 (2H, s), 7.05 (6H, s), 2.39 (12H, s). ^{13}C NMR (600 MHz, $CDCl_3$, r.t.) δ/ppm: 143.1, 139.5, 137.8, 135.2, 129.8, 127.1, 121.3, 21.5. FT-IR (KBr) υ/cm^{-1}: 3004, 2910, 1605, 1449, 1374, 1345, 1233, 1107, 1051, 907, 876, 844, 705, 635, 577, 482, 459. HRMS (ESI): calcd. for $C_{22}H_{20}Br_2$ 441.99; found 441.99279.

The spectral data for this compound are indicated in Figure 2-33, 2-34 and 2-35.

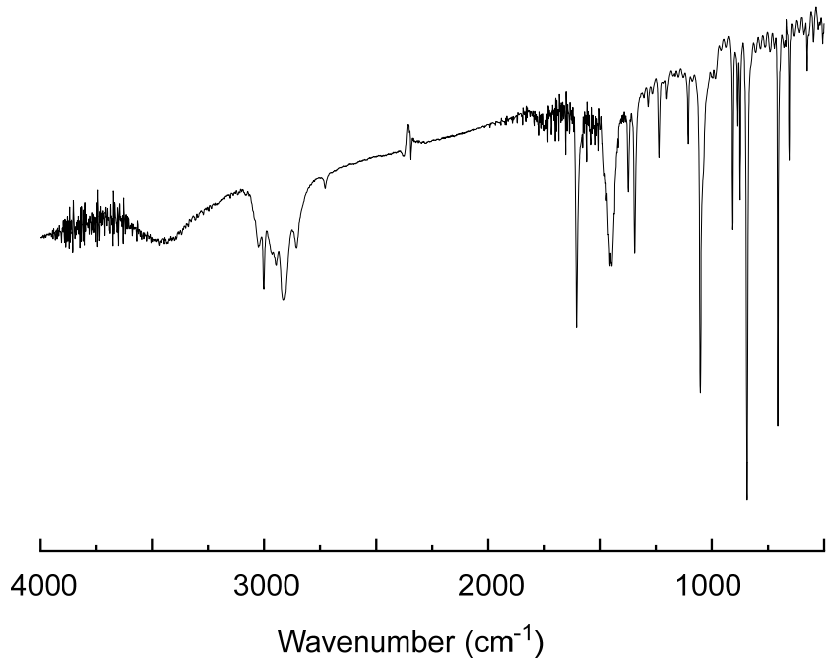

Figure 2-33. IR spectrum of 1,4-dibromo-2,5-bis(3,5-dimethylphenyl)benzene.

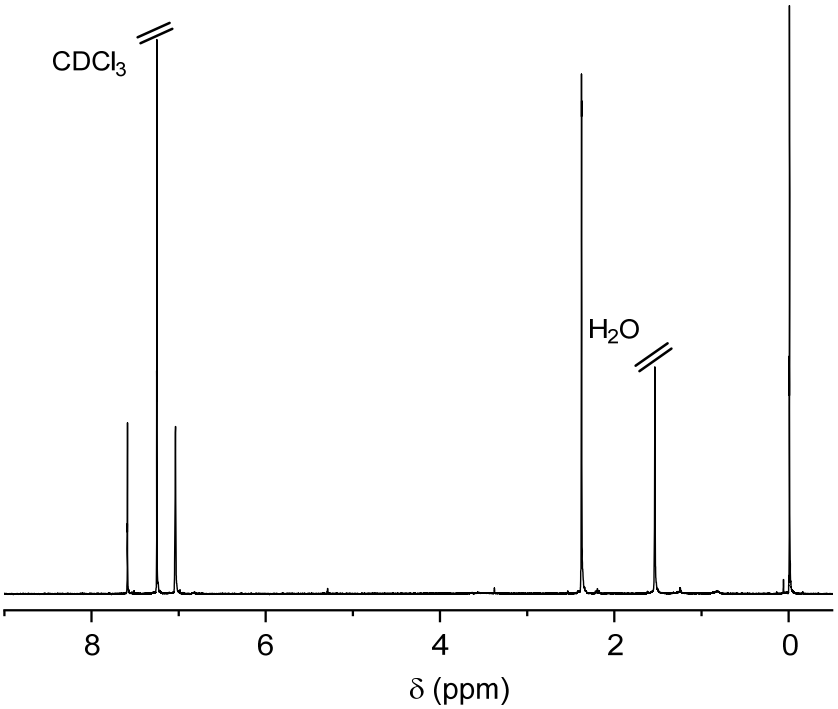

Figure 2-34. ^{1}H NMR spectrum of 1,4-dibromo-2,5-bis(3,5-dimethylphenyl)benzene. [400 MHz, $CDCl_3$, r.t.].

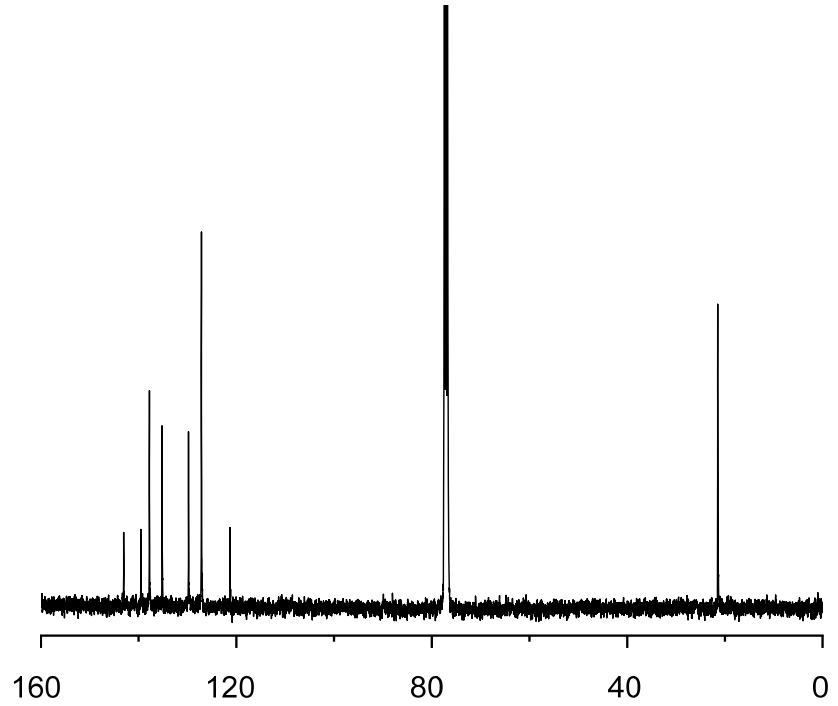

Figure 2-35. ^{13}C NMR spectrum of 1,4-dibromo-2,5-bis(3,5-dimethylphenyl)benzene. [600 MHz, $CDCl_3$, r.t.].

2.12.3 1,4-Dibromo-2,5-bis(3,5-bis(trifluoromethyl)phenyl)benzene

1,4-Dibromo-2,5-diiodobenzene (1.22 g, 2.5 mmol),

3,5-bis(trifluoromethy)benzeneboronic acid (1.55 g, 6.0 mmol), K_2CO_3 (1.38 g, 10 mmol) and tetrakis(triphenylphosphine)palladium (0.28 g, 0.25 mmol) were with a degassed mixture of DGDME (20 mL) and H_2O (5 mL) in a 100-mL flask under nitrogen, and the reaction mixture was stirred at 90ºC for 24 h. The mixture was poured into water after cooling at ambient temperature, and the raw material was extracted with DCM. The organic layer was washed with water and dried over anhydrous $MgSO_4$. The organic layer was washed by water and dried over anhydrous $MgSO_4$. Removal of the solvent led to the crude product which was recrystallized from DGDME to lead to a white powder as the pure monomer: yield 0.88 g (53 %). ^{1}H NMR (400 MHz, $CDCl_3$, r.t.) δ/ppm: 7.97 (2H, s), 7.91 (4H, s), 7.71 (2H, s). ^{13}C NMR (600 MHz, $CDCl_3$, r.t.) δ/ppm: 141.4, 140.8, 135.4, 131.9, 129.6, 124.1, 122.5, 121.7. FT-IR (KBr) υ/cm^{-1}: 3100, 2927, 1457, 1383, 1331, 1280, 1228, 1195, 1172, 1131, 1038, 909, 889, 847, 716, 708, 687, 670, 535. HRMS (ESI): calcd. for $C_{22}H_8Br_2F_{12}$ 657.88; found 657.88028.

The spectral data for this compound are indicated in Figure 2-36, 2-37 and 2-38.

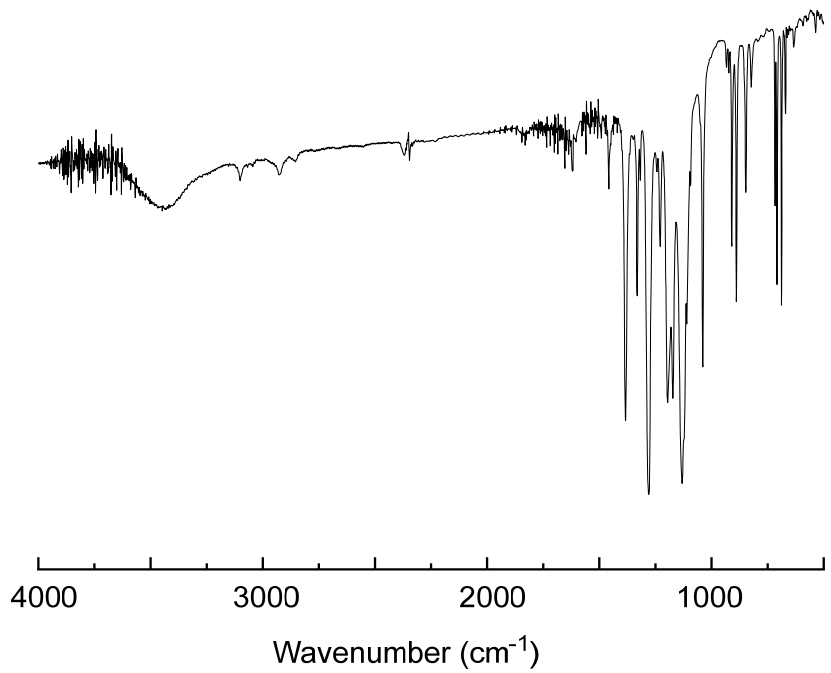

Figure 2-36. IR spectrum of 1,4-dibromo-2,5-bis(3,5-bis(trifluoromethyl)phenyl)benzene.

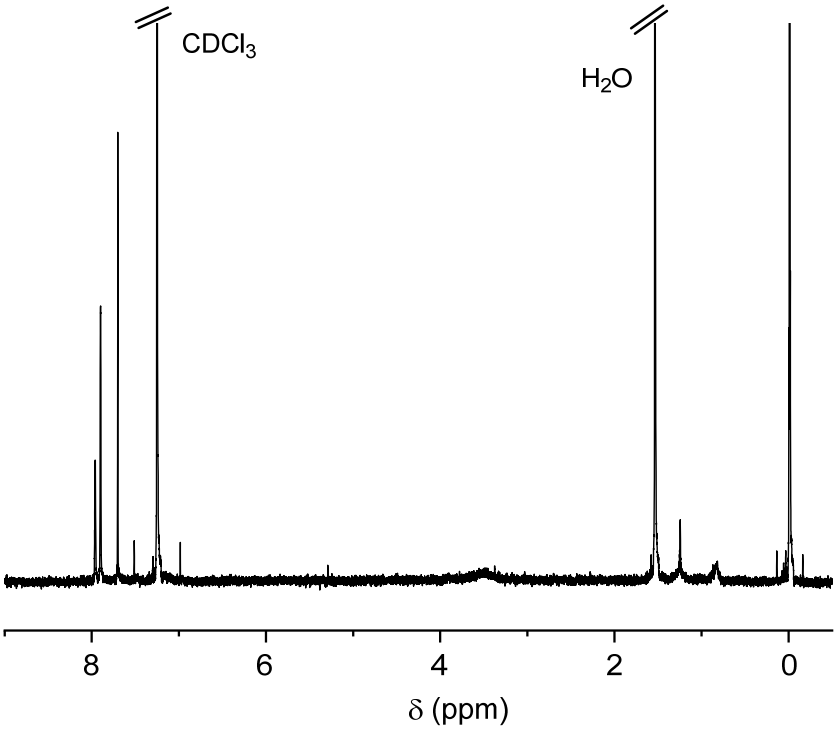

Figure 2-37. ^{1}H NMR spectrum of 1,4-dibromo-2,5-bis(3,5-bis(trifluoromethyl)phenyl)benzene. [400 MHz, $CDCl_3$, r.t.].

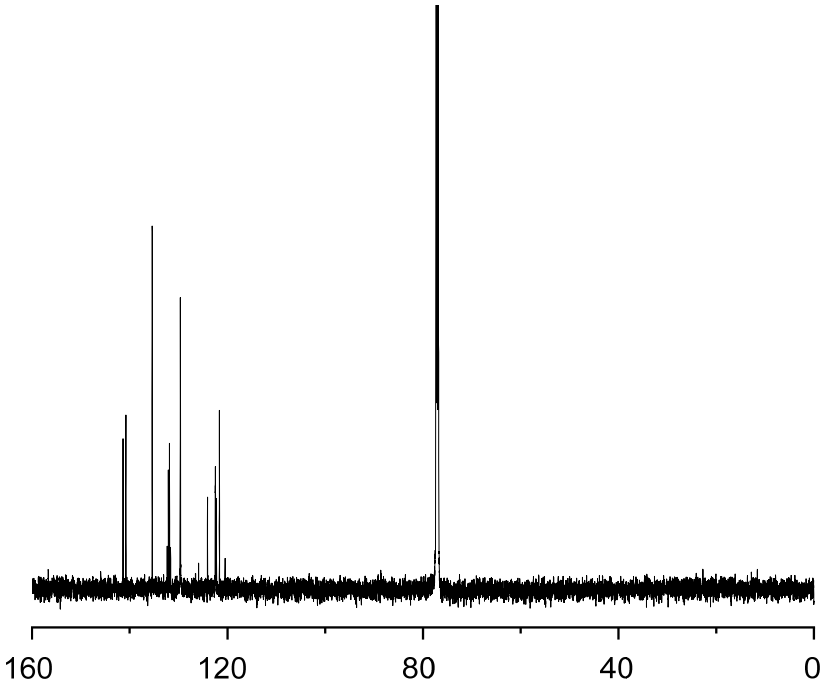

Figure 2-38. ^{13}C NMR spectrum of 1,4-dibromo-2,5-bis(3,5-bis(trifluoromethyl)phenyl)benzene. [600 MHz, $CDCl_3$, r.t.].

2.12.4 1,4-Dibromo-2,5-bis(3,5-diphenylphenyl)benzene

1,4-Dibromo-2,5-diiodobenzene (0.49 g, 1.0 mmol), [(3,5-diphenylphenyl) boronic acid] (0.58 g, 2.1 mmol), K_2CO_3 (0.55 g, 4.0 mmol) and tetrakis(triphenylphosphine)palladium (0.11 g, 0.10 mmol) were with a degassed mixture of DGDME (20 mL) and H_2O (5 mL) in a 100-mL flask under nitrogen, and the reaction mixture was stirred at 90ºC for 24 h. The mixture was poured into water after cooling at ambient temperature, and the raw material was extracted with DCM. The organic layer was washed by water and dried over anhydrous $MgSO_4$. The organic layer was washed by water and dried over anhydrous $MgSO_4$. Removal of the solvent led to the crude product which was recrystallized from DGDME to lead to a white powder as the pure monomer: yield 0.31 g, (45 %). ^{1}H NMR (400 MHz, $CDCl_3$, r.t.) δ/ppm: 7.87 (2H, t, *J* = 1.7 Hz), 7.82 (2H, s), 7.69-7.73 (12H, m), 7.48-7.52 (8H, m), 7.39-7.42 (4H, m). ^{13}C NMR (600 MHz, $CDCl_3$, r.t.) δ/ppm: 143.0, 141.9, 140.8, 140.4, 135.5, 129.0, 127.8, 127.5, 127.2, 126.0, 121.6. FT-IR (KBr) υ/cm^{-1}: 3056, 3033, 1592, 1579, 1496, 1481, 1452, 1407, 1382, 1357, 1308, 1280, 1183, 1136, 1063, 1033, 1010, 876, 759, 695, 648, 612. HRMS (ESI): calcd. for $C_{42}H_{28}Br_2$ 690.06; found 690.05478.

The spectral data for this compound are indicated in Figure 2-39, 2-40 and 2-41.

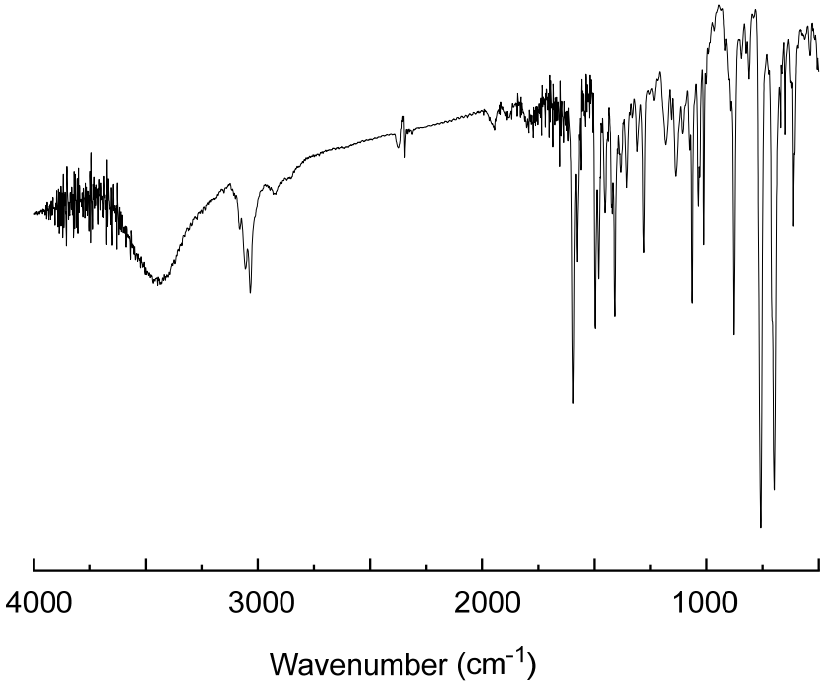

Figure 2-39. IR spectrum of 1,4-dibromo-2,5-bis(3,5-diphenylphenyl)benzene.

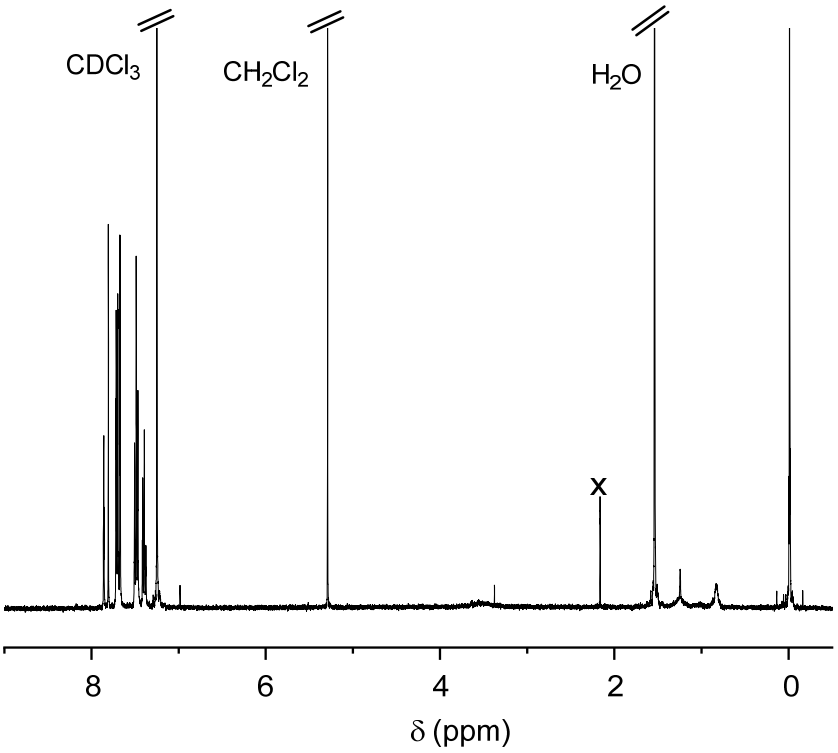

Figure 2-40. ^{1}H NMR spectrum of 1,4-dibromo-2,5-bis(3,5-diphenylphenyl)benzene. [400 MHz, $CDCl_3$, r.t.].

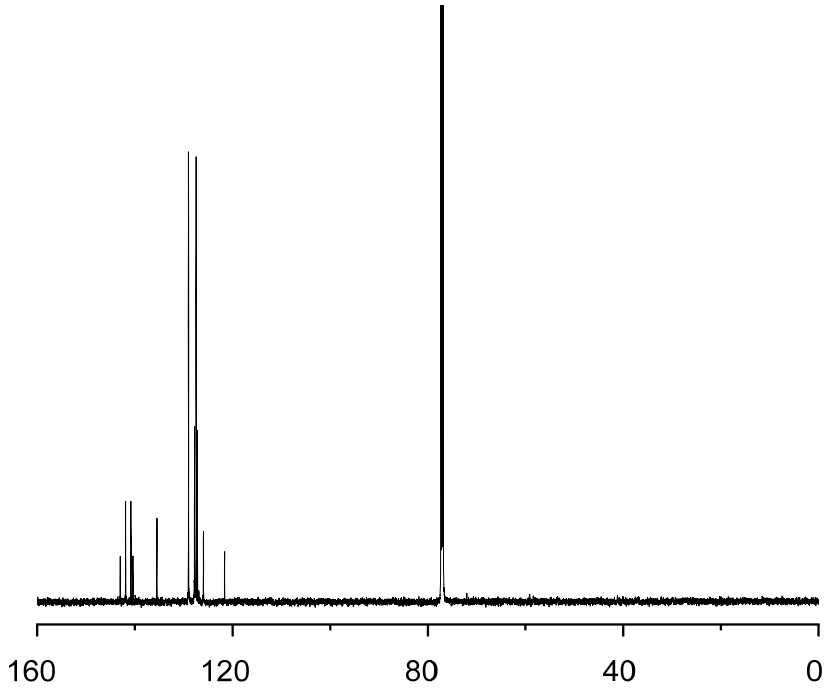

Figure 2-41. ^{13}C NMR spectrum of 1,4-dibromo-2,5-bis(3,5-diphenylphenyl)benzene. [600 MHz, $CDCl_3$, r.t.].

2.12.5 1,4-Dibromo-2,5-bis((*S*)-2-methylbutoxy)benzene[55]

A solution of (*S*)-(-)-2-methylbutanol (7.93 g, 90 mmol) in pyridine (45 mL) was placed in a 100-mL flask at 0 ºC to which *p*-toluenesulfonyl chloride (20.59 g, 108 mmol) was add slowly. After stirring at 4 ºC for 24 h, the reaction was quenched by adding excess aq. HCl (2M). The crude products were extracted with diethyl ether and water, and the organic layer was washed with saturated aq. sodium bicarbonate and dried over anhydrous $MgSO_4$. Removing the solvent resulted in pure (S)-2-methylbutyl 4-methylbenzenesulfonate: yield 19.45 g (89%).

A solution of 2,5-dibromohydroquinone (2.3 g, 8.7 mmol) and (*S*)-2-methylbutyl 4-methylbenzenesulfonate (5.25 g, 21.7 mmol) in distilled DMF (60 mL) was placed in a 100-mL flask. After the addition of Cs_2CO_3 (7.34 g, 22.5 mmol) the solution, the system was homogenized and stirred at 100 ºC for 24 h. Insoluble materials were removed from the reaction mixture, and the solvent was removed from the soluble part to give a crude material which was purified by silica gel column chromatography using chloroform as eluent: yield 3.25 g (91 %). ^1H NMR (400 MHz, $CDCl_3$, r.t.) δ/ppm: 7.07 (2H, s), 3.71-3.83 (4H, m), 1.85-1.93 (2H, m), 1.56-1.62 (2H, m),

1.26-1.35 (2H, m), 1.05 (6H, d, J = 6.8 Hz), 0.95 (6H, t, J = 7.5 Hz). ^{13}C NMR (600 MHz, $CDCl_3$, r.t.) δ/ppm: 150.2, 118.3, 111.2, 75.0, 34.9, 26.1, 16.6, 11.4. FT-IR (KBr) υ/cm^{-1}: 2957, 2873, 1499, 1467, 1362, 1264, 1216, 1105, 1058, 1024, 988, 957, 846, 829, 799, 629, 598.

The spectral data for this compound are indicated in Figure 2-42, 2-43 and 2-44.

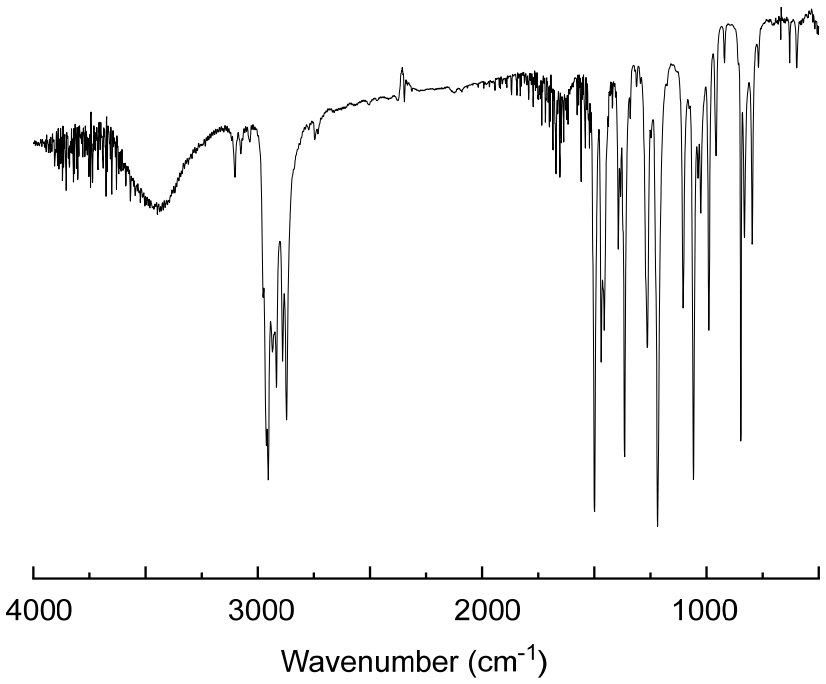

Figure 2-42. IR spectrum of 1,4-dibromo-2,5-bis((*S*)-2-methylbutoxy)benzene.

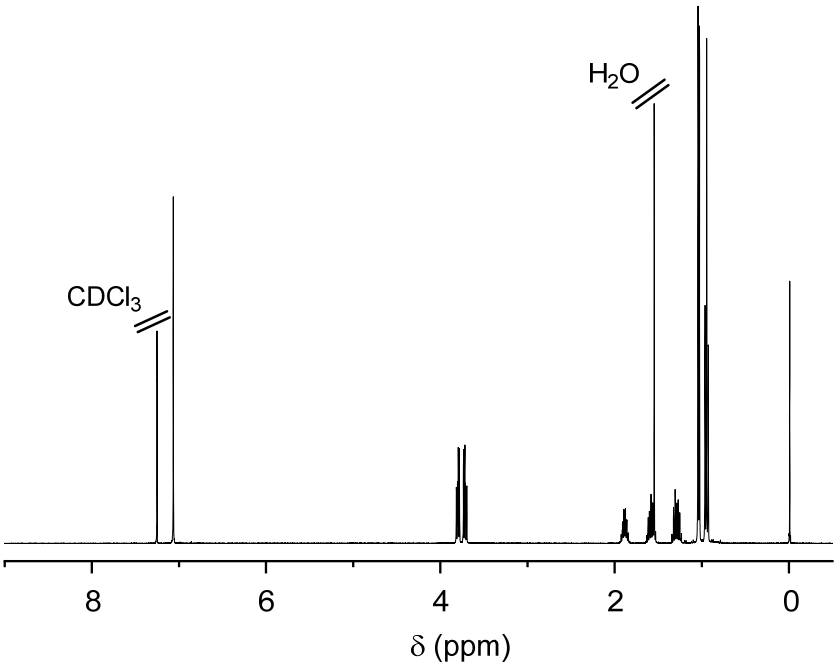

Figure 2-43. ^{1}H NMR spectrum of 1,4-dibromo-2,5-bis((*S*)-2-methylbutoxy)benzene. [400 MHz, $CDCl_3$, r.t.].

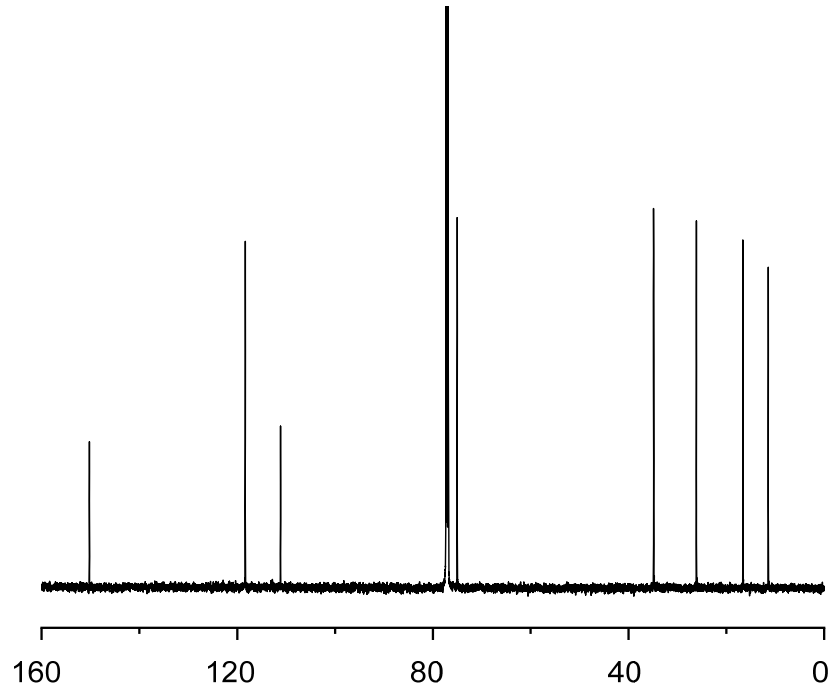

Figure 2-44. ^{13}C NMR spectrum of 1,4-dibromo-2,5-bis((*S*)-2-methylbutoxy)benzene. [600 MHz, $CDCl_3$, r.t.].

2.12.6 1,4-Bis(dihyroxyboranyl)-2,5-bis((*S*)-2-methylbutoxy)benzene[55]

A solution of 2,5-bis((*S*)-2-methylbutoxy)-1,4-dibromobenzene (2000 mg, 4.90

mmol) in THF (20 mL) was placed in a 100-mL flask equipped with a three-way stopcock under N_2 at -78 ºC. *n*-BuLi (1.6 M in hexane, 6.82 mL, 10.80 mmol, 2.2 eq.) was slowly added with a syringe, and the mixture was stirred for 2 hours at -78 ºC. Trimethyl borate (2040 mg, 19.60 mmol) was added, and the mixture was stirred ambient temperature for 24 h. Aq. HCl (2M) was added to the system in excess, and the resulting mixture was vigorously stirred for 2 h. The raw material was extracted with diethyl ether and washed with water. Removal of the solvent from the soluble led to the crude product which was washed with hexane to yield the targeted compound: yield 0.46 g (27 %). ^{1}H NMR (400 MHz, $CDCl_3$, r.t.): 7.38 ppm (2H, s), 6.38 ppm (4H, s), 3.88-4.01 ppm (4H, m), 1.87-1.95 ppm (2H, m), 1.50-1.61 ppm (2H, m), 1.28-1.35 ppm (2H, m), 1.06 ppm (6H, d, J = 6.8 Hz), 0.97 ppm (6H, t, J = 7.5 Hz). ^{13}C NMR (600 MHz, $CDCl_3$, r.t.) δ/ppm: 158.4, 118.3, 73.8, 34.9, 26.4, 16.9, 11.4. FT-IR (KBr) υ/cm^{-1}: 3358, 2964, 2927, 2877, 1497, 1430, 1390, 1308, 1270, 1199, 1135, 1096, 1060, 779, 712, 640, 553.

The spectral data for this compound are indicated in Figure 2-45, 2-46 and 2-47.

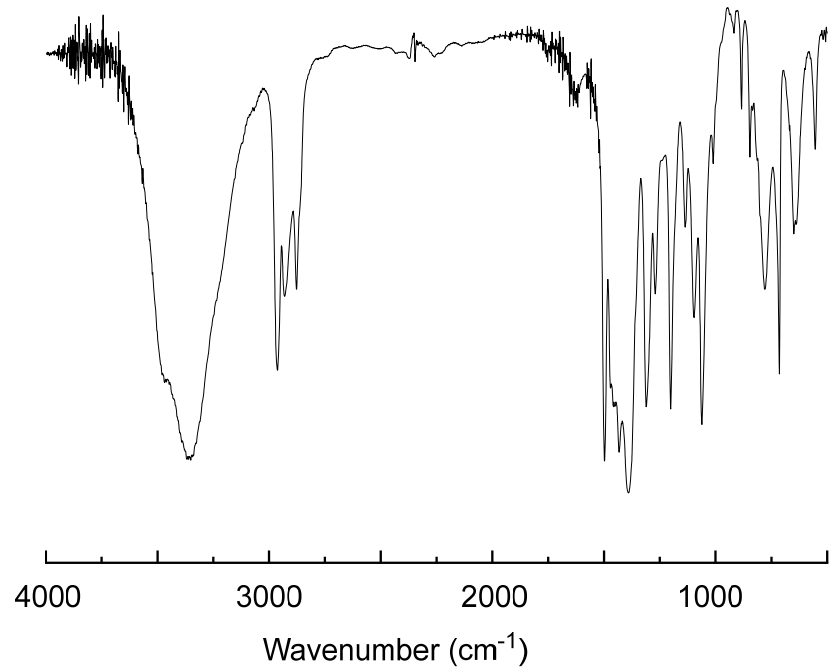

Figure 2-45. IR spectrum of 1,4-dihyroxyboranyl-2,5-bis((*S*)-2-methylbutoxy)benzene.

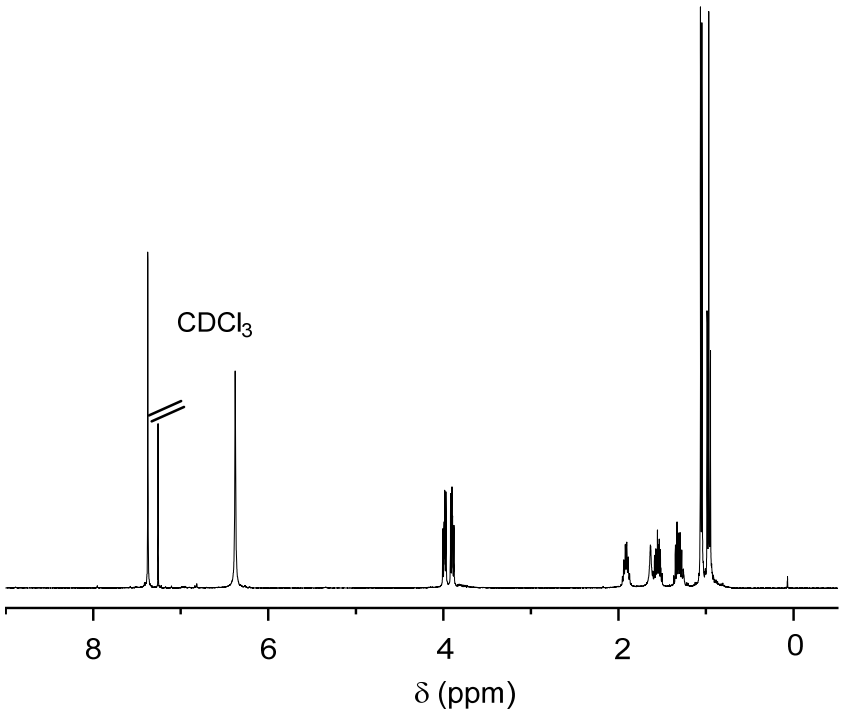

Figure 2-46. ^{1}H NMR spectrum of 1,4-dihyroxyboranyl-2,5-bis((*S*)-2-methylbutoxy)benzene. [400 MHz, $CDCl_3$, r.t.].

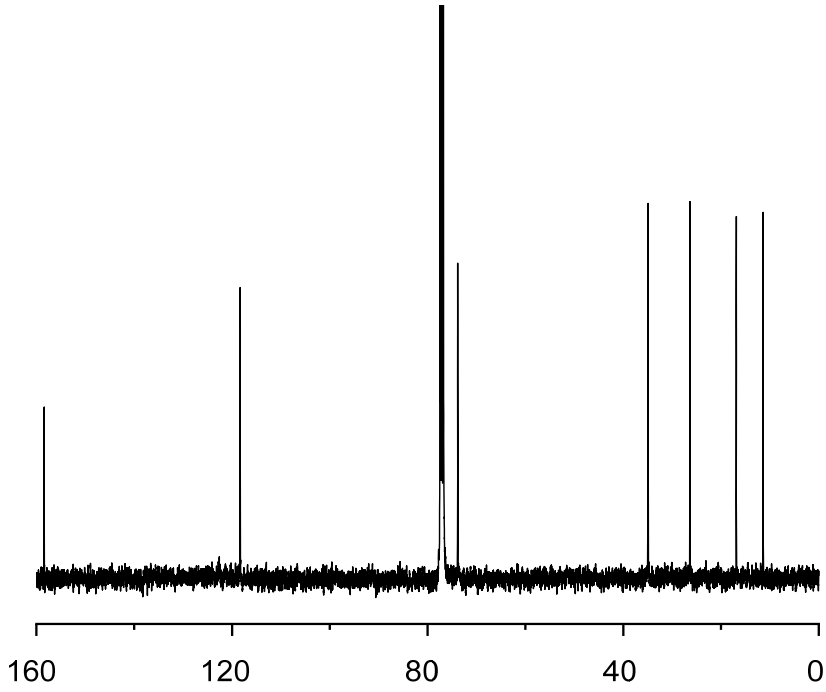

Figure 2-47. ^{13}C NMR spectrum of 1,4-dihyroxyboranyl-2,5-bis((*S*)-2-methylbutoxy)benzene. [600 MHz, $CDCl_3$, r.t.].

References

1. Yashima, E.; Ousaka, N.; Taura, D.; Shimomura, K.; Ikai, T.; Maeda, K. *Chem. Rev.* **2016**, *116*, 13752-13990.

2. Yashima, E.; Maeda, K.; Iida, H.; Furusho Y.; Nagai, K. *Chem. Rev.* **2009**, *109*, 6102-6211.

3. Nakano, T.; Okamoto, Y. *Chem. Rev.* **2001**, *101*, 4013-4038.

4. Okamoto, Y.; Nakano, T. *Chem. Rev.* **1994**, *94*, 349-372.

5. Nakano, T.; Nakagawa, O.; Tsuji, M.; Tanikawa, M.; Yade, T.; Okamoto, Y. *Chem. Commun.* **2004**, 144-145.

6. Nakano, T. *J. Chromatogr. A* **2001**, *906*, 205-225.

7. Kovacic, P.; Jones, M. B. *Chem. Rev.* **1987**, *87*, 357-379.

8. Yamamoto, T.; Hayashi, Y.; Yamamoto, A. *Bulletin of the Chemical Society of Japan* **1978**, *51*, 2091-2097.

9. Ballard, D. G. H.; Courtis, A.; Shirley, I. M.; Taylor, S. C. *Macromolecules* **1988**, *21*, 294-304.

10. Rehahn, M.; Schlüter, A.-D.; Wegner, G.; Feast, W. J. *Polymer* **1989**, *30*, 1054-1059.

11. Rehahn, M.; Schlüter, A.-D.; Wegner, G.; Feast, W. J. *Polymer* **1989**, *30*, 1060-1062.

12. Fiesel, R.; Huber, J.; Apel, U.; Enkelmann, V.; Hentschke, R.; Scherf, U.; Cabrera, K. *Macromol. Chem. and Phys.* **1997**, *198*, 2623-2650.

13. Chen, S. H.; Conger, B. M.; Mastrangelo, J. C.; Kende, A. S.; Kim, D. U. *Macromolecules* **1998**, *31*, 8051-8057.

14. Fiesel, R.; Huber, J.; Scherf, U.; Cabrera, K. *Enantiomer* **1998**, *3*, 383-389.

15. Fiesel, R.; Scherf, U. *Acta Polymerica* **1998**, *49*, 445-449.

16. Chen, S. H.; Katsis, D.; Schmid, A. W.; Mastrangelo, J. C.; Tsutsui, T.; Blanton, T. N. *Nature* **1999**, *397*, 506-508.

17. Chen, H. P.; Katsis, D.; Mastrangelo, J. C.; Marshall, K. L.; Chen, S. H.; Mourey, T. H. *Chem. Mater.* **2000**, *12*, 2275-2281.

18. Hayasaka, H.; Miyashita, T.; Tamura, K.; Akagi, K. *Adv. Funct. Mater.* **2010**, *20*, 1243-1250.

19. Okamoto, Y.; Suzuki, K.; Ohta, K.; Hatada, K.; Yuki, H. *J. Am. Chem. Soc.* **1979**, *101*, 4763-4765.

20. Nakano, T.; Okamoto, Y.; Hatada, K. A *J. Am. Chem. Soc.* **1992**, *114*, 1318-1329.

21. Nakano, T. *Polym. J.* **2010**, *42*, 103-123.

22. Nakano, T.; Yade, T. *J. Am. Chem. Soc.* **2003**, *125*, 15474-15484.

23. Nakano, T.; Takewaki, K.; Yade, T.; Okamoto, Y. *J. Am. Chem. Soc.* **2001**, *123*, 9182-9183.

24. Okamoto, Y.; Hatada, K. *Journal of Liquid Chromatography* **1986**, *9*, 369-384.

25. Okamoto, Y.; Honda, S.; Okamoto, I.; Yuki, H.; Murata, S.; Noyori, R.; Takaya, H. *J. Am. Chem. Soc.* **1981**, *103*, 6971-6973.

26. Yuki, H.; Okamoto, Y.; Okamoto, I. *J. Am. Chem. Soc.* **1980**, *102*, 6356-6358.

27. Okamoto, Y.; Ikai, T. *Chemical Society Reviews* **2008**, *37*, 2593-2608.

28. Okamoto, Y.; Yashima, E. *Angew. Chem. Int. Edit.* **1998**, *37*, 1020-1043.

29. Shen, J.; Okamoto, Y. *Chem. Revi.* **2015**, *116*, 1094-1138.

30. Yashima, E. *Journal of chromatography A* **2001**, *906*, 105-125.

31. Wehrmann, C. M.; Charlton, R. T.; Chen, M. S. *J. Am. Chem. Soc.* **2019**, *141*, 3240-3248.

32. Yamamoto, T.; Choi, B.-K.; Kubota, K. *Polym. J. (Tokyo)* **2000**, *32*, 619-621.

33. Mori, T.; Akagi, K. *Macromolecules* **2013**, *46*, 6699-6711.

34. Sun, H. *J. Phys. Chem.* **1998**, *102*, 7338-7364.

35. Tanaka, S.; Sato, K.; Ichida, K.; Abe, T.; Tsubomura, T.; Suzuki, T.; Shinozaki, K. *Chem. Asian J.* **2016**, *11*, 265-273.

36. Nakano, T.; Satoh, Y.; Okamoto, Y. *Macromolecules* **2001**, *34*, 2405-2407.

37. Cheng, X.; Miao, T.; Yin, L.; Ji, Y.; Li, Y.; Zhang, Z.; Zhang, W.; Zhu, X. *Angew. Chem. Int. Ed.* **2020**, *59*, 9669-9677.

38. Cheng, X.; Miao, T.; Ma, Y.; Zhang, W. *ChemPlusChem* **2022**, *87*, e202100556.

39. Song, Z.; Sato, H.; Pietropaolo, A.; Wang, Q.; Shimoda, S.; Dai, H.; Imai, Y.; Toda, H.; Harada, T.; Shichibu, Y.; Konishi, K.; Bando, M.; Naga, N.; Nakano, T. *Chem. Commun.* **2022**, *58*, 1029-1032.

40. Zhang, Z.; Harada, T.; Pietropaolo, A.; Wang, Y.; Wang, Y.; Hu, X.; He, X.; Chen, H.; Song, Z.; Bando, M.; Nakano, T. *Chem. Commun.* **2021**, *57*, 1794-1797.

41. Wang, Q.; Pietropaolo, A.; Fortino, M.; Song, Z.; Bando, M.; Naga, N.; Nakano, T. *Chirality* **2021**, *34*, 1-8.

42. Wang, Y.; Wang, R.; Imai, Y.; Hara, N.; Wan, X.; Nakano, T. *New J. Chem.* **2018**, *42*, 14713-14716.

43. Zhang, Z.; Wang Y.; Nakano, T. *Molecules* **2016**, *21*, 1541.

44. Wang, Y.; Kanibolotsky, A. L.; Skabara, P. J.; Nakano, T. *Chem. Commun.* **2016**, *52*, 1919-1922.

45. Pietropaolo, A.; Wang, Y.; Nakano, T. *Angew. Chem. Int. Edit.* **2015**, *127*, 2726-2730.

46. Wang, Y.; Sakamoto, T.; Koyama, Y.; Takanashi, Y.; Kumaki, J.; Cui, J.; Wan, X.; Nakano, T. *Polymer Chemistry* **2014**, *5*, 718-721.

47. Nakano, T. *The Chemical Record* **2014**, *14*, 369-385.

48. Pietropaolo, A.; Nakano, T. *J. Am. Chem. Soc.* **2013**, *135*, 5509-5512.

49. Wang, Y.; Sakamoto, T.; Nakano, T. *Chem. Commun.* **2012**, *48*, 1871-1873.

50. Hattori, T.; Shimazumi, Y.; Yamabe, O.; Koshiishi, E.; Miyano, S. *Chem. Commun.* **2002**, *19*, 2234-2235.

51. Imamura, A.; Hoffmann, R. *J. Am. Chem. Soc.* **1968**, *90*, 5379-5385.

52. Fortino, M.; Cozza, C.; Bonomi, M.; Pietropaolo, A. *Chem Phys.* **2021**, *154*, 174108.

53. Fletcher, R.; Reeves, C. M. *Comput. J.* **1964**, *7*, 149-154.

54. Berendsen, H. J. C.; Postma, J. P. M.; van Gunsteren, W. F.; DiNola, A.; Haak, J. R. *J. Chem. Phys.* **1984**, *81*, 3684-3690.

55. Fiesel, R.; Scherf, U. *Acta Polymerica* **1998**, *49*, 445-449.

Chapter 3. Distinctive Form Chirality Induced to Poly(naphthalene-1,4-diyl)

3.1 Introduction

Optically active poly(naphthalene-1,4-diyl) was prepared through helix-sense-selective polymerization (HSSP) of the corresponding monomers and through circularly polarized light (CPL) irradiation, resulting in distinctive circular dichroism (CD) spectral patterns. Chirality of the HSSP-based polymer is ascribed to preferred-handed helicity while that of the CPL-based polymer to inter-chain arrangement or a non-helical, chiral conformation with preferred-handedness which was stable only in the solid state. The helix of the HSSP-based polymer gradually racemized in tetrahydrofuran while it was stabilized by aggregate formation in a hexane-dichloromethane solution. Both HSSP- and CPL-based polymers exhibited efficient CPL emission in film.

Macromolecules having a single-handed helical structure are useful sources of optically active polymeric materials showing functions including resolution of racemic compounds, asymmetric catalysis, and circularly polarized light (CPL) emission.[1-8] One of the most established methods of polymer helix synthesis is helix-sense-selective polymerization (asymmetric helix-chirogenic polymerization) where single-handedness arises from chirality of ligands used in the polymerization or of monomeric units.[9-11] In addition, single-handed helix can be dynamically controlled through interactions of polymer chain with external, chiral molecules.[12-16] Apart from these established methodologies, a newer way to create single-handed helices has been developed employing CPL as the chirality source. By this method, single-handed helicity was introduced to polyfluorene derivatives as well as related small- to medium-sized molecules. In addition, various azobenzene-containing polymers have been made optically active using CPL. While there have been a number of reports on asymmetric polymerization resulting in helical polymers and also reports on CPL-driven chirality induction to polymers, direct comparisons between the two methods using the same macromolecules have never been conducted. This work for the first time makes a direct comparison between asymmetric polymerization and CPL

method in the preparation of optically active poly(naphthalene-1,4-d)yl) (poly(Naph)).[17-22]

Helix-sense-selective polymerization was carried out by Suzuki-Miyaura cross coupling (SMC) with Pd catalysis and Kumada-Tamao-Corriu cross coupling (KTCC) with Ni catalysis using (*R*)-2,2'-bis(diphenylphosphino)-1,1'-binaphthyl） (BINAP), (*R*)-(+)-4,4'-bis(diphenylphosphino)-3,3'-bi(1,2-methylenedioxybenzene) (Segphos), and (*R,R*)-2,3-Bis(tert-butylmethylphosphino)quinoxaline (Quinox-P*) as chiral ligands, and the CPL-method was conducted for the optically inactive, "racemic" samples prepared by SMC and Yamamoto coupling (YC) using Ni species (Scheme 3-1 A).

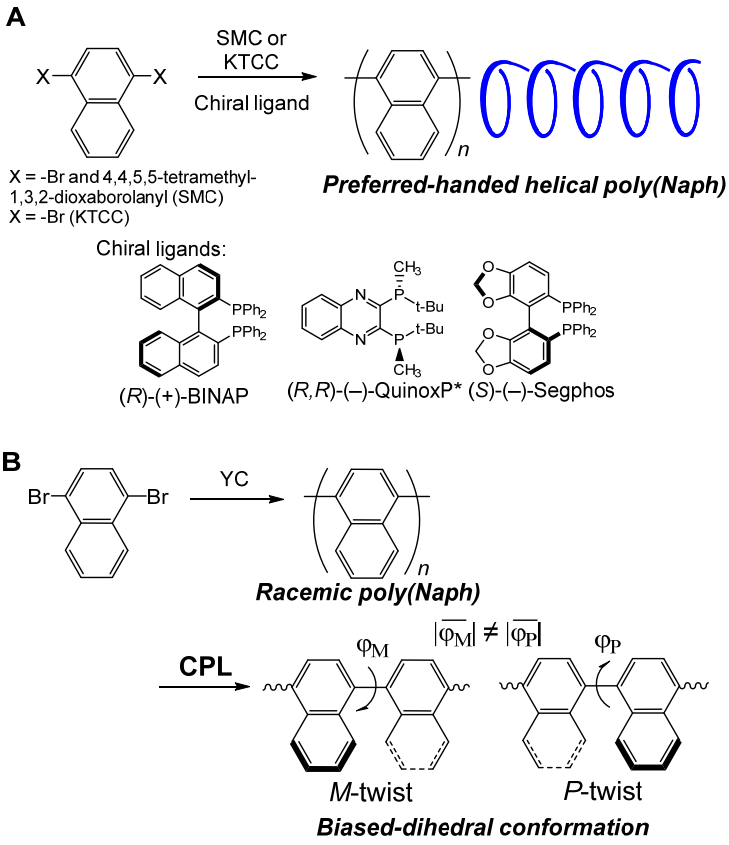

Scheme 3-1. Synthesis of preferred handed helical poly(Naph)s by helix-sense-selective polymerization (A), synthesis and resolution of model 2-mer, and preparation of optically active poly(Naph)s having "biased-dihedral-angle conformation" by CPL irradiation (B).

3.2 Polymerization of Naphthalene

The SMC, KC, and YC polymerization of 1,4-dibromonaphthalene produced at high conversions tetrahydrofuran- and $CHCl_3$-soluble poly(Naph)s with Mn's of around 1900 in addition to a relatively small amount of THF-insoluble products (Tables 1).

Table 3-1. Synthesis of poly(naphthalene-1,4-diyl)[a]

Entry	Solvent	Catalyst	Chiral Ligand	Temp (°C)	Time (h)	Conv.[b] (%)	MeOH-insol. part			
							THF-soluble.			THF-insol.
							Yield (%)	M_n[c]	M_w/M_n[c]	Yield (%)
1	THF	$Ni(acac)_2$	-	r.t.→70	10→0.5	>99	49	3816	1.31	40
2	THF	$Ni(acac)_2$	-	r.t.→70	10→1	>99	48	3498	1.23	45
3	THF	$Ni(acac)_2$	-	r.t.→70	10→18	>99	55	3498	1.27	39
4	THF/$CHCl_3$[d]	$Ni(acac)_2$	-	r.t.→70	10→18	>99	18	2449	1.12	-
5	THF/Toluene[d]	$Ni(acac)_2$	-	70	1	>99	49	3498	1.22	19
6	THF/Toluene[d]	$Ni(acac)_2$	-	70	18	>99	30	3816	1.26	24
7	Toluene	$Ni(cod)_2$	-	85	24	>99	19	2270	1.79	71
8	DME	$Pd(oac)_2$	-	85	24	>99	7	1970	1.69	91
9	THF	$Ni(acac)_2$	(R)-QuinoxP*	r.t.	3	76	16	1590	1.26	-
10	THF	$Ni(acac)_2$	(S)-Segphos	r.t.	3	83	26	2544	1.60	>1
11	THF	$Ni(acac)_2$	(R)-BINAP	r.t.	3	86	45	3050	1.85	2
12	DME	$Pd(oac)_2$	(R)-BINAP	85	24	93	64	1612	1.49	-
13	DME	$Pd(oac)_2$	(R)-BINAP	85	24	92	46	2137	1.99	-
14	Ethanol	$Pd(oac)_2$	(R)-BINAP	85	24	85	99	1145	1.16	-
15	Toluene	$Pd(oac)_2$	(R)-BINAP	85	24	94	69	1889	1.49	-
16	Toluene	$Pd(oac)_2$	(S)-BINAP	85	24	91	53	2000	1.32	-
17	Toluene	$Pd(oac)_2$	(R)-Segphos	85	24	>99	43	2019	1.30	-
18	Toluene	$Pd(oac)_2$	(R)-QuinoxP*	85	24	97	44	1650	1.42	-

[a][Monomer]$_0$ = 0.175 M (entry 1-6, 9-11), 0.04 M (entry 7), 0.2 M (entry 8, 12-18). [$Ni(acac)_2$] = 1.65×10^{-3} M (1 mol%, entry 1-6, 9-11), [$Ni(cod)_2$] = 0.12 M (entry 7), [$Pd(oac)_2$] = 0.002 M (entry 13); 0.02 M (entry 8, 12, 14-18). [Chiral ligand] = 1.65×10^{-3} M (1 mol%, entry 9-11), 0.002 M (entry 13); 0.02 M (entry 8, 12, 14-18).
[b]Determined by ^{1}H NMR spectral analysis of crude mixture. [c]Determined by SEC (vs standard polystyrene). [d]A mixture of THF and $CHCl_3$ or toluene (1/1, v/v).

3.3 Conformation of the Polymers

The polymers made SMC and KC using chiral ligands showed circular dichroism (CD) spectra (Figure 3-1). Because poly(Naph) does not have any centers or planes of chirality, the chiroptical properties are ascribed to a preferred-handed helical conformation based on biased twist hand between neighboring monomeric units. The polymers prepared by SMC using (R)-BINAP and by KTCC using (R)-QuinoxP* showed clearer CD spectra with higher intensities than the other polymers. These two polymers showed clear positive Cotton splitting patterns centered at 240 nm (SMC-(R)-BINAP) and 230 nm (KTCC-(R)-QuinoxP*), which resemble the CD

spectra of (S)-isomer of 1,1'-binaphthyl obtained by HPLC resolution as a model 2-mer compound prepared in racemic form by SMC between 1-bromonapthalene and 1-napthaleneboronic acid. Based on the spectral resemblance, the two optically active poly(Naph)s' absolute configuration of helix in excess may be assigned to S with positive twist between neighboring monomeric units. Also, on the basis of spectral intensities of 1,1'-binaphthyl and the two polymers of the negative signal of the Cotton splitting, helix-sense-excess is estimated to be about 3% (SMC-(R)-BINAP) and 1% (KTCC-(R)-QuinoxP*). The other polymers showing weaker CD signals are considered to have much lower helix-sense excesses. It is noteworthy that the two polymers showed different spectral patterns, especially in the range of 270-400 nm, where the polymer prepared by SMC with (R)-BINAP showed an additional positive Cotton splitting centered at around 300 nm while the one prepared by KTCC with (R)-QuinoxP* only a weak and monotonous negative signal. These observations may mean that the two polymers have different tacticities.

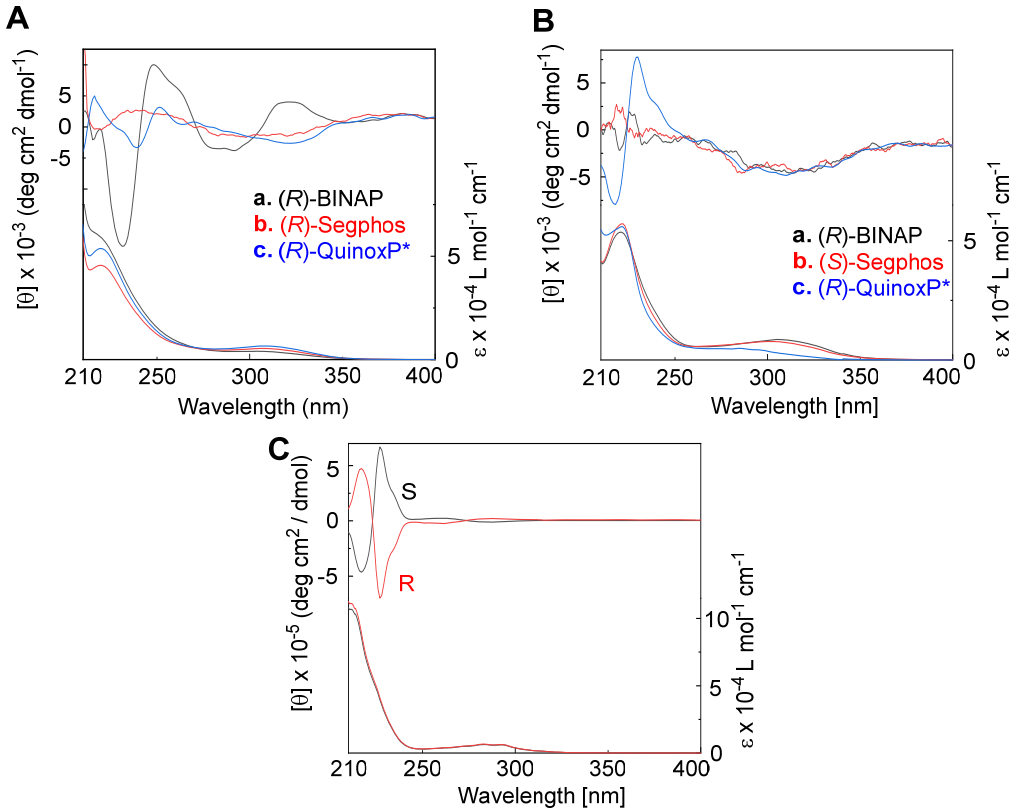

Figure 3-1. CD-UV spectra of poly(Naph)s prepared using (R)-BINAP by SMC (A) and KC (B) and those of enantiomers of 1,1'-binaphtyl obtained by HPLC resolution (C). [conc. = 3 x 10^{-3} M (per residue) (A,B), 1.0 x 10^{-3} M (C) cell path = 1-mm in (A)-(C)].

Stability of chiral conformation of the polymer obtained by SMC with (R)-BINAP as well as (R)-1,1'-binaphthyl as a 2-mer model was assessed by monitoring changes in CD spectra in solution. (R)-1,1'-binaphthyl (e.e. >99%) obtained by HPLC resolution showed a gradual decrease in CD intensity in hexane-dichloromethane (1/1, v/v) solution at 25 ºC (Figure 3-2 A), which is based on racemization as evidenced by HPLC resolution (Figure 3-3). On the other hand, the polymer prepared by did now show clear changes in SMC with (R)-BINAP in hexane-dichloromethane (1/1, v/v) solution (Figure 2 B) while it lost its CD signals in THF solution (Figure 3-2 C) due to racemization. These clear solvent effects on helix stability of poly(Naph) is explained in terms of aggregate formation of the polymer. Dynamic light scattering (DLS) measurements of the polymer in hexane-dichloromethane (1/1, v/v) solution indicated the presence of aggregates with a mean diameter of 200 nm while aggregate formation was not confirmed in THF. Aggregate formation of the polymer chains seems thus hampers racemization of the helix.

This conclusion was further supported by calculations of energy-barriers of rotation around the single bond connecting the two naphthyl groups of 1,1'-binaphthyl and around the single bond connecting the neighboring naphthyl groups at the center of a 4-mer model and a 10-mer model. The three species were predicted to have very similar barriers (around 23 kcal/mol) at the semiempirical PM6 level, suggesting that extending of the length of single chain itself does not contribute to helix stability but longer chains tend to form aggregates that hamper helix reversal.

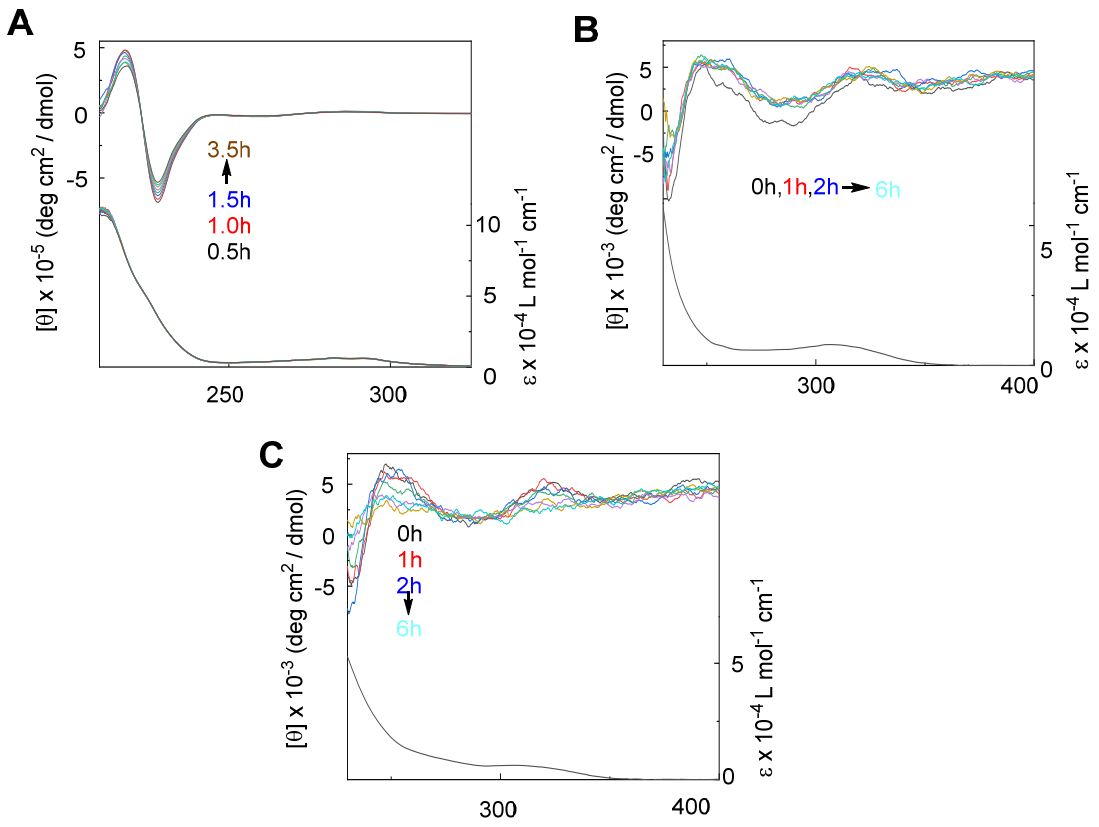

Figure 3-2. Changes in CD-UV spectra of (R)-1,1'-binaphthyl in hexane-dichloromethane (1/1, v/v) (A) and of poly(Naph) prepared by SMC with (R)-BINAP by SMC in hexane-dichloromethane (B) and in THF (C). [conc. = 3 x 10^{-3} M (per residue) (A), 1.0 x 10^{-3} M (B) cell path = 1 mm, temp. 25 °C].

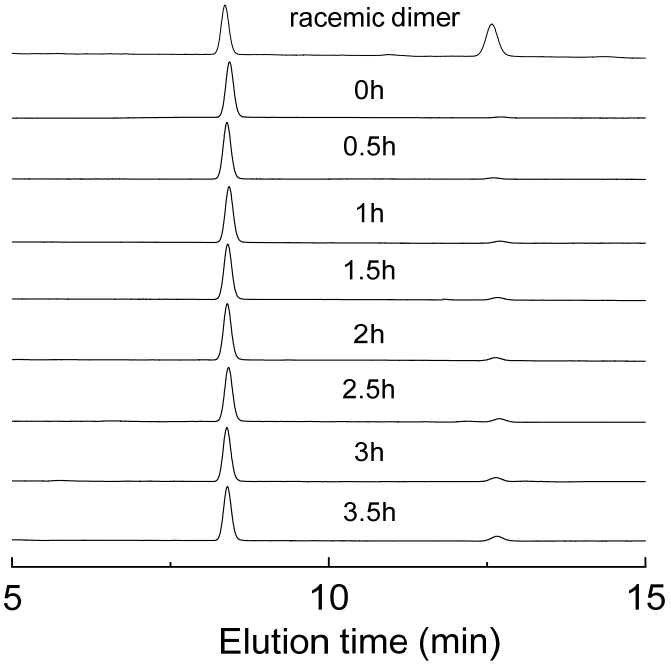

Figure 3-3. Changes in HPLC spectra of (R)-1,1'-binaphthyl in hexane-dichloromethane (1/1, v/v) (ChiralPAK IA, flow rate 0.5 ml/min).

Next, chirality induction using CPL was studied for the racemic polymer prepared by YC without using chiral ligands. This method was applied to film samples of the polymer prepared by casting a THF solution to quartz glass plate. In order to minimize the effects of linear dichroism, CD spectra were obtained by averaging those recorded at four different film orientations (angles) at an interval of 90o with the film face positioned vertically to the incident light beam for measurement. The CPL-irradiated films showed clear and intense CD spectra where L- and R-CPL irradiation resulted in mirror image spectra (Figure 3A), indicating that oppositely handed chiral conformations were induced by using opposite-handed CPL for irradiation. In addition, IR spectral studies indicated that no remarkable changes in the chemical structure of poly(Naph) was caused by irradiation. In addition, chirality induction was reversible where the positive CD signals induced by L-CPL were changed into the negative CD signals by additional R-CPL irradiation, and the positive signals were recovered by through further irradiation by L-CPL (Figure 3-4 B).

Maximum CD intensities were reached within about 15 min of irradiation, which was much faster than induction for helix-induction to polyfluorene derivatives and related molecules (Figure 3-4 C). Further, a decrease in UV intensity was also observed by CPL irradiation, this may be ascribed not to chemical modifications but to a decrease in the dihedral angle between neighboring naphthalene-1,4-diyl units which has been reported for biphenyl.

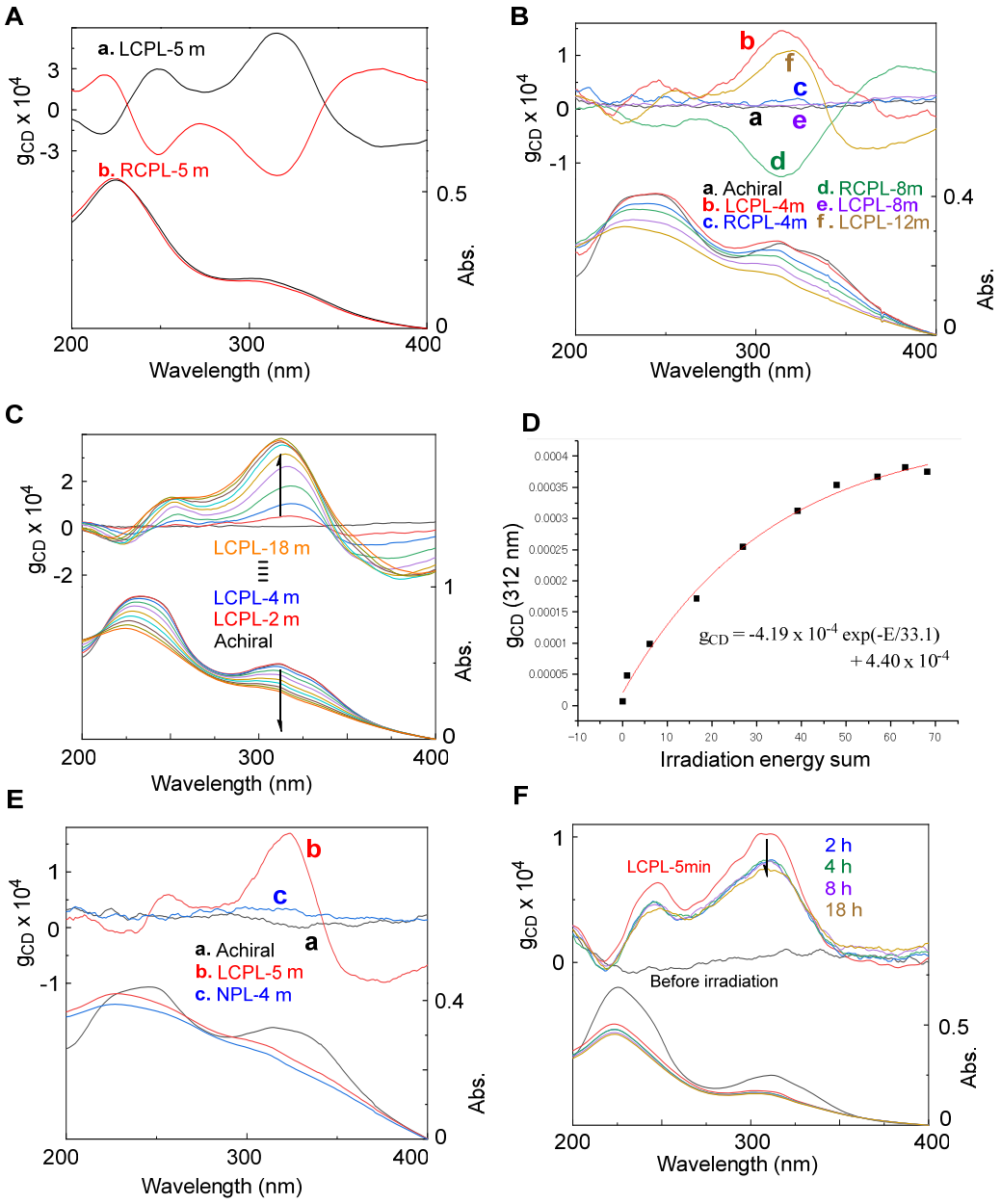

Figure 3-4. CD-UV spectra of poly(Naph) films prepared by P- and M-CLP irradiation (top and bottom, respectively) (A), changes in CD-UV spectra of the film prepared by L-CPL irradiation on R-CPL irradiation [reversibility of chirality induction] (B), changes in CD-UV spectra depending on L-CPL irradiation time (C), g_{CD}-vs.-irradiation energy sum plot corresponding to the data in C (D), changes in CD-UV spectra of the film prepared by L-CPL irradiation on achiral NPL irradiation (E), and changes in CD-UV spectra of the film prepared by L-CPL irradiation upon heating at 100 ºC (F).

The chirality induction rate was evaluated by plotting g_{CD} against the irradiation energy sum where the plot was well approximated by an exponential decay in increasing form (Figure 3-4 D). This result was in a sharp contrast to that the

reported helix induction to a polyfluorene derivative was approximated by a power function implying chirality amplification where helix formation was established by metadynamics calculations, suggesting that chirality induction to poly(Naph) is not based on helix formation. This aspect is supported by the fact that CD spectral shapes induced by CPL are rather different from those of the polymers prepared by asymmetric polymerization and also by the fact that chirality was immediately lost when the CPL-irradiated films were dissolved in hexane-dichloromethane (1/1, v/v) in which helix can be stabilized as discussed for the polymer prepare by SMC with (R)-BINAP.

As a chiral structure of poly(Naph) induced by CPL, "biased-dihedral conformation" is proposed (Scheme 3-1 B). This conformation is composed of right- and left-handed twists between the neighboring naphthyl groups of the same number (racemic from a view of twist hand population) but the right- and left-handed twists are not mirror images having different average angles. As changes in dihedral angle is induced by irradiation to aryl-aryl compounds including biphenyl and related molecules and polymers, CPL can induce changes in dihedral to different extents for right- and left-handed twists even if it does not induce full rotation modifying right-handed twist to left-handed twist (helix induction). The chiral structure of poly(Naph) induced by CPL was rather stable on heating. At 100 deg, the CD intensity was decreased by about 15% in 18 h and thereafter almost unchanged (Figure 3-4 F) whereas at 60 deg, the loss of CD was only 5% in 18h. On the other hand, on irradiation with intense linearly polarized light (LPL), the CD spectrum was swiftly erased.

Optically active poly(Naph) samples prepared by asymmetric polymerization and CPL irradiation exhibited efficient CPL emission properties. The polymer synthesized by SMC with (R)-BINAP showed the CPL spectrum centered at around 400 nm with positive sign of glum of the 10^{-3} order in film (Figure 3-5 A). The films of the polymers synthesized by YC without chiral ligand and irradiated by CPL also indicated CPL emission with glum of the 10-3 order where the film irradiated with L- and R-CPL exhibited positive and negative CPL emission, respectively. These results indicate that the polymers irradiated with L- and R-CPL have enantiomeric

structures in excited states and also that CPL emission handedness of poly(Naph) can be tuned by choosing the handedness of CPL used to induce the biased-dihedral conformation.

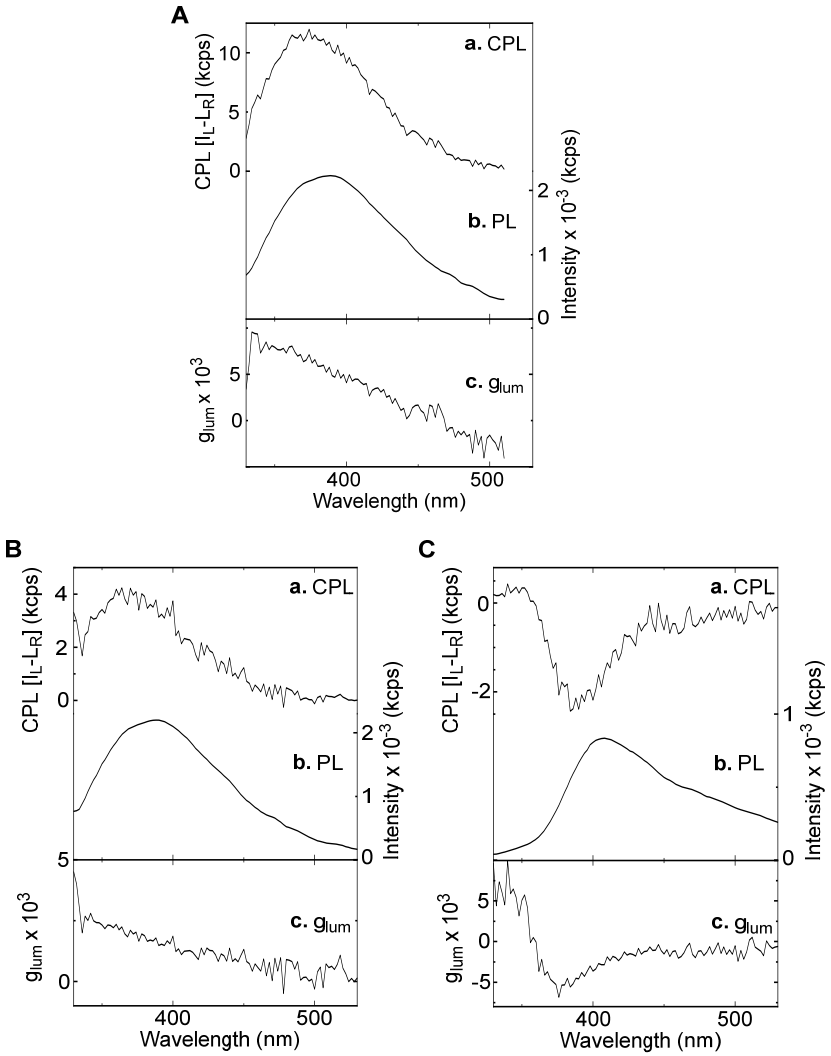

Figure 3-5. CPL spectra of cast film samples of poly(Naph)s prepared by SMC with (R)-BINAP (A) and prepared by YC without chiral ligand and irradiated by L-CPL (B) and R-CPL (C). [λ_{ex} 260 nm].

3.4 Conclusions

Racemic In conclusion, optically active poly(Naph)s were prepared by asymmetric polymerization using chiral ligands and by CPL irradiation, resulting in distinctive chiral conformations. The former method led to a preferred-handed helical

conformation of the chain that is maintained in solution where chain aggregation stabilizes helix. The helix-sense excess was estimated by comparing CD intensities between the polymers and 1,1'-binaphthyl as a dimer model with e.e. of >99%. The latter method led to biased-dihedral conformation whose populations of P- and M-twists are equal and average dihedral angles of the opposite-handed twists are unequal. This structure may be regarded as a new chiral conformation of polymers. Poly(Naph)s prepared by the two methods exhibited efficient blue CPL emission, and facile control over CPL emission signs was realized by the CPL-irradiation method by simply choosing signs of irradiation CPL. While chiral polymers composed of 2,2'-dihydroxy-1,1'-biphenyl units with high rotational stability have been well studied, chirality control over poly(Naph), one of the simplest poly(bezene-1,4-diyl) derivatives, has not been reported possibly due to a general impression that poly(Naph) would be unstable with a low rotation barrier. This work clarified that poly(Naph) can assume a stable helix supported by aggregate formation and also it can assume biased-dihedral conformation, a non-helical chiral conformation and that both conformations can result in efficient CPL emission. Studies are under way to shed light on details of the non-helical, chiral conformation, to extend it to other polymers.

3.5 Experimental

3.5.1 General Instrumentation

^{1}H NMR spectra in solution were recorded on a JEOL JNM-ECX400 spectrometer (400 MHz for ^{1}H measurement) and a JEOL JNM-ECA600 spectrometer (600 MHz for ^{1}H measurement). SEC measurements were carried out using a chromatographic system consisting of a Hitachi L-7100 chromatographic pump, a Hitachi L-7420 UV detector (254 nm), and a Hitachi L-7490 RI detector equipped with TOSOH TSK gel G3000HHR and G6000HHR columns (30 x 0.72 (i.d.) cm) connected in series (eluent THF, flow rate 1.0 mL/min). Preparative SEC analyses were carried out using JAI LC-9201 recycling preparative HPLC with UV/VIS detector S-3740 and column

JAIGEL-1H, 2H (eluent $CHCl_3$, flow rate 3.0 mL/min), JAI LC-9201 recycling preparative HPLC with UV/VIS detector UV-50, RI detector RI-50 and column JAIGEL-1H, 2H (eluent $CHCl_3$, flow rate 3.0 mL/min), A Laboace LC-5060 recycling preparative HPLC with UV/VIS detector 4ch800LA and RI detector 700LA equipped with JAIGEL-1RH, 2RH, and 3RH columns connected in series (eluent $CHCl_3$, flow rate 10.0 mL/min). UV-vis absorption spectra were measured at room temperature with a JASCO V-570 spectrophotometers. Steady-state emission spectra were taken on a JASCO FP-8500 fluorescence spectrophotometer. Circular dichroism (CD) spectra were taken with a JASCO-820 spectrometer. The spectra of films were obtained by averaging those recorded at four different film orientations (angles) at an interval of 90° with the film face positioned vertically to the incident light beam for measurement. The anisotropy factor (g_{CD}) was calculated according to g_{CD} = ΔAbs/Abs = (ellipticity/32980)/Abs. DLS measurements were performed using an Otsuka Electronics FDLS-3000 fiber-optics dynamic light scattering spectrophotometer. CPL spectra were measured with a JASCO-300 spectrometer and also with an assembled apparatus based on a photo elastic modulator and a photomultiplier. The emission anisotropy factor (g_{lum}) was calculated according to $g_{lum} = 2(I_L - I_R)/(I_L + I_R)$ where I_L and I_R are the emission intensities of *L*- and *R*-CPL, respectively. TEM images were obtained on a JEM-2100F microscope at 200 kV using a microgrid. XRD profiles were measured using a Rigaku MiniFlex600-C diffractometer.

3.5.2 Computer Simulation

Molecular mechanics structure optimization was conducted using the COMPASS force field implemented in the Discover module of the Material Studio 2.0 (Accelrys) software package with the Fletcher-Reeves conjugate gradient algorithm until the RMS residue went below 0.01 kcal/mol/Å. Molecular dynamic simulation was performed under a constant NVT condition in which the numbers of atoms, volume, and thermodynamic temperature were held constant.

Berendsen's thermocouple was used for coupling to a thermal bath. The step time was 1 fs and the decay constant was 0.1 ps.

3.5.3 Materials

1,4-Dibromonaphthalene (TCI), $Pd(OAc)_2$ (TCI), $PdCl_2$ (Wako), (*R*)-2,2'-bis(diphenylphosphino)-1,1'-binaphthyl) (BINAP) (TCI), (*R*)-(+)-4,4'-bis(diphenylphosphino)-3,3'-bi(1,2-methylenedioxybenzene) Segphos (TCI), (*R,R*)-2,3-Bis(tert-butylmethylphosphino)quinoxalineQinoxP* (Sigma), *t*-BuOK (TCI), potassium hydroxide (Kanto), $CHCl_3$ (Kanto), methanol (Kanto), acetone (Kanto), dimethylformamide (Wako) and Silica-gel 60 N (neutral) (Kanto) were used as purchased. Tetrahydrofuran (THF) (Wako) was dried with calcium hydride under nitrogen flow.

2,2'-(1,4-Naphthalenediyl)bis[4,4,5,5-tetramethyl-1,3,2-dioxaborolane] (1).[23] 1,4-Dibromonaphthalene (10.00 g, 34.97 mmol), bis(pinacolato)diborane (19.54 g, 76.93 mmol), CH_3COOK (7.55 g, 76.93 mmol) and dichlorobis(triphenylphosphine)palladium (2.45 g, 3.50 mmol) were mixed with a degassed mixture of 1,4-dioxane (200 mL) in a 500-mL flask under nitrogen, and the reaction mixture was stirred at 100ºC for 24 h. Add 100 mL water and 100 mL ethyl acetate to the mixture after cooling at ambient temperature, and the raw material was extracted with ethyl acetate. The organic layer was washed by water and dried over anhydrous $MgSO_4$, and removal of the solvent resulted in the crude product which was purified by silica gel column chromatography using hexane/ethyl acetate (20/1, V/V) as eluent: yield 11.08 g (83 %). ^{1}H NMR (400 MHz, $CDCl_3$, r.t.) δ/ppm: 8.76-8.73 (2H, dd, *J* = 3.4, 3.4 Hz), 8.02 (2H, s), 7.52-7.50 (2H, dd, *J* = 3.4, 3.4 Hz), 1.42 (24H, s).

Synthesis of poly(naphthalene-1,4-diyl) by Kumada-Tamao-Corriu coupling (Scheme 3-2). Polymers were synthesized according to the Kumada-Tamao-Corriu cross coupling using $Ni(acac)_2$ as catalyst. As an example, the synthetic procedure for run **5** is described. A solution of Mg (1.05 mmol, 25.5 mg) and a small amount of I_2 in

distilled THF (1.0 mL) was placed in a dried 10-mL flask equipped with a three-way stopcock under N_2. The mixture was heated to 70 ºC and reflux for 30 min. 1,4-dibromonaphthalene (0.70 mmol, 200.0 mg) dissolved in distilled THF (1 mL) was introduced into the mixture slowly with stirring and reflux for 1 h. Then $Ni(acac)_2$ (0.007 mmol, 1.8 mg) dissolved in distilled toluene (2 mL) was add into the mixture slowly with stirring and reflux for 1 h. The polymerization was quenched by the addition of aq. HCl solution (1.4 N, 0.5 mL) and methanol (0.5 mL). Crude products were extracted with chloroform and remove the organic solvent resulted in the crude polymer. Washed it with THF (50 mL) and collected with a centrifuge, resulting in THF-insoluble part (yield 16.6 mg, 19 %). Then reprecipitation THF-soluble in methanol (50 mL) after concentrate the THF solution to about 5mL and collected the polymer with a centrifuge to get a light yellow powder (yield 43.3 mg, 49 %, M_n 3498, M_w/M_n 1.22 (SEC using polystyrene standard)): ^{1}H NMR (400 MHz, $CDCl_3$, r.t.) δ/ppm: 8.07-7.27.

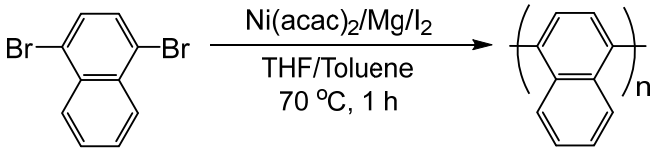

Scheme 3-2. Synthesis of poly(naphthalene-1,4-diyl) by Kumada-Tamao-Corriu coupling polymerization using $Ni(acac)_2$ as catalyst in THF/toluene.

Synthesis of poly(naphthalene-1,4-diyl) by Yamamoto coupling (Scheme 3-3). Polymers were synthesized according to the Yamamoto coupling using $Ni(COD)_2$ as catalyst. As an example, the synthetic procedure for run **7** is described. A solution of 1,5-cyclooctadiene (2.1 mmol, 227.0 mg), 2,2'-bipyridine (2.1 mmol, 328.0 mg) and $Ni(COD)_2$ (2.1 mmol, 577 mg) in distilled toluene (7 mL) was placed in a dried 30-mL flask equipped with a three-way stopcock under N_2. The mixture was heated to 85 ºC for 30 min, leading to a deep purple solution. 1,4-dibromonaphthalene (0.70 mmol, 200.0 mg) dissolved in distilled toluene (10 mL) was introduced into the Ni-species-containing, deep purple solution with stirring. The polymerization reaction

was carried out at 85 ºC for 24 h. Crude products were washed twice with methanol (100 mL) and then twice with aq. EDTA (pH= 5 and 9, 100 mL) in this order and were collected with a centrifuge. The washed material was washed twice with THF (50mL) and collected with a centrifuge, resulting in THF-insoluble part (yield 62.7 mg, 71 %) and THF-soluble part (yield 16.7 mg, 19 %, M_n 2270, M_w/M_n 1.79 (SEC using polystyrene standard)). THF-soluble polymer was further purified by preparative SEC: ^{1}H NMR (400 MHz, $CDCl_3$, r.t.) δ/ppm: 8.03-7.27.

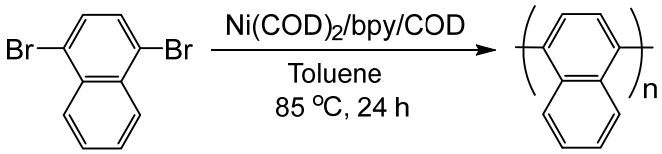

Scheme 3-3. Synthesis of poly(naphthalene-1,4-diyl) by Yamamoto coupling polymerization using $Ni(COD)_2$ as catalyst in toluene.

Synthesis of poly(naphthalene-1,4-diyl) by Suzuki-Miyaura coupling (Scheme 3-4). Polymers were synthesized according to the Suziki-Miyaura cross coupling using $Pd(PPh_3)_4$ as catalyst. As an example, the synthetic procedure for run **8** is described. To a solution of 1,4-dibromonaphthalene (0.35 mmol, 100.0 mg) and 2,2'-(1,4-Naphthalenediyl)bis[4,4,5,5-tetramethyl-1,3,2-dioxaborolane] (0.35 mmol, 133.0 mg) in a degassed DME (1.8 mL) was added a degassed aqueous solution of K_2CO_3 (4 M, 0.6 mL) in a dried 10-mL flask equipped with a three-way stopcock under N_2. $Pd(OAc)_2$ (10 mol%, 7.9 mg) was then introduced to the system, and the reaction mixture was stirred under N_2 at 85 ºC for 24 h. The reaction mixture was quenched by the addition of aq. HCl solution (4 N, 1.2 mL). Crude products were washed twice with H_2O (50 mL) and twice with methanol (50 mL×2 times) in this order and collected with a centrifuge. The washed material was washed twice with THF (50mL) and collected with a centrifuge, resulting in THF-insoluble part (yield 80.4 mg, 91 %) and the obtained THF-soluble polymer was further purified by preparative SEC (yield 6.2 mg, 7 %, M_n 1970, M_w/M_n 1.69 (SEC using polystyrene standard): ^{1}H NMR (400 MHz, $CDCl_3$, r.t.) δ/ppm: 8.40, 8.00-7.93, 7.79-7.27.

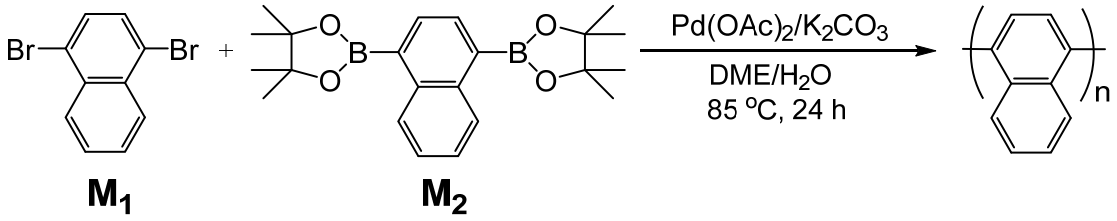

M1 **M2**

Scheme 3-4. Synthesis of poly(naphthalene-1,4-diyl) by Suzuki-Miyaura cross coupling polymerization using $Pd(OAc)_2$ as catalyst in DME.

CPL irradiation to films of poly(Naph)s. Thin-film samples were prepared by drop casting a tetrahydrofuran solution of the polymer (3.0 g/L) on to a quartz plate (1 cm x 2 cm x 0.1 cm). CPL was generated by passing light from an Ushio Optical Modulex SX-UID500MAMQQ 500-W Hg-Xe lamp through a Gran-Taylor prism and a glass-construction Fresnel Rhomb (50 mW (Jsec-1)). LPL was generated using a Gran-Taylor prism only. Irradiation experiments were conducted under N_2 atmosphere at ambient temperature (ca. 23°C). The films of the polymers prepared by SMC with BINAP for CD measurements were prepared in the same manner.

References

[1] E. Yashima, K. Maeda, H. Iida, Y. Furusho, K. Nagai, *Chem. Rev.* **2009**, *109*, 6102-6211.

[2] E. Yashima, N. Ousaka, D. Taura, K. Shimomura, T. Ikai, K. Maeda, *Chem. Rev.* **2016**, *116*, 13752-13990.

[3] T. Nakano, Y. Okamoto, *Chem. Rev.* **2001**, *101*, 4013-4038.

[4] Y. Okamoto, T. Nakano, *Chem. Rev.* **1994**, *94*, 349-372.

[5] M. M. Green, J. W. Park, T. Sato, A. Teramoto, S. Lifson, R. L. B. Selinger, J. V. Selinger, *Angew. Chem. Int. Ed.* **1999**, *38*, 3138-3154.

[6] J. H. K. K. Hirschberg, L. Brunsveld, A. Ramzi, J. A. J. M. Vekemans, R. P. Sijbesma, E. W. Meijer, *Nature* **2000**, *407*, 167-170.

[7] S. Cai, J. Chen, S. Wang, J. Zhang, X. Wan, *Angew. Chem. Int. Ed.* **2021**, 60, 9686-9692; *Angew. Chem.* **2021**, *133*, 9772-9778.

[8] H. Goto, H. Katagiri, Y. Furusho, E. Yashima, *J. Am. Chem. Soc.* **2006**, *128*, 7176.

[9] S. Sakurai, K. Okoshi, J. Kumaki, E. Yashima, *Angew. Chem. Int. Ed.* **2006**, *45*, 1245-1248.

[10] R. Ho, M. Li, S. Lin, H. Wang, Y. Lee, H. Hasegawa, E. L. Thomas, *J. Am. Chem. Soc.* **2012**, *134*, 10974-10986.

[11] H. Gilch, W. Wheelwright, J. *Polym. Sci.* A1 **1966**, *4*, 1337-1349.

[12] S. Jin, H. Park, J. Kim, K. Lee, S. Lee, D. K. Moon, H. Lee, Y. S. Gal, *Macromolecules* **2002**, *35*, 7532-7534.

[13] C. C. Lee, C. Grenier, E. W. Meijer, A. P. H. J. Schenning, *Chem. Soc. Rev.* **2009**, *38*, 671-683.

[14] T. M. Clover, C. L. O'Neill, R. Appavu, G. Lokhande, A. K. Gaharwar, A. E. Posey, M. A. White, J. S. Rudra, *J. Am. Chem. Soc.* **2020**, *142*, 19809-19813.

[15] A. J. Varni, A. Fortney, M. A. Baker, J. C. Worch, Y. Qiu, D. Yaron, S. Bernhard, K. J. T. Noonan, T. Kowalewski, *J. Am. Chem. Soc.* **2019**, *141*, 8858-8867.

[16] K. Suda, K. Akagi, *Macromolecules* **2011**, *44*, 9473-9488.

[17] T. J. Deming, *Chem. Rev.* **2016**, *116*, 786-808.

[18] J. Venkatraman, S. C. Shankaramma, P. Balaram, *Chem. Rev.* **2001**, *101*, 3131-3152.

[19] D. Priftis, L. Leon, Z. Song, S. L. Perry, K. O. Margossian, A. Tropnikova, J. Cheng, M. Tirrell, *Angew. Chem. Int. Ed.* **2015**, *54*, 11128-11132.

[20] D. J. Hill, M. J. Mio, R. B. Prince, T. S. Hughes, J. S. Moore, *Chem. Rev.* **2001**, *101*, 3893-4012.

[21] J. C. Nelson, J. G. Saven, J. S. Moore, P. G. Wolynes, *Science* **1997**, *277*, 1793-1796.

[22] R. S. Lokey, B. L. Iverson, *Nature* **1995**, *375*, 303-305.

[23] S. Werner, T. Vollgraff, J. Sundermeyer, *Angew. Chem. Int. Ed.* **2021**, *60*(24), 13631-13635.

Chapter 4. General Conclusions

This thesis work aimed at creating optically active poly(bezene-1,4-diyl)s including poly(naphthalene-1,4-diyl)s with conformational chirality through catalytic polymerization and through CPL irradiation. We first targeted to shed light on effects of side-chain bulkiness on the formation and stability of chiral conformation of poly(bezene-1,4-diyl)s having random and alternating copolymer architectures. The bulkiness concept and effects established in the helix synthesis of polymetharcrylates have not yet been extended to non-vinyl polymers. As novel poly(benzene-1,4-diyl)s, Random and alternating copoly(bezene-1,4-diyl)s composed of chiral 2,5-bis((S)-2-methylbutoxy)bezene-1,4-diyl units and bulky, achiral 2,5-disubstituted bezene-1,4-diyl units were prepared by Ni-mediated Yamamoto coupling and Pd-catalyzed Suzuki-Miyaura coupling, respectively, and their chiroptical properties were investigated in solution as well as in the solid state (cast film). Poly(benzene-1,4-diyl)s have been studied mainly as conducting polymers having long π-conjugation, and publication about chirality has been rather limited. In this work, systematic studies using the polymers having different bulkiness with an aim to stabilized helix were conducted for the first time for poly(benzene-1,4-diyl)s. Although stabilization of helix by bulkiness of monomeric units that is well known for poly(meth)acrylates was found not successful for the poly(benzene-1,4-diyl) prepared in this work, the copolymers exhibited remarkable chiroptical properties in the solid state (cast film form) while they did not show such properties in solution. It was thus presented that inter-chain interactions between macromolecules can stabilize even rather unstable helical conformation and enhance chiroptical properties. From a view of polymeric materials, this finding is significant because the materials are used basically as solid and what matters about functional materials is solid-state properties and not the solution properties. It may be said that control of helical conformation in solution is not necessarily mandatory and may even be regarded as "overdoing" as far as desired solid-state properties can be attained. In addition, some of the copolymers exhibited resolution abilities for *trans*-stilbene oxide, Tröger's base,

and flavanone, which are typically used to evaluate chiral recognition ability in HPLC, in the batch experiments, which suggests that poly(benzene-1,4-diyl)s may be good candidates of chiral HPLC stationary phases if proper structure is designed. Further, some of the copolymers showed efficient CPL emission properties, which suggests that poly(benzene-1,4-diyl)s may be good candidates of CPL-OLED's. This work thus largely expanded the scope of chiral structure and function of poly(benzene-1,4-diyl)s.

Second, poly(naphthalene-1,4-diyl) was studied as bulky derivatives of poly(bezene-1,4-diyl)s. Indeed, 1,1'-binaphthyl, a dimer model of the polymers, can maintain its axial chirality in solution while biphenyl has a low rotation barrier that allows rather free rotation around the bond connecting the two benzene ring. Preferred-handed helical poly(naphthalene-1,4-diyl) was prepared using chiral P-atom containing ligands through Suzuki-Miyaura cross coupling and Kumada-Tamao-Corriu cross coupling polymerizations. The obtained polymers had helical conformation stable in solution. The stability was attained by chain aggregates formation, and when aggregates did not form due to a solvent property, the preferred-handed helix gradually racemized. It is noteworthy that helix-sense excesses were evaluated for the optically active polymers using optically active 1,1'-binaphthyl obtained by HPLC resolution as a reference compound. This is a very rare example of determination of helix-sense excess of helical polymers. In most examples of helical polymer studies, helix-sense excess has been completely unknown and even not discussed. This work thus made a significant contribution of polymer helix sciences. Further, a racemic poly(naphthalene-1,4-diyl) prepared by Yamamoto coupling polymerization without using chiral ligands was successfully made optically active by CPL-irradiation in film. The CPL-method has been applied only for polyfluorene derivatives to crease helical conformation, but it is now extended to poly(naphthalene-1,4-diyl), suggesting versatility of this method. It should be noted here that helix was induced to polyfluorenes by CPL while CPL created a chiral non-helical conformation of poly(naphthalene-1,4-diyl) where discrepancy in averaged dihedral angle of right- and left-handed twists of diads is proposed. Also,

both the asymmetric polymerization-based polymers and CPL-based polymers with optical activity showed CPL emission, indicating that the two methods are useful in making functional chiral polymers.

This work thus expanded the scope of helical polymers to poly(benzene-1,4-diyl)s which are rather simple to be made and have robust chemical structures from the other examples discussed in Chapter 1. It is especially important that chiral conformation was found to be readily stabilized by solidification (film fabrication), which means useful chiral polymeric materials may possibly prepared even from macromolecules showing poor chiroptical properties in solution. The author hopes that the information disclosed in this thesis may be useful those who work in functional polymers disciplines.

Acknowledgement

I am indebted to my supervisor, Prof. Dr. Tamaki Nakano, whose stimulating motivation, valuable ideas, and warm encouragement were indispensable in completing this thesis work.

I gratefully acknowledge Prof. Dr. Takanori Suzuki, Prof. Dr. Toshihumi Sato, and Prof. Dr. Jun-ya Hasegawa for their reviewing my thesis and helpful advises.

Also, I would love to thank Prof. Dr. Adriana Pietropaolo (Catanzaro University), Prof. Dr. Masamichi Ogawawara (Tokushima University), and Prof. Dr. Nino Zavraddashvili (Agricultural University of Georgia) for their experimental support.

I feel grateful to all members of Nakano Laboratory and ICAT for their friendship and encouragement. Also, great gratitude goes to all of my friends who helped me complete this work.

Finally, I want to show deep love to my parents and all family members for their comprehension and supporting.

In the end, I would like to extend my sincere appreciation to the DX program, and a research associate program of ICAT for financial support for my doctoral research in Japan.

Thank you all,

2023/3/24
Qingyu WANG